DETERMINATION OF ABSOLUTE AND RELATIVE PERMEABILITY USING WELL TEST ANALYSIS

A DISSERTATION

SUBMITTED TO THE DEPARTMENT OF PETROLEUM ENGINEERING

AND THE COMMITTEE ON GRADUATE STUDIES

OF STANFORD UNIVERSITY

IN PARTIAL FULFILLMENT OF THE REQUIREMENTS

FORTHEDEGREEOF

DOCTOR OF PHILOSOPHY

By

Abdul-Jaleel Abdullah Al-Khalifah

February 1988

I certify that I have read this thesis and that in my opinion it is fully adequate, in scope and quality, as a dissertation for the degree of Doctor of Philosophy.

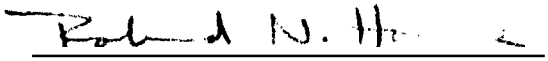

(Co-advisor)

I certify that I have read this thesis and that in my opinion it is fully adequate, in scope and quality, as a dissertation for the degree of Doctor of Philosophy.

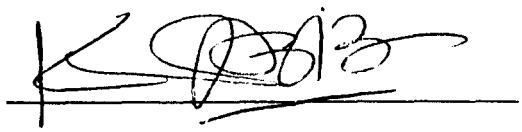

(Co-advisor)

I certify that I have read this thesis and that in my opinion it is fully adequate, in scope and quality, as a dissertation for the degree of Doctor of Philosophy.

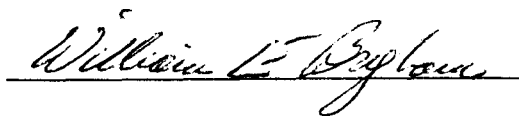

I certify that I have read this thesis and that in my opinion it is fully adequate, in scope and quality, as a dissertation for the degree of Doctor of Philosophy.

Approved for the University Committee on Graduate Studies:

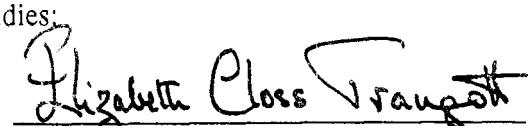

Dean of Graduate Studies

To my father who is no longer

but present in my thought

Among those whom I respect

for their endless support

Acknowledgement

I would like to acknowledge first and foremost. Dr. Roland N. Home and Dr. Khalid *Aziz* for their continued inspiration, support throughout this study. When no hope seemed in sight, Dr. Home's ever optimistic view kept me going.

I am also grateful to Dr. H. J. Ramey, Jr., and Dr. W. E. Brigham for their excellent suggestions and constructive criticism. Their kindness, I will never forget.

Very many thanks are due to *ARAMCO* for providing my scholarship. While I am elated at this opportunity, I remain deeply indebted to many friends in ARAMCO for their kind assistance and on going support.

During the course of this work computer facilities and software provided by Apollo, Gould and ECL were used. I am grateful to all these organizations. *Also,* computer facilities supported by the Reservoir Simulation Industrial Affiliates Program (SUPRI-B) and the Stanford Center for Reservoir Forecasting (SCRF) were used.

Fellow graduate students: I. Kocabas, M. Riley, A. Ambastha, J. Kikani and R. Bratfold, I appreciate your stimulating discussions and review of the manuscript.

Finally, my deepest sincere appreciation goes to my family. Their patience and kindness gave me the faith and support to amve at this point.

ABSTRACT

Multiphase flow is modeled with a diffusivity equation using p^2 as the dependent variable. Such a model applies to systems in which a gas phase is present (i.e. gas-oil and gas-oil-water reservoirs) where it represents the physics of multiphase flow better than existing models and with fewer restrictive assumptions. This new approach allows reasonable estimates of reservoir and wellbore parameters such as effective oil permeability and wellbore skin.

This dissertation also presents a new method to estimate two- and three-phase relative permeabilities in-situ, using pressure transient analysis. The technique requires a short drawdown test, consisting of a number of steps of increasing flow rate. The resulting estimates of relative permeabilities reflect the properties of the entire drainage area, rather than those of a small laboratory core. The method estimates the relative permeabilities at sandface saturations. which cover a range of reservoir conditions that will take place in the future.

The proposed relative permeability method applies solutions of a multiphase diffusivity equation in terms of the pseudopressure function, $m(p)$. These solutions had already been reported for constant rate tests in solution gas-drive reservoirs by Raghavan (1976). This work extends the pseudopressure solutions to three-phase systems. Two- and three-phase solutions were then superposed to obtain multiple-rate solutions. The saturation equation developed by Bøe et al. (1981) for solution gas-drive reservoirs, is extended to three-phase reservoirs. These solutions are then used to estimate relative permeability-saturation values during the test.

When reservoir absolute permeability is not known, the proposed relative permeability technique results in estimates of the effective permeability as a function of the saturation. These results can then be fitted with a simple relation to infer the absolute permeability.

A rate-normalization method applicable to multiphase well tests is formulated and applied to simulated tests with varying flow rates. Such a normalization results in reasonable estimates of individual phase permeabilities and thereby an accurate value of total system mobility.

TABLE OF CONTENTS

LIST OF TABLES

LIST OF FIGURES

1. INTRODUCTION

Reliable description of petroleum reservoirs is essential for accurate performance forecasting. Besides geology and seismology, several branches of the petroleum industry have contributed in describing petroleum reservoirs, e.g. well testing, well logging and core analysis. Well testing is an efficient tool capable of estimating in-situ reservoir properties. Normally, the flow rate is perturbed while monitoring the flowing or shut-in pressure during a test. This pressure transient can be matched to analytical solutions that are functions of some significant reservoir properties, e.g. conductivity and storativity. The reservoir properties inferred from matching the data are usually insensitive to small scale features, and therefore represent some average of the entire scale of investigation.

Well testing in single-phase reservoirs is commonly used to obtain an estimate of the absolute permeability, k, which fully characterizes the conductivity for single-phase flow. The situation is different for multiphase reservoirs. The conductivity for each of the phases is less than that of single phase flow. For multiphase flow, the phase conductivity is the effective phase permeability, k_l, which is normalized to a specific base permeability, yielding the phase relative permeability. These phase relative permeabilities are strong functions of the saturation, the fraction of the pore space filled with the specific fluid. Therefore, an entire set of relative permeability-saturation curves is needed to characterize multiphase flow. The objective of this work was to explore whether well testing may be used to generate relative permeability-saturation curves.

The flow mechanism in multiphase reservoirs is more complicated than that in single-phase reservoirs. A single flow equation is capable of describing single-phase flow. For multiphase flow, there is one flow equation for each component. These flow equations are coupled by the saturation terms. Almost all rock and fluid properties are pressure and/or saturation dependent, leadiig to highly nonlinear coupled equations. This explains why well testing is not as advanced in describing multiphase reservoirs as it is in single phase reservoirs. Pemne's (1956) approach, later verified by Martin (1959), and Raghavan's (1976) approach are

currently used to analyze multiphase well tests. Penine pointed out the possibility of estimating reservoir relative permeability without need for total system compressibility (Ramey, 1987). Perrine's idea has not been considered since none of the current well testing approaches yields relative permeability curves. Raghavan's approach can estimate the absolute permeability of solution gas-drive reservoirs assuming laboratory relative permeability curves apply to reservoir conditions. In summary, multiphase well testing is at an early stage of investigation, and awaits the development of accurate approaches capable of estimating both the absolute and the relative permeability.

The aim of this work was to explore the development of new methads for describing multiphase reservoirs utilizing well test analysis. A physical understanding of multiphase flow allowed some simplification of highly nonlinear terms encountered in the flow equations. Upon simplification, new solutions were developed which made it possible to retrieve estimates of reservoir parameters. These reservoir parameters are relative permeability-saturation curves and the absolute permeability.

Chapter 2 presents a background of multiphase flow theory, and reviews the literature on multiphase well test analysis. After summarizing the state of the art in this field, Chapter 3 states the problem to be considered in this work.

Chapter 4 describes the simplification of multiphase flow equations to a difisivity equation in terms of p^2. This equation can be solved for linearized sets of initial and boundary conditions. As an example, the line source solution is derived and utilized to analyze several simulated, and previously published well tests. This practical approach is shown to yield reasonable estimates of effective phase permeabilities and wellbore skin. Moreover, it is the basis of several multiphase relations that have already been reported in the literature. i.e. the Fetkovich empirical isochronal testing approach (1973) and the Fetkovich empirical material balance relation for solution gasdrive reservoirs (1980). In the course of deriving the diffusivity quation, Martin's total compressibility (1959) is rederived from basic principles, and his pressure-saturation relations are rederived and investigated.

Chapter 5 introduces a technique to estimate two-phase relative permeabilities under reservoir conditions of wettability, heterogeneity and fluid composition. This technique utilizes a drawdown test consisting of a number of steps of increasing flow rates. The pressure response during such a test is analyzed analytically to estimate the sandface saturations and relative permeabilities. Since the sandface saturation reaches values that can only be attained by the reservoir saturation very much later in its life, this approach is a good forecasting tool with no need for extrapolation or extensive historical production data. Several multiple-rate tests were generated using the ECLIPSE simulator for both homogeneous and composite systems. These tests were then analyzed and found to produce matching relative permeability results with the input curves.

Chapter 6 extends the theory of Chapter 5 to three-phase reservoirs. A three-phase diffusivity equation in terms of the pseudopressure function, $m(p)$, is derived and solved to obtain the line source solution, which was used to derive the relative permeability equations. Also, the two-phase saturation equation of Bøe et al. (1981) is extended to three-phase flow, where two pressure-saturation relations are obtained. These analytical relations are used to analyze simulated three-phase multiple-rate tests whereby relative penneabilities are obtained.

A rate-normalization applicable to multiphase well tests is formulated and applied to buildup tests with afterfiow effects and drawdown tests with wellbore unloading behavior. The proposed normalization was shown to be practical and superior to that currently used.

Three main objectives achieved in this work are:

1). the development of a new approach to analyze multiphase well tests which yields reasonable estimates of effective phase penneabilities and wellbore skin,

2). development of an approach to estimate two- and three-phase relative permeabilities, as well as the absolute permeability at reservoir conditions, and

3). a rate-normalization for multiphase tests with varying flow rates.

2. BACKGROUND

Petroleum reservoirs often encounter multiphase flow during normal production operations. Typical examples = solution gas-drive, gas cap, water drive and enhanced recovery processes. The most common representation of multiphase flow is a modification of single phase theory using several redefined parameters. The modifications of the single-phase theory, the nature of the multiphase flow parameters, and methods currently available to measure them are discussed in the following sections.

2.1 Single Phase Theory

The single phase flow equation is a combination of Darcy's law (1856) and the conservation principle. For single phase flow, Darcy's law may be written as follows:

$$v = -\frac{k}{\mu}(\nabla p - \gamma \nabla z) \tag{2-1}$$

where

k = absolute permeability of the rock

μ = flowing fluid viscosity

v = Darcy velocity

p = pressure

z = vertical elevation, positive in the downward direction

γ = hydrostatic pressure gradient

In Darcy's equation, the absolute permeability is a macroscopic statistical average of complex behavior at the microscopic level. When Darcy's equation is combined with the principle of conservation of mass, the resulting single phase flow equation can be written as follows:

$$\nabla \cdot \left[\frac{\rho k}{\mu}(\nabla p - \gamma \nabla z)\right] = \frac{\partial}{\partial t}(\phi \rho) \tag{2-2}$$

where:

ρ = fluid density

ϕ = formation porosity

t = time

Rock properties (porosity and permeability) and single phase fluid properties (viscosity and density) are the only parameters in **Eq. 2-2. This** is not the case with multiphase flow where several other parameters are needed to describe the flow, as will **be discussed** in **the** following sections.

2.2 Multiphase **Theory**

Darcy's (1856) law can **be** modified to accommodate multiphase flow. **During** multiphase flow, two or three phases flow simultaneously in the reservoir. The conductivity of the formation differs for each of the phases and is less **than** that for a single phase fully saturating the formation. While the single phase conductivity is represented by the absolute penneabiiity, **k,** the multiphase conductivities **are** specific for each phase and are called effective phase permeabilities, k_l. When phase l effective permeability, k_l, is normalized to a specific base permeability, such **as** absolute permeability, k; the relative permeability, k_{rl}, results. **Based on this** view, Darcy's equation for multiphase flow may be written as:

$$v_l = - \frac{k\, k_{rl}}{\mu_l} \cdot (\nabla p - \gamma_l \nabla z) \qquad (2\text{-}3)$$

where the subscript l represents a specific phase.

Phase l relative permeability, k_{rl}, **is** a macroscopic statistical average of the complex multiphase behavior at the pore scale. Rapoport and Leas (1951) verified this definition of relative permeability, and found it to be valid provided the following conditions **exist:**

1. flowing phases are continuous,
2. microscopic flow is laminar, and
3. a flow path exists along which saturation can be defined.

Muskat and Meres (1936) modified Darcy's equation, Eq. 2-1, to accommodate multiphase flow. They viewed a multiphase flow system as a fluid structure of dynamic properties superimposed on a rock structure of static properties. As fluid saturations change with space and time, rock structure retains the same properties, but fluid structure properties continue to change. These changing properties are rock-fluid interaction parameters (relative permeability and capillary pressure curves) and fluid-fluid interaction parameters (total system compressibility). Although relative permeability and saturation terms are explicitly used in the multiphase equations, total system compressibility is not. However it is imbedded in the three phase accumulation terms. Assuming negligible gravity and capillary pressure effects, no mass transfer between water and both gas and oil phases, and no evaporation into the gas phase, the following multiphase equations were derived:

For Oil:

$$\nabla \cdot \left[\frac{k\, k_{ro}}{\mu_o B_o} \nabla p \right] = \frac{\partial}{\partial t} \left[\frac{\phi\, S_o}{B_o} \right] \qquad (24\text{-a})$$

For Gas:

$$\nabla \cdot \left[k \left[\frac{k_{rg}}{\mu_g B_g} + \frac{R_s\, k_{ro}}{\mu_o B_o} \right] \nabla p \right] = \frac{\partial}{\partial t} \left[\phi \left[\frac{S_g}{B_g} + \frac{R_s\, S_o}{B_o} \right] \right] \qquad (2\text{-}4\text{-b})$$

For Water:

$$\nabla \cdot \left[\frac{k\, k_{rw}}{\mu_w B_w} \nabla p \right] = \frac{\partial}{\partial t} \left[\frac{\phi\, S_w}{B_w} \right] \qquad (24\text{-c})$$

where:

B_l = phase l formation volume factor,

R_s = solution gas-oil ratio,

S_l = saturation of phase l.

This set of equations describes multiphase flow under the following conditions:

1. Darcy's law applies.
2. thermodynamic equilibrium exists, and
3. fluid PVT properties reflect interphase mass transfer.

2.3 Multiphase flow parameters

The only parameters required to describe single phase flow are the fluid properties (PVT data), and the rock properties (porosity and permeability). On the other hand, when several phases flow in a reservoir, they interact with each other as well as with the rock surface. Therefore, both the PVT data and the relative permeability-saturation curves are required for each of the phases present, as can be seen in Eq. 2.4. Amyx et al. (1960), Marle (1981) and Honarpour et al. (1986) studied the characteristics of relative permeability curves and found them to depend on:

1. pore size,
2. pore size distribution,
3. wettability,
4. fluid saturation and composition, and
5. fluid saturation history (drainage - decreasing wetting phase saturation; imbibition - increasing wetting phase saturation)

Fig. 2-1 shows a typical set of two-phase relative permeability curves. Current methods to measure these relative permeability curves, rock absolute permeability and fluid PVT properties are discussed in the following sections.

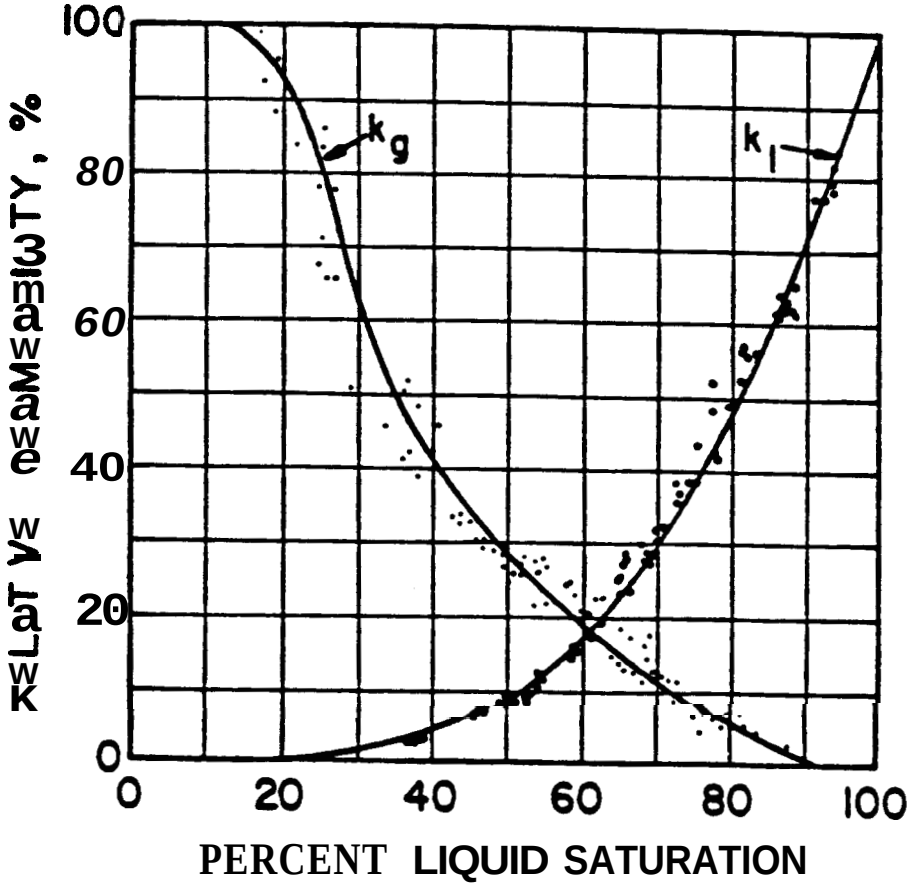

Figure 2.1: A typical example of two-phase relative permeability curves (Wyckoff and Botset, 1936; Scheidegger, 1974)

2.4 Current Measurement Methods

Measurement of multiphase parameters has been the subject of hundreds of publications. Published literature has considered laboratory measurement of PVT properties, from which phase and total system compressibilities are determined. Most of the literature has been concerned with laboratory methods to measure relative permeability curves. While a few publications have proposed performance methods which utilize historical production data of the field, to my knowledge there has been no successful attempt to apply well testing for such applications. The next sections present a brief review of the laboratory and performance methods, and a survey of multiphase well testing literature.

2.4.1 Laboratory Methods

Fluid PVT properties may be measured directly in the laboratory. The basis for almost all laboratory methods is the Dodson et al. (1953) approach. Their approach combines both reservoir differential liberation and wellbore-stock tank flash liberation processes. However this experimental procedure is tedious and costly. Therefore laboratory reports correct the differential liberation results using the correlation given by Amyx et al. (1960) and later by Dake (1978). Moses (1986) has reviewed the subject in detail.

Macias and Ramey (1986) showed that the total system compressibility, calculated using total formation volume factor, B_t, is much higher than Martin's total compressibility calculated using the individual phase formation volume factors. The Macias-Ramey compressibility is defined for an adiabatic system as:

$$c_t = -\frac{1}{B_t}\left[\frac{\partial B_t}{\partial p}\right|_A + c_f \qquad (2\text{-}5)$$

where:

c_t = total system compressibility

c_f = formation rock compressibility

Martin's compressibility was expressed as:

$$c_t = S_o \left[-\frac{1}{B_o}\frac{dB_o}{dp} + \frac{B_g}{B_o}\frac{dR_s}{dp} \right] + S_g \left[-\frac{1}{B_g}\frac{dB_g}{dp} \right] + S_w \left[-\frac{1}{B_w}\frac{dB_w}{dp} + \frac{B_g}{B_w}\frac{dR_{sw}}{dp} \right] + c_f \qquad (2\text{-}6)$$

where R_{sw} is the solution gas-water ratio.

Macias and Ramey concluded that Martin's relation underestimates the total compressibility for most flow conditions, due to thermodynamic equilibrium effects which neglect heat exchange from the rock. In Chapter 4 Martin's relation is derived from basic principles without Martin's assumption of negligible saturation and pressure gradients. There is another possible reason for underestimation of the total compressibility, besides that of the thermodynamic effects. It is that current laboratory measurement methods, based on the Dodson et el. (1953) approach, do not represent the liberation processes occurring in the formation. When gas is liberated from the oil, some time is required to reach the critical gas saturation before gas can move in the reservoir. Throughout this production period, reservoir fluids undergo a flash process, which can not be represented by a differential process as is done in laboratory experiments. After gas starts to move, the process is neither a complete flash nor a complete differential process, rather it is somewhere in between. Again, the laboratory methods do not consider such a mixed process. In general, laboratory methods do not reflect interphase mass transfer as it actually happens in a reservoir, This results in an underestimation of the total isothermal compressibility obtained using individual phase PVT properties measured in a laboratory. This basic difficulty deserves further investigation in future research.

Extensive work has been done on the theory, instrumentation and procedure of several laboratory methods used to measure two-phase relative permeability curves. Steady-state and unsteady-state methods are the two conventional choices in the laboratory. In the steady-state method, the two phases flow simultaneously until stable flow rates are measured at both ends

of the core. In the unsteady-state method, the core is saturated with one phase and then the other phase is injected into one end and produced from the other end. Several variations of these two methods are currently in use.

Three-phase relative permeabilities are not easily measured in a laboratory. Experimental procedure is tedious and is less advanced than that of two-phase flow (e.g. Honarpour et al., 1986). Results of measurements reported in the literature are often controversial. An alternate approach to estimate three-phase relative penneabilities is to use probability models proposed by Stone (1970); see the discussion by Aziz and Settari (1979). These models combine two sets of two-phase relative permeabilities to obtain three-phase relative penneabilities. Such a combination assumes that both water and gas relative penneabilities are only functions of their individual saturations. It also assumes that there is at most one mobile phase in each channel of the porous medium. Not only do probability models distort the physics of three-phase flow. they also involve the problems associated with two-phase relative permeability measurements discussed later. Nevertheless, these models provide a practical approach for reservoir simulation studies.

Relative penneabilities for unsteady state flow are difficult to measure in a laboratory. Kimbler and Caudle (1957) stated that the steady-state fluid distribution is different from the unsteady state one. Hence, relative permeability curves should be different. In another study, Rafigul-Islam and Bentsen (1986) concluded that the application of steady-state relative permeability curves to describe unsteady-state flow is questionable. This argument is still subject to investigation.

Core wettability and fluid composition are two other problems of laboratory methods. Although relative permeability curves are strong functions of both wettability and fluid composition, drilling and core recovery operations normally alter both of them. Cores are either preserved, or restored in an attempt to represent conditions existing in a reservoir. Nevertheless, none of these methods appears to be particularly successful in doing so.

Corey and Rathjens (1956) studied the effects of stratification on laboratory relative permeability curves. Flows both parallel and perpendicular to stratifications were considered. The critical gas saturation, S_{gc}, was found to be low in the first case, but high in the second. Oil relative permeability was a severe function of high oil saturations for the perpendicular flow case. Gas relative permeability was sensitive to slight stratification, while oil relative permeability was not. This experiment supported the fact that relative permeability is a strong function of rock heterogeneity. Such a conclusion was also reached by Huppler (1970) and Johnson and Sweeney (1971).

Laboratory experiments use small pieces of reservoir rocks, i.e. cores. These cores represent small-scale heterogeneities, compared to the entire formation. Such drawback of laboratory methods necessitated the search for other methods to measure relative permeability-saturation curves that reflect the whole reservoir.

2.4.2 Performance Methods

In an attempt to resolve problems with laboratory procedures, performance methods were proposed to measure relative permeability curves from long-term production data. These methods are applicable to depletion reservoirs (e.g. Mueller et al., 1955), and apply after a long production time for which performance data are available. These methods also assume uniform average pressure, saturation, and gas-oil ratio over the entire reservoir. Finally, these methods only produce a short segment of the relative permeability ratio, k_{rg}/k_{ro}, vs. saturation curve. Since these results are limited to historical values of saturations (to the most recent data point), they must be extrapolated to forecast future performance.

Fetkovich et al.(1986) utilized decline curves to analyze performance data for depletion reservoirs. Their method assumed uniform average pressure, saturation and gas-oil ratio over the well drainage area. Pore volume was only calculated at the start of pressure decline and was assumed constant over flow rate changes. Their method was based on another important assumption, which is that $k_{ro} / \mu_o B_o$ is a linear function of average reservoir pressure. Besides

these assumptions, Fetkovich et al. (1986) method requires both extensive production history data and extrapolation beyond present values of saturation in order to be useful for future reservoir calculations.

2.4.3 Well Testing

One of the major tools used to characterize petroleum reservoirs is well test analysis. The monographs by Matthews and Russell (1967). and Earlougher (1977) and the text book by Lee (1982) have reviewed pressure transient theory and application for many reservoir and testing conditions. Of the many publications in this field, only a few have considered multiphase flow theory and only one, Nygård (1982), studied the possibility of estimating relative permeability curves from well test data. The few publications reported on multiphase flow can be divided into two main categories. First is the pressure approach by Penine (1956). Second is the pseudopressure approach by Raghavan (1976). These approaches and their related Literature are reviewed as follows.

2.4.3.1 Perrine's Approach

Penine (1956), based on empirical observations, modified single-phase flow theory to incorporate multi-phase flow effects. This was done by:

1. replacing single-phase mobility k / μ, by the total mobility:

$$\lambda_t = \left(\frac{k}{\mu}\right)_o + \left(\frac{k}{\mu}\right)_g + \left(\frac{k}{\mu}\right)_w \qquad (2\text{-}7)$$

2. replacing single-phase compressibility by the total-system compressibility obtained by weighting phase compressibilities by their average saturations, as defined in Eq. 2-6.

Perrine's approach results in the total-system mobility, the individual phase mobilities, and the wellbore skin. The solution for individual phase mobilities summarized by Earlougher (1977) may be expressed as:

$$k_l = \frac{162.6\, q_l\, \mu_l\, B_l}{m^*\, h} \qquad (2\text{-}8)$$

The solution for total system mobility, λ_t, applied by Fetkovich and Vienot (1984) as well as Raghavan (1986). may be written as:

$$\lambda_t = (k / \mu)_t = \frac{162.6\, q_t}{m^* h} \tag{2-9}$$

where:

$$q_t = q_o B_o + [\, q_g - q_o R_s - q_w R_{sw} \,] B_g + q_w B_w \tag{2-10}$$

and m^* is the slope of the semilog straight line in the p versus log t or log $\left(\frac{\Delta t + t_p}{A t} \right)$ plot.

The solution for wellbore skin, based on Penine's approach, may be written as:

$$s = 1.151 \left[\frac{p_{1\,hr} - p_i}{m^*} - \log \left(\frac{\lambda_t}{\phi c_t r_w^2} \right) + 3.23 \right] \tag{2-11}$$

Martin (1959) showed that Pemne's approach was based on the following pressure diffusivity equation:

$$\nabla^2 p = \frac{\phi c_t}{\lambda_t} \frac{\partial p}{\partial t} \tag{2-12}$$

Martin derived this equation assuming negligible pressure and saturation gradients. The total compressibility-mobility ratio was assumed constant with pressure to linearize Eq. 2-12.

Martin did not discuss the linearization of the inner boundary conditions (constant oil rate) written as:

$$\lim_{r \to r_w} \left[r \left(\frac{k_{rl}}{\mu_l B_l} \right) \frac{\partial p}{\partial r} \right] = \frac{q_l}{2\pi kh} \tag{2-13}$$

Weller (1966) discussed testing depletion reservoirs, where both oil and gas are flowing. His study was an evaluation of Pemne's approach. He concluded that such an approach is valid for engineering accuracy. He also stated that as gas saturation increases, Pemne's results become less reliable. This was not reported by Earlougher et al. (1967) who studied the same

problem.

Kazemi (1975) developed a near-wellbore simulator to study multiphase well testing. In his runs, pressure started above the bubble point and declined until abandonment. Kazemi's simulator considered wellbore storage, skin effect, and non-uniform gas saturation. He simulated several transient tests and compared his results with those of Penine's. He concluded that when gas saturation develops only in the region around the wellbore, liquid compressibility should be used to calculate the skin and the average reservoir pressure. He stated that the results improve rapidly as gas saturation becomes uniform in the drainage area of the well. He also found that in most cases Pemne's method produced very good approximations to the correct values, but in a few cases it led to large errors.

Raghavan (1986) reviewed the state of the art in this field and reported a field application, which he analyzed using Perrine's approach. Raghavan concluded that for solution gas-drive reservoirs the drawdown rate normalization suggested by Winestock and Colpitts (1965) applies using the instantaneous total rate (q_t in Rb/D), and the buildup rate normalization given by Uraiet and Raghavan (1980) applies using the total rate at shut-in (q_t at $\Delta t = 0$ in Rb/D). Raghavan also reported identical pressure changes for both buildup and drawdown ($p_i - p_{wf} = p_{ws} - p_{wf,s}$).

Chu et al. (1986) investigated the sensitivity of Pemne's approach to saturation gradient for two phase, oil-water, systems. They simulated several testing conditions with and without saturation gradients. They concluded that, in general, a good estimate of total mobility, λ_t, can be obtained using Eq. 2-9. However to determine individual phase mobilities using Eq. 2-8, one of two conditions should prevail. Either the saturation distribution must be uniform, or the producing fluid ratio must be representative of the flow ratio in the investigated zone. They also considered the case of a saturated wellbore region within an undersaturated reservoir. They reported that using the total fluid rate the oil mobility could be estimated.

Ayan and Lee (1986) considered the effect of non-uniform saturation distribution within the well drainage area during buildup tests. They concluded that Pemne's approach

overestimates the wellbore skin. They found that calculated skin was a function of the saturation distribution and the "blockage" caused by the buildup of gas around the wellbore. This overestimation in skin increases as completion interval and vertical permeability decreases.

Penine's approach can be applied to two- and three-phase reservoirs without need for tedious calculations. Unfortunately, Pemne's method neither estimates the absolute permeability nor the the relative permeability-saturation curves.

2.4.3.2 Raghavan's Approach

Evinger and Muskat (1942) studied the effects of multiphase flow on the productivity index of a well. They examined the radial flow of both oil and gas on a steady state problem. They expressed the oil flow rate as:

$$q_o = \frac{k\,h}{141.2\,\ln\left[\frac{r_e}{r}\right]} \int_{p}^{p_e} \frac{k_{ro}}{\mu_o\,B_o}\,dp \qquad (2\text{-}14)$$

where:

r_e = external radius

h = thickness

Note that k_{ro} is a function of oil saturation. Therefore, this integral can be evaluated if the saturation-pressure relationship is available, an example of which is the producing gas-oil ratio:

$$GOR = R_s + \frac{k_{rg}}{k_{ro}}\,\frac{\mu_o\,B_o}{\mu_g\,B_g} \qquad (2\text{-}15)$$

Equation 2-15 may be used, as follows, to relate k_{rg}/k_{ro} to the pressure at which the *GOR* is monitored. For a transient test, both bottomhole pressure and *GOR* may be monitored along the test. The k_{rg}/k_{ro} term can then be evaluated using Eq. 2-15 for any monitored *GOR*. The k_{rg}/k_{ro} values obtained can then be tabulated versus monitored bottomhole pressures. Utilizing a k_{rg}/k_{ro} - saturation plot, saturations may be used instead of k_{rg}/k_{ro} in the previous table, resulting in a pressure-saturation table. Using a k_{ro}-saturation graph, saturations may be

replaced by corresponding k_{ro} values, leading to a new table of k_{ro} versus pressure. Such a table can then used to evaluate the integral of Eq. 2-14.

Levine and Pratts (1961) studied the behavior of solution gas-drive reservoirs. Using numerical simulation, they found that the maximum variation of the gas-oil ratio from the outer to the inner boundary was only 10 % for the cases they considered. However they did not discuss the variation of gas-oil ratio with time.

Fetkovich (1973) studied the isochronal testing of oil wells in solution gas-drive reservoirs. He compared oil well behavior with that of a gas well. Based on his empirical observations, he proposed the following deliverability equation:

$$q_o = J'_o \left(\bar{p}^2 - p_{wf}^2 \right)^n \tag{2-16}$$

where:

J_o = back-pressure curve coefficient,

$\bar{p}$ = average reservoir pressure,

p_{wf} = wellbore flowing pressure, and

n = exponent.

This relation is identical to the back pressure equation for gas wells. This approach has been in use since 1973. Chapter 4 derives this empirical approach, and discusses the inherent assumptions behind it.

Fetkovich (1973) also proposed the use of a pseudopressure function, m(p), for both transient and pseudosteady state solutions. The pseudopressure function suggested was:

$$m(p) = \int_{p_{ref}}^{p} \frac{k_{ro}}{\mu_o B_o} \, dp \tag{2-17}$$

where p_{ref} is a base pressure.

He formulated the two-phase, gas-oil, equations utilizing this m(p) , and obtained the solutions for both the transient and the pseudosteady state periods, which can be written as:

For the transient period:

$$q_o = \frac{k\,h}{141.2\left[0.5 \ln t_D + 0.4045 + s\right]} \left[m(p_i) - m(p_{wf})\right] \tag{2-18}$$

For the pseudosteady state period:

$$q_o = \frac{k\,h}{141.2\left[\ln\frac{0.472\,r_e}{r_w} + s\right]} \left[m(\bar{p}) - m(p_{wf})\right] \tag{2-19}$$

where:

q_o = oil rate,

p_i = initial pressure,

$\bar{p}$ = average pressure,

s = skin

t_D = dimensionless time, given by:

$$t_D = \frac{0.000264\,k\,t}{\phi\,(\mu\,c_t)_i\,r_w^2} \tag{2-20}$$

Raghavan (1976) utilized this pseudopressure approach for analyzing buildup and drawdown tests in solution gas-drive reservoirs to estimate absolute permeability and wellbore skin. Raghavan used the producing gas-oil ratio, *GOR*, given by Eq. 2-15 to relate saturation to pressure and thereby to evaluate the integral of Eq. 2-17 as explained earlier. For drawdown, he used the instantaneous producing gas-oil ratio, while for buildup he utilized the producing gas-oil ratio at the instant of shut-in. Since these pressure-saturation relations are different from each other, Raghavan concluded that superposition does not apply in solution gasdrive reservoirs.

Perhaps due to the tedious nature of the computations required for the evaluation of m@) as a function of pressure for every value of GOR, only one application was reported (see Verbeek, 1982). Moreover, Aanonsen (1985,a) stated that the pseudopressure approach is sensitive to the accuracy of the relative permeability curves. Since reservoir relative permeability curves are not available, laboratory curves were used to evaluate the pseudopressure function, $m(p)$.

Considering the fact that resewoir relative permeability curves may be different from laboratory Curves, Raghavan's approach may lead only to approximate results. Furthermore, Raghavan (1976) reported that his approach does not apply during the pseudosteady state period, where the slope of 2π cannot be observed.

Bϕe et. al. (1981) presented a theoretical background for Raghavan's approach and his use of the producing gas-oil ratio to evaluate the integral of Eq. 2-17. They simplified the two phase equations by using the Boltzman transformation ($y = \frac{\phi r^2}{4kr}$), as follows:

$$\frac{d}{dy}\left[y\frac{dm}{dy}\right] = -\left[\frac{c}{\lambda}\right]^* y\frac{dm_o}{dy} \tag{2-21}$$

where :

$$\left[\frac{c}{\lambda}\right]^* = \frac{1}{\alpha}\left[\dot{\beta}\frac{dS_o}{dp} + \beta'\right] \tag{2-22}$$

$$\alpha = \frac{k_{ro}}{\mu_o B_o} \tag{2-23}$$

$$\beta = \frac{S_o}{B_o}. \tag{2-24}$$

For any two-phase variable, x_2 (such as α and β), the derivatives can be defined as:

$$\dot{x}_2 = \left(\frac{\partial x_2}{\partial S_o}\right)_p \tag{2-25}$$

$$x_2' = \left(\frac{\partial x_2}{\partial p}\right)_{S_o} \tag{2-26}$$

Assuming that the $\left[\frac{c}{\lambda}\right]^*$ term is constant, Bϕe et al. (1981) solved Eq. 2-21 and reported the following logarithmic approximation of the line source solution of Eq. 2-21:

$$m(p_w) = m(p_i) - \frac{141.2\, q_o}{kh}\left[0.5\left[\ln t_D + 0.80907 + 2s\right]\right] \tag{2-27}$$

where :

$$t_D = \frac{0.000264\, k\, t}{\phi\, r_w^2 \left(\frac{c}{\lambda}\right)} \tag{2-28}$$

Bφe et al. (1981) presented an analytical pressure-saturation relation which is applicable assuming Boltzman's transformation applies. This relation relates saturation changes at the sandface to changes in flowing bottomhole pressure. This important relation can be written as:

$$\frac{dS_o}{dp} = \frac{(\alpha\, a' - a\alpha')\, \frac{N}{Y} + (ab' - a\beta')}{(a\dot{\alpha} - a\dot{a})\, \frac{N}{Y} + (a\dot{\beta} - a\dot{b})} \tag{2-29}$$

where:

$$a = \frac{R_s\, k_{ro}}{\mu_o\, B_o} + \frac{k_{rg}}{\mu_g\, B_g}, \tag{2-30}$$

$$b = \frac{R_s\, S_o}{B_o} + \frac{S_g}{B_g}, \tag{2-31}$$

and:

$$\frac{N}{Y} = \frac{q_o\, t}{13.44\, r_w^2\, h\, \phi\, a} \tag{2-32}$$

Bφe et al. verified this relation using simulated drawdown and buildup tests. They also suggested that this relation could eliminate the need to measure the producing gas-oil ratio. In addition, they concluded that the producing gas-oil ratio quickly stabilizes and remains constant during the infinite-acting period of a drawdown test. For buildup, Raghavan's approach which uses the producing gas-oil ratio before shut-in, works better for evaluating the integral of Eq. 2-17. The reason for this was explored by Aanonsen (1985,a), and is reviewed later.

Nygård (1982) attempted to estimate oil and gas relative permeability curves using a drawdown test. He tried to calculate the pseudopressure, $m(p)$, curves using different sets of relative permeabilities. These sets of relative permeability curves were functions of the pore distribution factor, λ, and the critical gas saturation, S_{gc}. However, he obtained the same

pseudopressure curves for all different combinations of λ and S_{gc}. Therefore, his method was not capable of retrieving the input parameters for the different sets of relative permeability curves he had used.

Whitson (1983) applied Evinger-Muskat's (1942) approach to multiple-rate tests. Whitson found his results to agree with those obtained using Fetkovich's (1973) empirical approach Every rate in both Whitson's and Fetkovich's multiple-rate tests extended into the pseudosteady state period.

Al-Khalifah (1985) developed a theory for pulse testing in solution gas-drive reservoirs in terms of the pseudopressure function, $m(p)$, defined by Eq. 2-17. He reported that the same set of revised pulse testing correlation charts applies for both single- and two-phase tests provided the corresponding variables are used.

Aanonsen (1985,a) studied non-linear effects during transient flow in solution gasdrive reservoirs. He indicated that for constant-rate drawdown, pressure is monotonic with radius, r, and time, t, which is not strictly the case for pressure buildup. However, for practical applications, it can be assumed so. He also reported that for any given test, fluid saturation is a specific function of both radius and time. He argued against Bϕe et al.'s (1981) conclusion that saturation is a unique function of pressure in an infinite reservoir. He concluded that theoretically, the non-linear two-phase equations do not indicate such a conclusion, even though both pressure and saturation are strictly monotonic with Boltzman transform variable, y. However, Aanonsen agreed that both physical understanding and numerical application verify Bϕe et al.'s relation, to a good approximation. Aanonsen also gave a rigorous definition of the pseudopressure function as follows:

$$m\left[r,t\right] = \int_{p_i}^{p_w(t)} \alpha\left[p', t\right] dp' + \int_{p_w(t)}^{p(r,t)} \alpha\left[p', t\right] dp' \qquad (2\text{-}25)$$

Therefore, the pseudopressure function can be evaluated for any radius at any time using two terms. the first term is an integral over time at a given point while the second term is an integral over radius for a fixed time. At the wellbore, the second term of Eq. 2-25 drops and

Eq. 2-17, applied by Raghavan (1976), is obtained.

Aanonsen (1985,a-b) described different flow regions in the well drainage area, in which he considered different simplifying assumptions. For drawdown, he designated the first region as the nearest to the wellbore, in which he neglected the time derivative of the flow equations shortly after the start of the test. The second region was the outside one in which dependent variables change slowly, and their functional coefficients could be assumed constant. The relative sizes of those different regions depend on the degree of non-linearity of the equations.

Aanonsen (1985,a) studied the variation of both $(c/\lambda)^*$, defined by Eq. 2-20, and c_t/λ_t, the total compressibility mobility ratio, with pressure for both buildup and drawdown. Both appeared to increase in value as pressure declined. However their relation with pressure did not seem reversible. Therefore, buildup values of $(c/h)^*$ and c_t/λ_t at any pressure value, may be different from their values at the same pressure of a drawdown test. Aanonsen's reported results show that $(c/\lambda)^*$ and c_t/λ_t are both independent of radial position for drawdown, but not for buildup. A possible reason is that the producing gas-oil ratio in a drawdown test is approximately constant with time during the infinite-acting period, and with space during the pseudosteady state period, while for the buildup test the gas-oil ratio vanes with both space and time. Aanonsen used drawdown values of c_t/λ_t to replace $(c/h)^*$ in an empirical definition of a pseudotime for buildup tests.

Aanonsen (1985,a) also stated that superposition should not apply to the non-linear two-phase solutions. However he considered multiple-rate testing, in which each rate extends into the pseudosteady state period, a special case where superposition should work. He also warned that care should be taken when superposition is applied to other test conditions. In this dissertation, superposition was found to apply to transient multiple-rate testing, as will be justified in Section 5.3.1.

One of Aanonsen's (1985,a) important conclusions was that small inaccuracies in relative permeabilities greatly influence the accuracy of Raghavan's approach. Since laboratory curves were used to evaluate the pseudopressure function, $m(p)$, it is fair to state that unless reservoir

and laboratory curves are identical, Raghavan's pseudopressure approach would not be reasonable. Thus, laboratory curves should not be used in the pseudopressure approach. unless approximate results only are needed.

Jones and Raghavan (1985) studied well test analysis for gas-condensate reservoirs. They introduced two new pseudopressure integrals, one for the sandface pressure and the other for the reservoir pressure. Making use of the steady flow solutions, they were able to evaluate the pseudopressure transformation proposed in their work. Based on their results, a drawdown test results in estimates of both the permeability-thickness product and the wellbore skin. On the other hand, a buildup test results in estimates of the permeability-thickness product, the average pressure, and only the upper and lower bounds of the wellbore skin.

2.4.33 State of the Art

Multiphase well test analysis has been a trade-off between the two current approaches of Penine (1956) and Raghavan (1976). Pemne's approach was reported in two forms. The first form is expressed by Eq. 2-9 and is used to obtain reasonable estimates of total system mobility. The second form is expressed by Eq. 2-8 and was reported to underestimate individual phase permeabilities for some cases. Raghavan's approach is sensitive to the accuracy of the relative permeability curves used in the analysis. On the other hand, Raghavan's approach needs a tedious computation for almost every test, which apparently made it less friendly in practice.

Neither of the current approaches, Pemne's or Raghavan's, is capable of estimating relative pemeability-saturation curves. Measurements of absolute permeability for oil-gas-water or oil-water reservoirs are still unavailable. In summary, neither the absolute permeability nor the relative permeability-saturation curves can be estimated using current well testing techniques.

3. STATEMENT OF THE PROBLEM

Development and Management of petroleum reservoirs relies heavily on the available descriptive picture for the reservoir. To insure a high recovery of valuable petroleum resources, several fields of science and engineering are involved in characterizing reservoir rock and fluid properties. Among those is pressure-transient analysis which has proven efficiency in describing single-phase reservoirs. Because normal situations in practice involves multiphase flow, this dissertation explored the development of new methods for describing multiphase reservoirs using well test analysis.

In multiphase flow, a phase permeability is the absolute permeability of the formaticn multiplied by the relative permeability at the existing phase saturation. While rock absolute permeability may be considered a static property, phase saturations change with space and time and so do their relative permeabilities. Thus, the management of multiphase reservoirs requires the entire relative permeability-saturation curves, together with rock absolute permeability.

The prime objective of this work was the development and application of new multiphase well testing theories for accurate estimation of effective phase pemeabilities, wellbore skin, absolute permeability and relative permeability-saturation curves.

4. NEW APPROACH TO MULTIPHASE WELL TEST ANALYSIS

Multiphase flow is commonly encountered in reservoirs of interest to petroleum engineers. Equations describing multiphase flow are nonlinear and do not yield simple analytical solutions. Hence, very little work has been done in the estimation of reservoir properties from multiphase well tests.

This chapter presents a new approach to analyze multiphase well tests. In this approach, multiphase flow is modeled using the diffusivity equation with p^2 as the dependent variable. This approach is applied to analyze simulated and literature multiphase tests for a range of PVT properties. Results of this approach are compared to those obtained by the pressure approach (Perrine, 1956), which is shown to be a special case of the new approach.

Fetkovich's empirical approach (1973) for isochronal oil-well testing has been in use without theoretical justification. His approach is derived here using the pseudosteady state solution of the diffusivity equation in terms of p^2. The possibility of extending isochronal testing to three phase systems is also discussed.

This chapter also derives the pressure-saturation relations, reported by both Muskat (1949) and Martin (1959). Martin's total compressibility is derived without the assumption of negligible pressure and saturation gradients.

4.1 Mathematical Model

The flow of a three-phase, three-component, oil-gas-water system can be represented by the following equations:

For oil:

$$\nabla \cdot \left[\frac{k\, k_{ro}}{\mu_o B_o} \nabla p \right] = \frac{\partial}{\partial t} \left[\frac{\phi S_o}{B_o} \right] \tag{4-1}$$

For gas:

$$\nabla \cdot \left[\left[\frac{k\, k_{rg}}{\mu_g B_g} + \frac{R_s\, k\, k_{ro}}{\mu_o B_o} \right] \nabla p \right] = \frac{\partial}{\partial t} \left[\frac{\phi S_g}{B_g} + \frac{\phi R_s S_o}{B_o} \right] \tag{4-2}$$

For water:

$$\nabla \cdot \left[\frac{k\, k_{rw}}{\mu_w\, B_w} \nabla p \right] = \frac{\partial}{\partial t} \left[\frac{\phi\, S_w}{B_w} \right] \tag{4-3}$$

Note that gravity and capillary effects have been neglected. This form of the equations also assumes that no gas dissolves in the water phase, and that oil does not evaporate into the gas phase.

Multiply Eq. 4-1 by $\left[B_o - B_g\, R_s\right]$, Eq. 4-2 by B_g and Eq. 4-3 by B_w to obtain:

$$\left[B_o - B_g\, R_s\right] \nabla \cdot \left[\frac{k\, k_{ro}}{\mu_o\, B_o} \nabla p \right] = \left[\frac{\partial}{\partial t} \left[\frac{\phi\, S_o}{B_o} \right] \right] \left[B_o - B_g\, R_s\right] \tag{4-4}$$

$$B_g \nabla \cdot \left[\left[\frac{k\, k_{rg}}{\mu_g\, B_g} + \frac{k}{R_{p0}} \frac{k_{ro}}{B_o} \right] \nabla p \right] = B_g \left[\frac{\partial}{\partial t} \left[\frac{\phi\, S_g}{B_g} + \phi\, \frac{R_s\, S_o}{B_o} \right] \right] \tag{4-5}$$

and

$$B_w \nabla \cdot \left[\frac{k\, k_{rw}}{\mu_w\, B_w} \nabla p \right] = B_w \left[\frac{\partial}{\partial t} \left[\frac{\phi\, S_w}{B_w} \right] \right] \tag{4-6}$$

The right hand side of Eq. 4-4 can be expanded to:

$$\left[B_o - B_g\, R_s\right] \frac{\partial}{\partial t} \left[\frac{\phi\, S_o}{B_o} \right] = \left[B_o - B_g\, R_s\right] S_o \left[-\frac{\phi}{B_o^2} \frac{dB_o}{dp} + \frac{1}{B_o} \frac{d\phi}{dp} \right] \frac{\partial p}{\partial t}$$

$$+ \phi \frac{\partial S_o}{\partial t} - \frac{\phi\, B_g\, R_s}{B_o} \frac{\partial S_o}{\partial t} \tag{4-7}$$

Similarly the right hand side of Eq. 4-5 can be expanded to:

$$B_g \frac{\partial}{\partial t} \left[\frac{\phi\, S_g}{B_g} + \frac{\phi\, R_s\, S_o}{B_o} \right] = \left[B_g\, S_o \left\{ -\frac{\phi\, R_s}{B_o^2} \frac{dB_o}{dp} + \frac{\phi}{B_o} \frac{dR_s}{dp} + \frac{R_s}{B_o} \frac{d\phi}{dp} \right\} \right.$$

$$\left. + B_g\, S_g \left\{ \frac{1}{B_g} \frac{d\phi}{dp} - \frac{\phi}{B_g^2} \frac{dB_g}{dp} \right\} \right] \frac{\partial p}{\partial t} + \phi \frac{\partial S_g}{\partial t} + \frac{\phi\, B_g\, R_s}{B_o} \frac{\partial S_o}{\partial t} \tag{4-8}$$

The right hand side of Eq. 4-6 is similarly expanded to:

$$B_w \frac{\partial}{\partial t}\left[\frac{\phi S_w}{B}\right] = B_w S_w \left[-\frac{\phi}{B_w^2}\frac{dB_w}{dp} + \frac{1}{B_w}\frac{d\phi}{dp}\right]\frac{\partial p}{\partial t} + \phi \frac{\partial S_w}{\partial t} \qquad (4\text{-}9)$$

Equations 4-7, 4-8, and 4-9 are substituted into Eqs. 4-4, 4-5 and 4-6 respectively, and the resulting equations are added to obtain:

$$\left[B_o - B_g R_s\right] \nabla \cdot \left[\frac{k\, k_{ro}}{\mu_o B_o} \nabla p\right] + B_g \nabla \cdot \left[\left[\frac{k\, k_{rg}}{\mu_g B_g} + \frac{R_s\, k\, k_{ro}}{\mu_o B_o}\right] \nabla p\right]$$

$$+ B_w \nabla \cdot \left[\frac{k\, k_{rw}}{\mu_w B_w} \nabla p\right] = \phi \left[-\frac{S_o}{B_o}\frac{dB_o}{dp} + \frac{S_o B_g}{B_o}\frac{dR_s}{dp}\right.$$

$$\left. - \frac{S_g}{B_g}\frac{dB_g}{dp} - \frac{S_w}{B_w}\frac{dB_w}{dp} + \frac{1}{\phi}\frac{d\phi}{dp}\right]\frac{\partial p}{\partial t} \qquad (4\text{-}10)$$

Note that when summing the equations, the saturation derivatives add up to zero. Equation 4-10 may then be reduced to :

$$\left[B_o - B_g R_s\right] \nabla \cdot \left[\frac{k\, k_{ro}}{\mu_o B_o} \nabla p\right] + B_g \nabla \cdot \left[\left[\frac{k\, k_{rg}}{\mu_g B_g} + \frac{R_s\, k\, k_{ro}}{\mu_o B_o}\right] \nabla p\right]$$

$$+ B_w \nabla \cdot \left[\frac{k\, k_{rw}}{\mu_w B_w} \nabla p\right] = \phi\, c_t \frac{\partial p}{\partial t} \qquad (4\text{-}11)$$

where c_t is the total system compressibility, defined as:

$$c_t = -\frac{S_o}{B_o}\frac{dB_o}{dp} + \frac{S_o B_g}{B_o}\frac{dR_s}{dp} - \frac{S_g}{B_g}\frac{dB_g}{dp} - \frac{S_w}{B_w}\frac{dB_w}{dp} + \frac{1}{\phi}\frac{d\phi}{dp} \qquad (4\text{-}12)$$

In general, if we allow for gas solution in the water phase, the preceding equation can be modified to:

$$c_t = -\frac{S_o}{B_o}\frac{dB_o}{dp} + \frac{S_o B_g}{B_o}\frac{dR_s}{dp} - \frac{S_g}{B_g}\frac{dB_g}{dp}$$

$$-\frac{S_w}{B_w}\frac{dB_w}{dp} + \frac{S_w B_g}{B_w}\frac{dR_{sw}}{dp} + \frac{1}{\phi}\frac{d\phi}{dp} \qquad (4\text{-}13)$$

The derivation of Eq. 4-13 does not require Martin's (1959) assumption of negligible pressure and saturation gradients. Therefore, Martin's definition of total compressibility applies to any flow condition provided thermodynamic equilibrium is reached and the PVT properties reflect the interphase mass transfer that takes place in the reservoir.

Expanding the flow terms in Eq. 4-11:

$$\phi c_t \frac{\partial p}{at} = (B_o - B_g R_s)\frac{k_o}{\mu_o B_o}\nabla^2 p + B_g\left(\overline{GOR}\frac{k_o}{\mu_o B_o}\right)\nabla^2 p$$

$$+ B_w \overline{WOR}\frac{k_o}{\mu_o B_o}\nabla^2 p + \left[B_o - B_g R_s\right]\nabla p \cdot \nabla\left[\frac{k_o}{\mu_o B_o}\right] +$$

$$B_g \nabla p \cdot \nabla\left[\overline{GOR}\frac{k_o}{\mu_o B_o}\right] + B_w \nabla p \cdot \nabla\left[\overline{WOR}\frac{k_o}{\mu_o B_o}\right] \qquad (4\text{-}14)$$

where the following definitions apply for all (r, t) :

total gas (both solution and free gas) per stock tank barrel of oil flowing in the reservoir is:

$$\overline{GOR} = R_s + \frac{k_g}{k_o}\frac{B_o \mu_o}{B_g \mu_g},$$

and total water per stock tank barrel of oil flowing in the reservoir is:

$$\overline{WOR} = \frac{k_w}{k_o}\frac{\mu_o B_o}{\mu_w B_w}.$$

Equation 4-14 may be reduced to:

$$\phi c_t \frac{\partial p}{\partial t} = \frac{k_o}{\mu_o} \nabla^2 p + \frac{k_g}{\mu_g} \nabla^2 p + \frac{k_w}{\mu_w} \nabla^2 p$$

$$+ \left[B_o - B_g R_s\right] \nabla p \cdot \nabla \left[\frac{k_o}{\mu_o B_o}\right] + B_g \overline{GOR} \nabla p \cdot \nabla \left[\frac{k_o}{\mu_o B_o}\right]$$

$$+ B_w \overline{WOR} \nabla p \cdot \nabla \left[\frac{k_o}{\mu_o B_o}\right] + B_g \left[\nabla \overline{GOR} \cdot \nabla p\right] \frac{k_o}{\mu_o B_o}$$

$$+ B_w \left[\nabla \overline{WOR} \cdot \nabla p\right] \frac{k_o}{\mu_o B_o} \qquad (4\text{-}15)$$

Equation 4-15 may be rearranged to:

$$\phi c_t \frac{\partial p}{\partial t} = \lambda_t \nabla^2 p$$

$$+ \left[B_o - B_g R_s + B_g \overline{GOR} + B_w \overline{WOR}\right] V p \cdot V \left[\frac{k_o}{\mu_o B_o}\right]$$

$$+ \frac{B_g k_o}{\mu_o B_o} \nabla p \cdot \nabla \overline{GOR} + \frac{B_w k_o}{\mu_o B_o} \nabla p \cdot \nabla \overline{WOR} \qquad (4\text{-}16)$$

where:

$$\lambda_t = \frac{k_o}{\mu_o} + \frac{k_g}{\mu_g} + \frac{k_w}{\mu_w} \qquad (4\text{-}17)$$

Penine's (1956) approach, discussed in Chapter 2, neglects all of the terms on the right hand side of Eq. 4-16 except the first. It will be seen later that the new approach neglects only the last two terms. Equation 4-16 reduces to:

$$\phi c_t \frac{\partial p}{\partial t} = \lambda_t \nabla^2 p + \frac{B_o \mu_o}{k_o} \left[\lambda_o + \lambda_g + \gamma\right] v p \cdot \nabla \left[\frac{k_o}{\mu_o B_o}\right]$$

$$+ \frac{k_o}{\mu_o B_o} \left[B_g \left[\nabla p \cdot \nabla \overline{GOR}\right] + B_w \left[\nabla p \cdot \nabla \overline{WOR}\right]\right] \qquad (4\text{-}18)$$

$$= \lambda_t \left[\nabla^2 p + \mathbf{v}\,\mathbf{p} \cdot \nabla \left[\ln\left(\frac{k_o}{p_o B_o} \right) \right] \right]$$

$$+ \frac{k_o}{\mu_o B_o} \left[B_g \left[\nabla p \cdot \nabla \overline{GOR} \right] + B_w \left[\nabla p \cdot \nabla \overline{WOR} \right] \right] \qquad (4\text{-}19)$$

Further simplification yields:

$$\frac{\phi c_t}{\lambda_t} \frac{\partial p}{\partial t} = \nabla^2 p + \nabla p \cdot \nabla \left[\ln \left(\frac{k_o}{\mu_o B_o} \right) \right]$$

$$+ \frac{k_o}{p_o B_o} \left[\frac{B_g}{\lambda_t} \left[\nabla p \cdot \nabla \overline{GOR} \right] + \frac{B_w}{\lambda_t} \left[\nabla p \cdot \nabla \overline{WOR} \right] \right] \qquad (4\text{-}20)$$

As shown by Handy (1957) and applied by Fetkovich (1973) the term $k_o / (\mu_o B_o)$ can reasonably be assumed to vary linearly with pressure in gas-oil systems. Fetkovich considered this linear relation to have a zero intercept at the origin. (Though this intercept is not zero in real systems, Appendix B justifies using a zero intercept). This linear relation of zero intercept and constant slope a can be expressed as:

$$\frac{k_o}{p_o B_o} = a\,p \qquad (4\text{-}21)$$

The linear relation, Eq. 4-21, may be utilized to change Eq. 4-20 to:

$$\frac{\phi c_t}{\lambda_t} \frac{\partial p}{\partial t} = \nabla^2 p + \nabla p \cdot \nabla \ln p$$

$$+ \frac{k_o}{p_o B_o} \left[\frac{B_g}{\lambda_t} \left[\nabla p \cdot \nabla \overline{GOR} \right] + \frac{B_w}{\lambda_t} \left[\nabla p \cdot \nabla \overline{WOR} \right] \right] \qquad (4\text{-}22)$$

$$= \nabla^2 p + \frac{1}{p} \left[\nabla p \right]^2$$

$$+ \frac{k_o}{p_o B_o} \left[\frac{B_g}{\lambda_t} \left[\nabla p \cdot \nabla \overline{GOR} \right] + \frac{B_w}{\lambda_t} \left[\nabla p \cdot \nabla \overline{WOR} \right] \right] \qquad (4\text{-}23)$$

When Eq. 4-23 is multiplied by 2p, the following equation in terms of p^2 results:

$$\frac{k_o}{\mu_o B_o}\left[\frac{B_g}{\lambda_t}\left(\nabla p^2 \cdot \nabla \overline{GOR}\right)+\frac{B_w}{\lambda_t}\left(\nabla p^2 \cdot \nabla \overline{WOR}\right)\right]+\nabla^2 p^2 = \frac{\phi c_t}{\lambda_t}\frac{\partial p^2}{\partial t} \qquad (4\text{-}24)$$

Levine and Prats (1961) performed simulation runs to investigate the change in GOR over the drainage area. They found a maximum variation of 10% over the drainage area. Numerical examples generated using ECLIPSE, also showed that:

$$\frac{k_o}{\mu_o B_o}\frac{B_g}{\lambda_t}\left[V\,\overline{GOR} \cdot \nabla p^2\right] cc\ \nabla^2 p^2$$

It can also be shown that:

$$\frac{k_o}{\mu_o B_o}\frac{B_w}{\lambda_t}\left[\nabla\,\overline{WOR} \cdot \nabla p^2\right] << \nabla^2 p^2.$$

For example. a drawdown test simulated at 10% initial gas saturation in a solution gas-drive reservoir resulted in a value for $(k_o B_g)/(\mu_o B_o \lambda_t)\left[V\,\overline{GOR} \cdot V p^2\right]$ which is less than one percent of that for $\nabla^2 p^2$. Based on such observations, Eq. 4-24 may be reduced to the following diffusivity equation in terms of p^2:

$$\nabla^2 p^2 = \frac{\phi c_t}{\lambda_t}\frac{\partial p^2}{\partial t} \qquad (4\text{-}25)$$

4.2 Line Source Solution

The multiphase diffusivity equation in terms of p^2 can be linearized by assuming that the total compressibility-mobility ratio, c_t / λ_t, is constant. Such an assumption was necessary to derive Pemne's (1956) and Raghavan's (1976) solutions. The linearized difisivity equation can then be solved for any linear set of initial and boundary conditions. The following is the derivation for a line source.

The reservoir is assumed to be infinite, homogeneous and isotropic. It is also assumed

that the flow is isothermal and that the well penetrates the entire thickness. It is worth noting that the proposed approach is based on the assumption that $k_{ro} / (\mu_o B_o)$ changes linearly with pressure, and that this assumption only holds for gas-oil and gas-oil-water systems. Section 4.6 shows that the new approach does not apply to oil-water systems with no flowing gas.

Initial and boundary conditions are:

initial:

$$p^2 = p_i^2 \qquad at\ t = 0, \quad for\ all\ r, \tag{4-26-a}$$

outer boundary:

$$p^2 = p_i^2 \qquad for\ r \to \infty\ , \quad for\ all\ t, \tag{4-26-b}$$

inner boundary (constant oil rate):

$$\lim_{r \to r_w} \left[r \left(\frac{k_o}{\mu_o B_o} \right) \frac{\partial p}{\partial r} \right] = \frac{q_o}{2 \pi h} \tag{4-26-C}$$

To linearize the inner boundary condition, $k_o / (\mu_o B_o)$ is assumed to vary linearly with pressure, $p(r \to 0\ , t)$. To verify this assumption, $k_o / (\mu_o B_o)$ is considered to be a combination of oil effective permeability k_o and PVT terms $1/(\mu_o B_o)$. It is an accepted assumption that the PVT term $1/(\mu_o B_o)$ varies linearly with pressure in saturated oil systems, an example is the PVT properties reported by Bφe et al. (1981) and plotted in Fig. 4-1. sandface saturation was found to adjust to a nearly stabilized value over most of a test (Fig. 4-2 shows the sandface saturation for a simulated drawdown test in a gas-oil system). When the sandface saturation stabilizes, so does the sandface effective oil permeability. Hence, for systems with gas phase present, k_o drops approximately to a constant value over most of the test Thereafter, the term $k_o / (\mu_o B_o)$ is approximately a linear function of pressure at the sandface. This was verified numerically using the ECLIPSE simulator. An example of computed ($k_{ro} / \mu_o B_o$) vs. p_{wf} is shown in Fig. 4-3 for a gas-oil system. The starting point $\left[k_o / (\mu_o B_o) \right]_i$ lies above the extrapolation of the approximately straight line (see Appendix B for more examples).

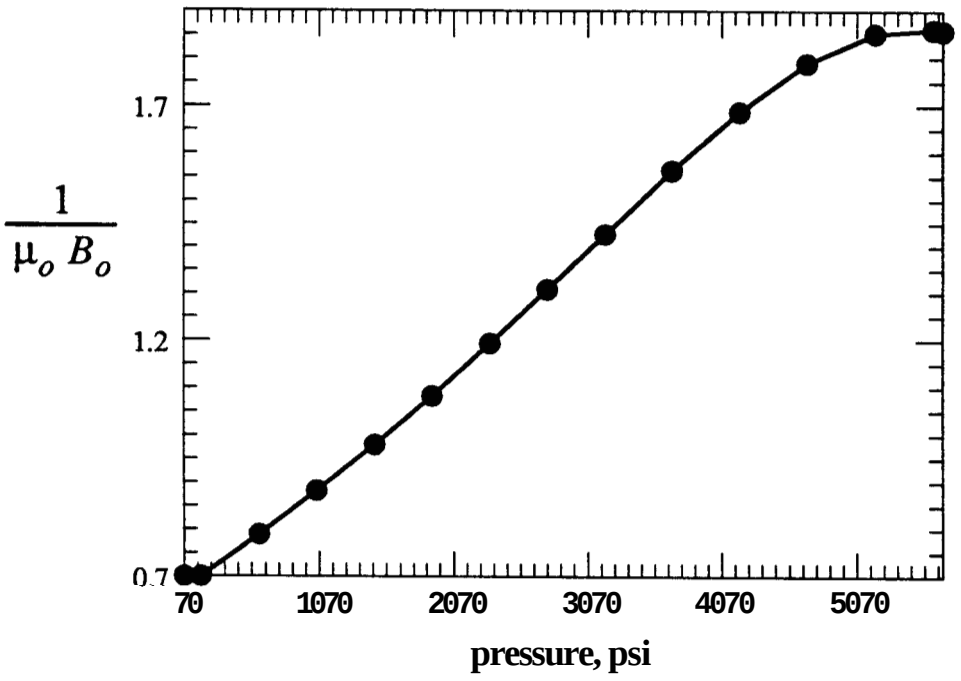

Figure 4.1: PVT properties, Bϕe et al (1981).

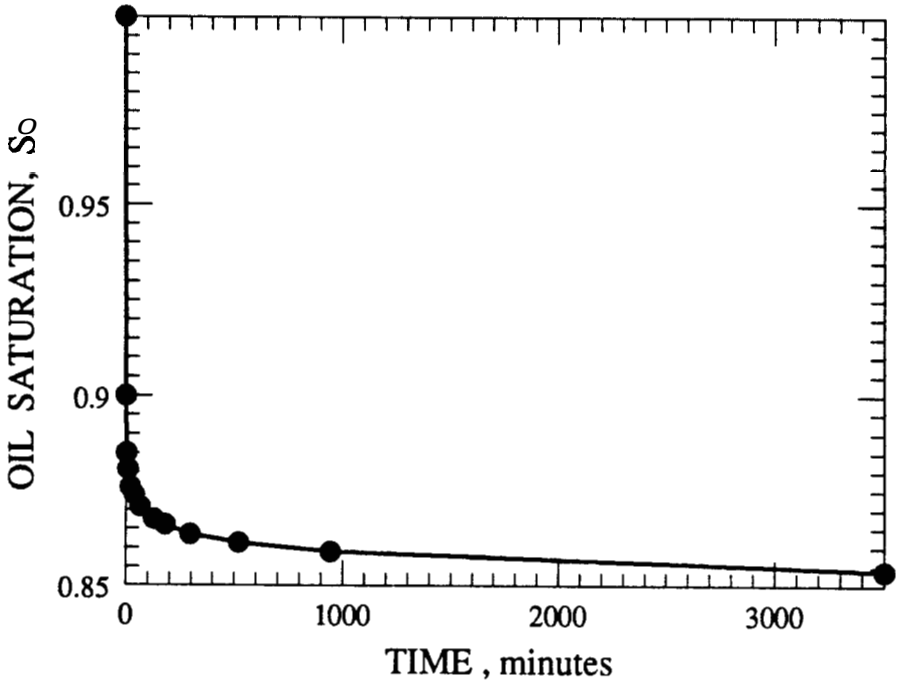

Figure 4.2: Sandface oil saturation vs. time for a simulated constant-rate drawdown test.

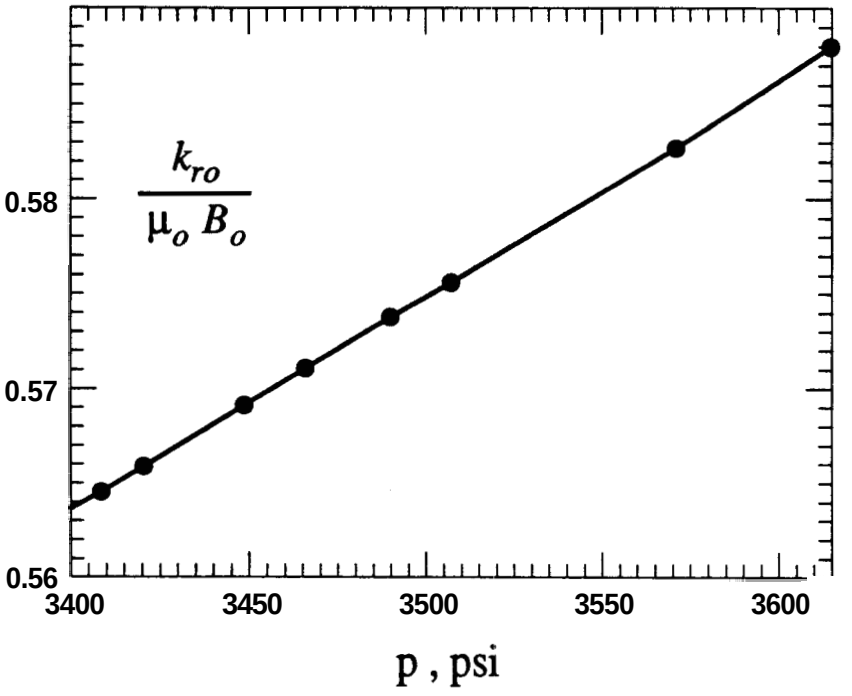

Figure 4.3: $k_{ro} / (\mu_o B_o)$ vs. p (r_w , t) for a simulated drawdown test.

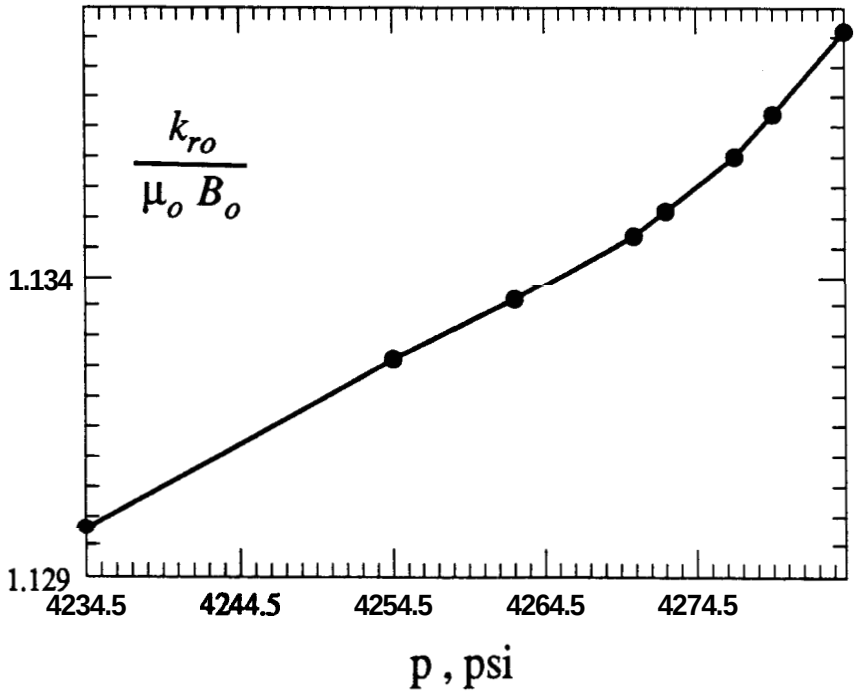

Figure 4.4: $k_{ro} / (\mu_o B_o)$ vs. p (r) at t_p = 41.05 days.

The term $k_{ro}/(\mu_o B_o)$ was assumed to be a linear function of $p(t)$ at any radial location for Eq. 4-21 to reduce to the diffusivity equation, Eq. 4-25. In general, $k_{ro}/(\mu_o B_o)$ involves highly nonlinear functions of pressure, e.g. $S_o(r,t)$. Since $S_o(r,t)$ keeps changing during a test, unlike the sandface saturation shown in Fig. 4.2, Eq. 4-21 is only an approximation to the actual behavior. Figure 4.4 is an example of the relationship between $k_{ro}/(\mu_o B_o)$ and $p(r)$ at a time of 4105 days. It may be argued that $k_{ro}/(\mu_o B_o)$ should be considered piecewise linear, but the results will not be as simple nor as practical. Through the course of this work, the simple linear relation, Eq. 4-21, was used assuming it reflects the overall behavior of the system. Appendix B justifies using a zero intercept in such a relation.

The inner boundary condition, for the constant oil rate, can be written as:

$$\lim_{r \to r_w} \left[r \left(\frac{k_o}{\mu_o B_o} \right) \frac{\partial p}{\partial r} \right] = \frac{q_o}{2 \pi h} \tag{4-27}$$

$$\lim_{r \to r_w} \left[r a p \frac{\partial p}{\partial r} \right] = \frac{q_o}{2 \pi h} \tag{4-28}$$

$$\lim_{r \to r_w} \left[r \frac{\partial p^2}{\partial r} \right] = \frac{q_o}{\pi a h} \tag{4-29}$$

Derivations of the solution to the pressure diffusivity equation, presented in the SPE Monograph 1 by Matthews and Russell (1967) and Monograph 5 by Earlougher (1977), as well as solutions in terms of p^2 documented in the ERCB manual (1975), were followed to obtain the line source solution. The initial and boundary conditions. Eqs. 4-26-a, 4-26-b and 4-29, were applied to solve the diffusivity equation in terms of p^2, Eq. 4-25. The following line source solution was obtained:

$$p_i^2 - p^2(r,t) = \frac{q_o}{2 \pi a h} \left[- E_i \left[- \frac{\phi r^2}{4 t} \frac{c_t}{\lambda_t} \right] \right] \tag{4-30}$$

When the logarithmic approximation applies, Eq. 4-30 can be written in field units as:

$$p_{wf}^2 - p_i^2 = -\frac{325.2\, q_o}{a\, h}\left[\log t + \log\left(\frac{\lambda_t}{\phi\, c_t\, r_w^2}\right) - 3.228 + 0.869\, s\right] \qquad (4\text{-}31)$$

where the skin effect has been added to obtain the wellbore flowing pressure. The skin equation is written for multiphase flow in terms of p^2 :

$$s = 1.1513\left\{\left[\frac{p_{1hr}^2 - p_i^2}{m}\right] - \log\left(\frac{\lambda_t}{\phi\, c_t\, r_w^2}\right) + 3.228\right\} \qquad (4\text{-}32)$$

where m is the slope of the semilog straight line in a p_{wf}^2 versus log t graph.

The line source solution is considered here as a simple application of the general approach For other reservoir or testing conditions, single-phase pressure solutions may be applied similarly to obtain the multiphase solutions in terms of p^2. In general, the difisivity equation, expressed by Eq. 4-25 can be solved for any linearized set of initial and boundary conditions.

4.3 Empirical Slope, a

The assumption that $k_o/(\mu_o B_o)$ is directly proportional to pressure is only valid for systems in which a gas phase is present (Section 4.6). This assumption was utilized to linearize both the diffusivity equation and its inner boundary condition for gas-oil and gas-oil-water systems. If this linear relation was exact, the slope, a, could be evaluated at any pressure. This relation is only approximately correct because highly nonlinear PVT and relative permeability data are involved. Therefore, the appropriate pressure at which the slope should be evaluated is the subject of the following investigation. Three choices for evaluating the slope, a, are considered:

1) The empirical slope, a, is evaluated at the average pressure over a semilog cycle from a p^2 vs log t plot, as described below. The slope, m, of the same cycle may then be used in the effective oil permeability calculation. For illustration, the semilog cycle, ($t = 1hr$ to $t = 10hr$) was chosen here, where the slope of the cycle is:

$$m = (p_{1hr}^2 - p_{10hr}^2), \qquad (4\text{-}33)$$

And the empirical slope, a, is evaluated at:

$$p = \frac{P1h + p_{10hr}}{2} \tag{4-34}$$

Hence:

$$a = \left(\frac{k_o}{\mu_o B_o}\right) \frac{2}{(p_{1hr} + p_{10hr})} \tag{4-35}$$

where $k_o / (\mu_o B_o)$ is evaluated at $(p_{1\,hr} + p_{10\,hr})/2$. Applying this in the line source solution of Eq. 4-31, the following relation was obtained:

$$k_o = \frac{325.2\, q_o \left[\frac{(p_{1hr} + p_{10hr})}{2}\right]\left[(\mu_o B_o)_{\frac{p_{1hr} + p_{10hr}}{2}}\right]}{m\ h} \tag{4-36}$$

which may be reduced to :

$$k_o = \frac{162.6\, q_o\, (\mu_o B_o)_{\frac{p_{1hr} + p_{10hr}}{2}}}{m^*\ h}\ , \tag{4-37}$$

where m^* is the slope per the cycle (1 hr to 10 hr) of a p_{wf} versus log t graph. Equation 4-37 is identical to Penine's (1956) solution, except for the different pressure at which the $(\mu_o B_o)$ term is evaluated. It seems that the estimate of effective oil permeability, obtained by Perrine's method, corresponds to the stabilized oil saturation shown in the saturation-time graph of Fig. 4-2 (i.e. it corresponds to $(p_{1hr} + p_{10hr})/2$). This estimate of k_o was less than k_o at p_i which corresponds to the average reservoir saturation. The higher the pressure drawdown, the lower the stabilized saturation compared to the average reservoir saturation, and therefore, the greater the underestimation of the effective oil permeability encountered in Penine's method. This behavior of Penine's method was investigated in this dissertation and discussed in detail in Section 4.5 and in Appendix C. To overcome this underestimation, it was proposed that $\frac{k_o}{P_0 B_o}$ should be evaluated at a pressure which is higher than that given by Eq. 4-34.

2) The empirical slope, a, is evaluated at the initial pressure, hence

$$a = \left(\frac{k_o}{\mu_o B_o}\right)_i \frac{1}{p_i} \tag{4-38}$$

This slope, when substituted in the line source solution of Eq. 4-31, yields:

$$k_o = \frac{325.2\, q_o\, p_i\, (\mu_o B_o)_i}{m\, h}, \tag{4-39}$$

For buildup tests, this empirical slope is evaluated at the average reservoir pressure. and the corresponding relation is :

$$k_o = \frac{325.2\, q_o\, \bar{p}\, (\overline{\mu_o B_o})}{m\, h}, \tag{4-40}$$

where $\bar{p}$ is average reservoir pressure, $(\overline{\mu_o B_o})$ term is evaluated at $\bar{p}$, m is the slope of Homer (1951) or Miller-Dyes-Hutchin (MDH) (1950) plots in terms of p^2.

These relations, Eqs. 4-39, and 4-40 were applied to well test simulations for reservoirs of both volatile and low volatile oils. As will be shown in Section 4.4, results were good for all ranges of pressure drawdown in volatile oils. For oils of low volatility, results were reasonable for drawdown of small pressure drop and following buildups. On the other hand, results tended to overestimate effective phase permeabilities for drawdowns of large pressure drop and subsequent buildups. Therefore, a third choice was investigated for drawdowns of large pressure drop and following buildups in oils of low volatility.

3) The empirical slope, a, was evaluated for oils of low volatility as follows. For drawdowns of large pressure drop, a was evaluated at $p = p_{wf}$ ($t = 0.1\ hr$). For the following buildups, a was evaluated at $p = p_{ws}$ ($\Delta t = 10\ hr$). Hence, the following relations were obtained:

drawdown of large pressure drop:

$$k_o = \frac{325.2\, q_o\, p_{0.1hr}\, (\mu_o B_o)_{p_{0.1hr}}}{m\, h}, \tag{4-41}$$

Following buildup:

$$k_o = \frac{325.2\, q_o\, p_{10hr}\, (\mu_o B_o)_{p_{10hr}}}{m\, h}. \qquad (4\text{-}42)$$

As can be seen in Section 4.4, these times (0.1 hour for drawdown and 10 hours for buildup) can not be related to the permeability of the system. These pressures were found to avoid the underestimation of the first choice (which reduces to Penine's approach, 1956), and the overestimation of the second choice.

When a drawdown test is dominated by wellbore storage, the semilog straight line may be extrapolated to obtain $p_{0.1hr}$. Though this procedure was not applied in this work, it is expected to work based on the storage-free, simulated tests presented next.

4.4 Applications

The validity of the new approach was investigated using several simulated drawdown and buildup tests including a buildup test reported by Raghavan (1976). These tests were simulated in systems where a gas phase was present, those were gas-oil and gas-oil-water systems. Effective phase permeabilities and wellbore skins were calculated and compared to the input values.

The simulated tests were generated using the ECLIPSE simulator with a 40-block radial model. Time step sizes were short at the beginning and increased with time, to allow close monitoring of the early time data. Three different sets of relative permeabilities were used in the simulation runs. These are shown in Fig. 4.5.

The proposed approach was applied for systems of both volatile and low volatile oils. Two sets of PVT data for volatile oils were used, firstly those reported by Bøe et al. (1981), and secondly the PVT set presented in Table 4-1. The first PVT data set for oils of low volatility is given in Table 4-2. The oil PVT properties of this set are approximately the Same as those reported by Raghavan (1976). Table 4-3 shows a second PVT data set for oils of low

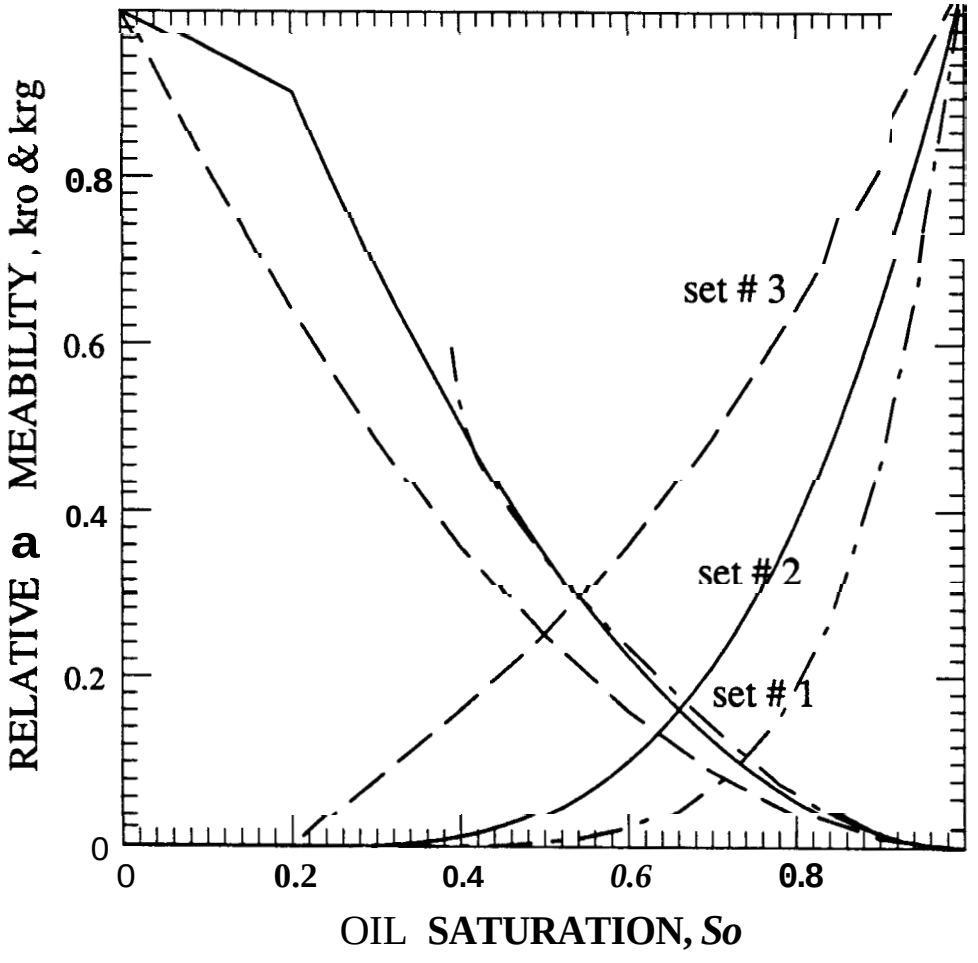

Figure 4.5: The three sets of relative permeability data used in the simulation runs.

Table 4.1: Second set of PVT data for a volatile oil

p, psi	B_g, RB/MSCF	μ_g, cp	R_s, MSCF/STB	B_O, RBBTB	μ_o, cp
14.7		0.0102	0.0	1.00	1.00
414.7	8.459	0.0137	0.044	1.0668	0.604
814.7	4.194	0.0148	0.129	1.1344	0.482
1214.7	2.755	0.0157	0.222	1.1707	0.419
1614.7	2.0445	0.0167	0.319	1.2152	0.373
2014.7	1.626	0.0178	0.411	1.2663	0.339
2414.7	1.3553	0.0191	0.515	1.3224	0.307
2814.7	1.1665	0.0206	0.637	1.3817	0.279
3214.7	1.031	0.0224	0.766	1.46	0.255
3614.7	0.9279	0.0246	0.931	1.5507	0.230
4014.7	0.8495	0.0274	1.108	1.6505	0.208
4214.7	0.8174	0.0292	1.224	1.7131	0.199
4414.7	0.7907	0.0311	1.356	1.7956	0.186
4514.7	0.7783	0.0323	1.450	1.85001	0.181
5014.7				1.8254	0.1891

Table 4.2: First set of PVT data for oils of low volatility

p, psi	B_g, RB/MSCF	μ_g, cp	R_s, MSCFBTB	B_o, RB/STB	μ_o, cp
14.7		0.011	0.102	1.0	3.0
500.0	4.54	0.0118	0.2	1.18	2.34
600.0	4.06	0.0122	0.22	1.195	2.2
700.0	3.3	0.0130	0.240	1.205	2.12
800.0			0.26	1.21	1.981
1000.0	2.85	0.0138	0.3	1.215	1.92
1200.0			0.34	1.23	1.82
1400.0			0.36	1.26	1.78
1500.0	1.958	0.0152	0.38	1.278	1.7645
1600.0	1.953	0.0154		1.274	1.77

Tabk 4 3 Second set of PVT data for oils of low volatility

p, psi	B_g, RB/MSCF	μ_g, cp	R_s, MSCF/STB	B_o, RB/STB	μ_o, cp
400.0	7.28	0.0122	0.102	1.123	1.76
520.0	5.54	0.0125	0.127	1.133	1.65
652.0	4.36	0.0128	0.155	1.144	1.56
777.0	3.62	0.0130	0.180	1.154	1.47
900.0	3.09	0.0133	0.204	1.163	1.40
1025.0	2.70	0.0135	0.226	1.172	1.34
1150.0	2.38	0.0138	*0.249*	1.181	1.29
1275.0	2.17	0.0141	0.270	1.189	1.27
1300.0	2.12	0.0142		1.188	1.28
1800.0	1.57	0.0156		1.183	1.32

volatility. These four sets represent a wide range of PVT properties over which the empirical slope, a, may be investigated.

For volatile oils, Eqs. 4-39 and 4-40 were applied to estimate effective oil permeability. The corresponding relations for oils of low volatility were:

drawdown of large pressure drop & following buildup: Eqs. 4-41 or 4-42,

drawdown of small pressure drop & following buildup: Eqs. 4-39 or 4-40.

The results were compared with those from Penine's solution obtained by Eq. 4-37, as well as to the input values. Effective gas permeability was estimated utilizing the producing GOR. The following relation was applied:

$$k_g = (GOR - R_s) \frac{\mu_g B_g}{\mu_o B_o} k_o \qquad (4\text{-}43)$$

The PVT properties in Eq. 4-43 were evaluated at the initial pressure.

Equation 4-43 was applied to Buildup tests after pseudosteady state drawdowns using the producing GOR before shutin with all PVT properties evaluated at the average reservoir pressure.

Effective water permeability for three-phase systems was evaluated using the producing water-oil ratio, WOR, as follows:

$$k_w = WOR \frac{\mu_w B_w}{\mu_o B_o} k_o \qquad (4\text{-}44)$$

The skin factor was evaluated for drawdown tests using Eq. 4-32. For buildup, that relation changes to the following:

$$s = 1.1513 \left\{ \left[\frac{p_{1hr}^2 - p_{wf,s}^2}{m} \right] - \log \left[\frac{\lambda_t}{\phi c_t r_w^2} \right] + 3.228 \right\} \qquad (4\text{-}45)$$

The Penine (1956) approach and the new approach were used to compute effective phase permeabilities and wellbore skin. Results were then compared with the input values.

Table 4.4: Reservoir and test data for volatile oil systems

Test No.	Test	p_i or $\bar{p}$ psi	S_{oi}	S_{gi}	k_r set	PVT set ft	h
1	First drawdown	4065.7	0.87	0.13	1	2	100
2	Second drawdown	3414.7	0.60	0.20	2	2	100
3	Third drawdown	5202.3	0.50	0.20	2	1	100
4	Fourth drawdown	5202.3	0.50	0.10	2	1	100
5	First buildup	3054.7	0.69	0.3 1	2	1	100
6	Second buildup	4147.7	0.87	0.13	1	2	100

Table 4.5: Reservoir and test data for drawdowns of small pressure drop and following buildups in systems of low volatiliy

Test No.	Test	p_i or $\bar{p}$ psi	S_{oi}	S_{gi}	k_r set	PVT set ft	h
1	First drawdown	1137.0	0.91	0.09	1	1	100
2	Second drawdown	1288.22	1.0	0	3	2	100
3	Third drawdown	1288.22	1.0	0	3	2	100
4	First buildup	1497.4	0.99	0.01	1	1	100

Table 4.6: Reservoir and test data for drawdowns of large pressure drop and following buildups in systems of low volatiliy.

TEST No.	Test	p_i or $\bar{p}$ psi	S_{oi}	S_{gi}	k_r set	PVT set ft	h
1	First drawdown	1137.0	0.91	0.09	1	1	100
2	Second drawdown	1281.22	1.0	0.0	3	2	100
3	First buildup	1180.9	0.79	0.21	1	1	100
4	Raghavan buildup (1976)	1000.0	0.88	0.12	Rag.	Rag.	25.0

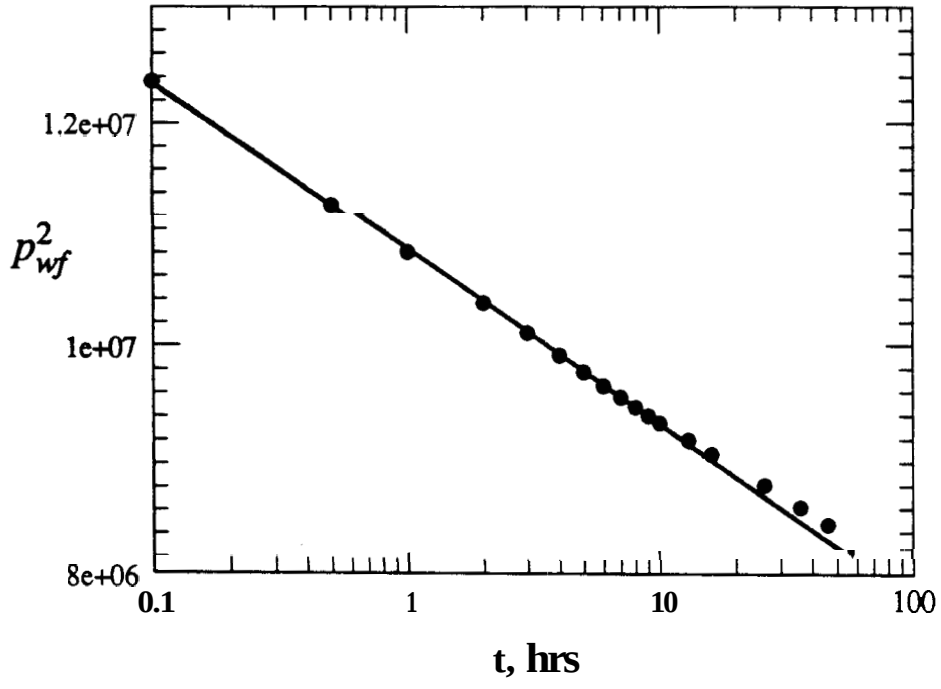

Figure 4.6: **First drawdown for volatile oil systems, Test** No. 1 **in Table 4.4**

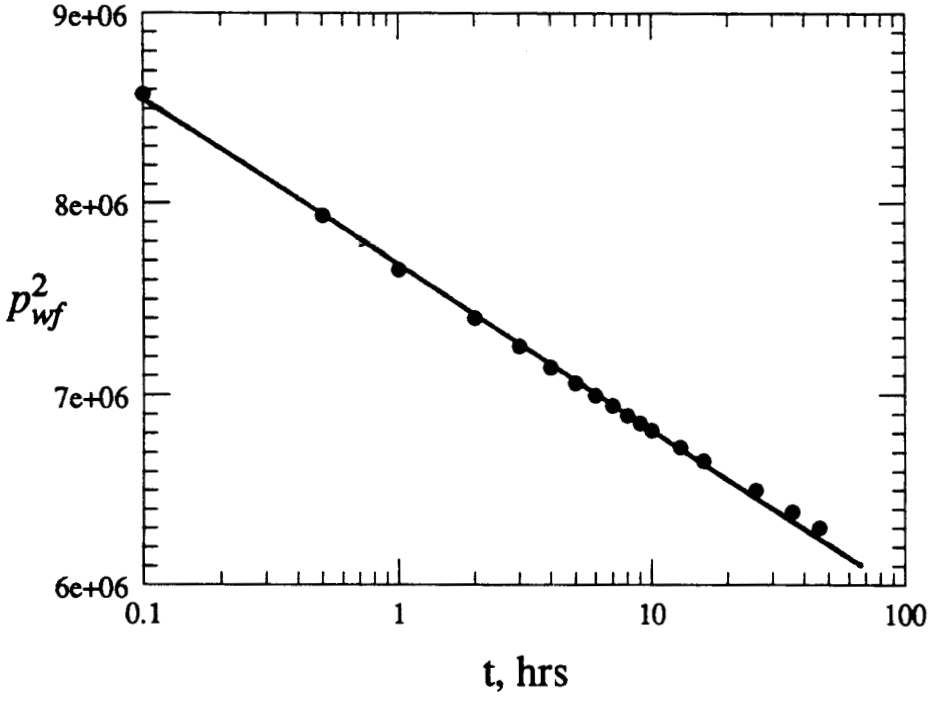

Figure 4.7: Second drawdown for volatile oil systems, Test No. 2 in Table 4.4

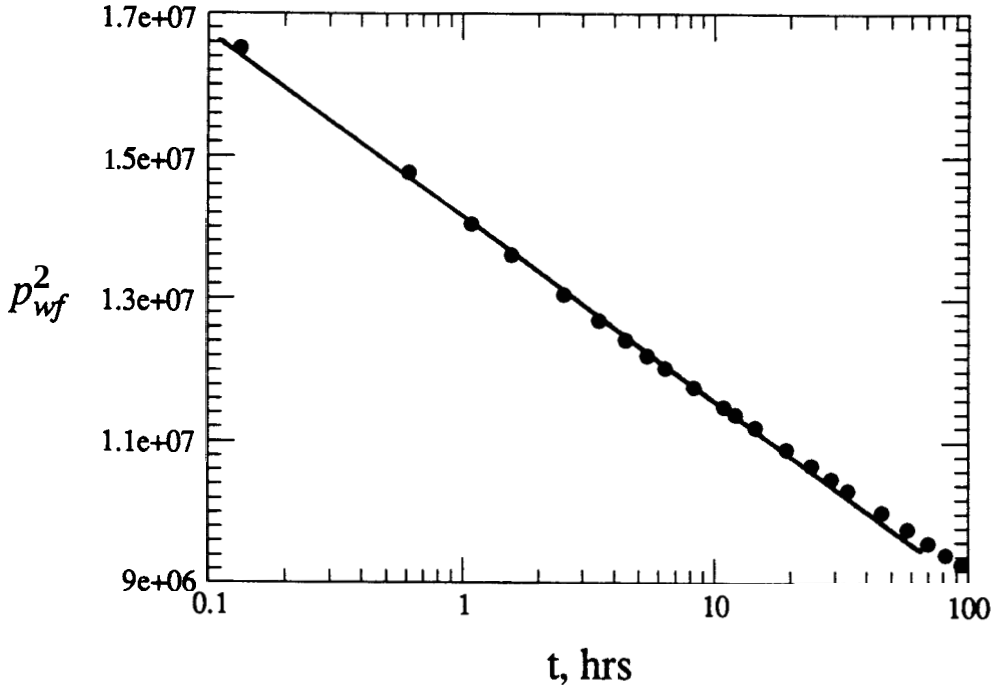

Figure 4.8: Third drawdown for volatile oil systems, Test No. 3 in Table 4.4

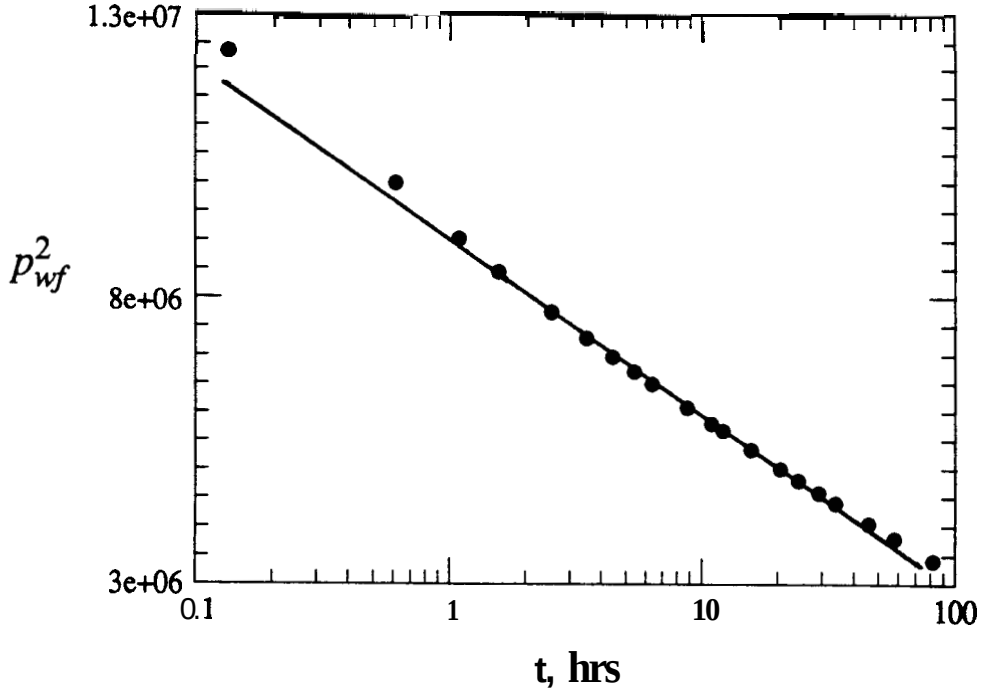

Figure 4.9: Fourth drawdown for volatile oil systems, Test No. 4 in Table 4.4

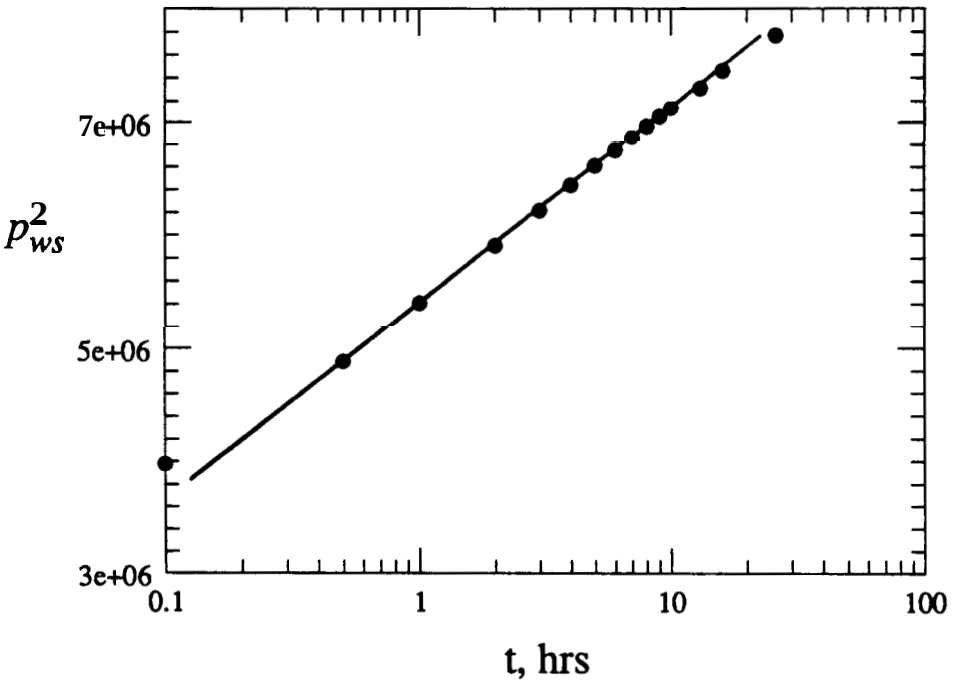

figure 4.10: First buildup for volatile oil systems, t_p = 310 Days, Test No. 5 in Table 4.4

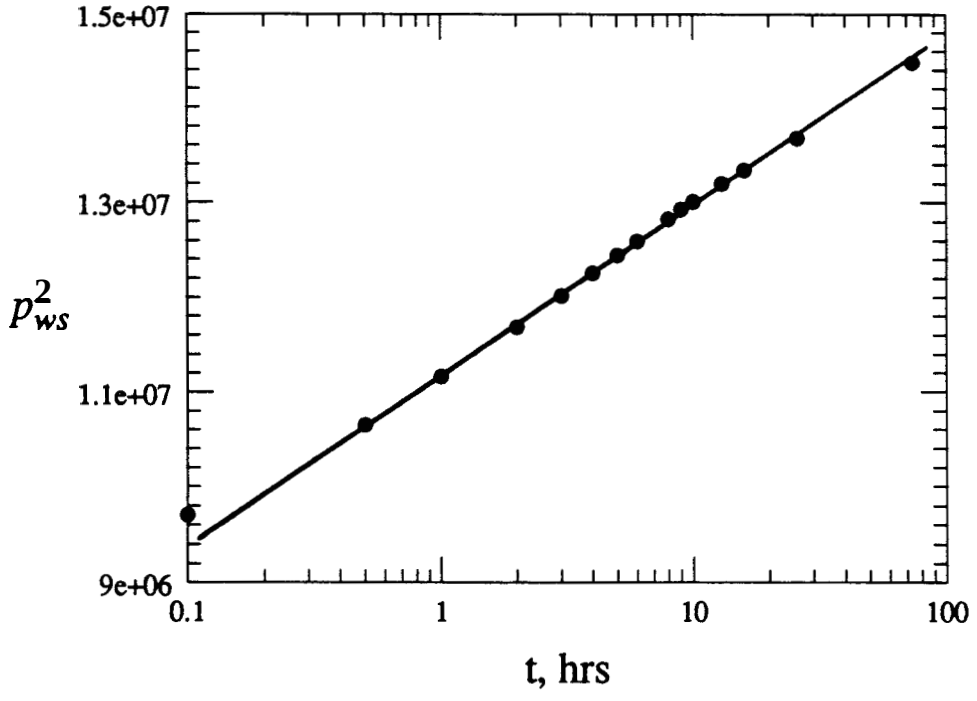

Figure 4.9: Second buildup for volatile oil systems, t_p = 1001 Days, Test No. 6 in Table 4.4

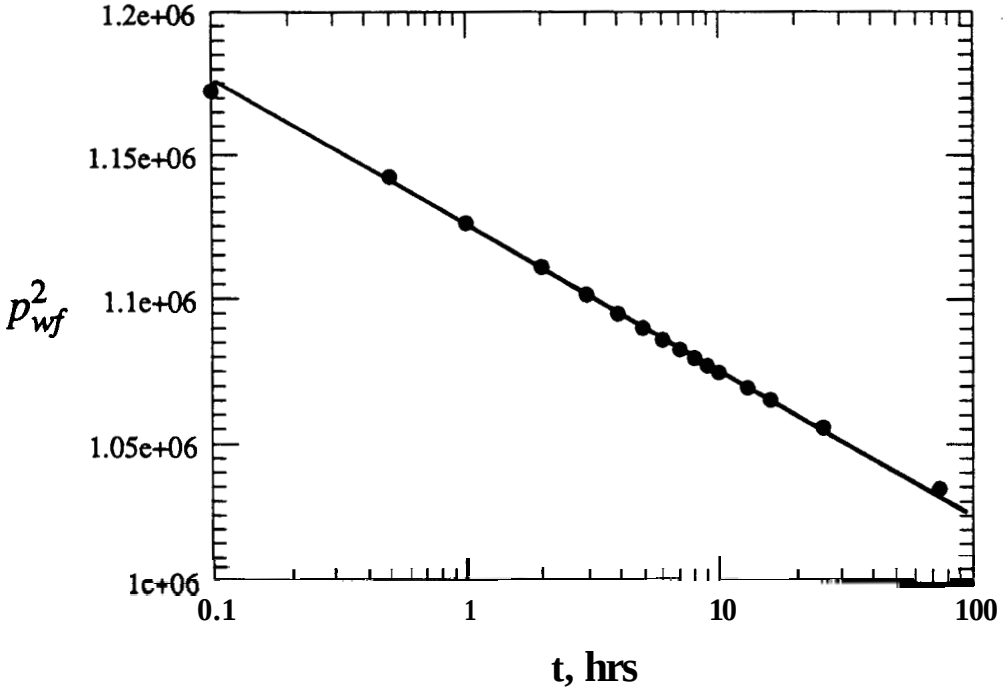

Figure 4.12: **First drawdown** of **small pressure drop in systems** of **low volatility, Test No. 1 in Table 4.5**

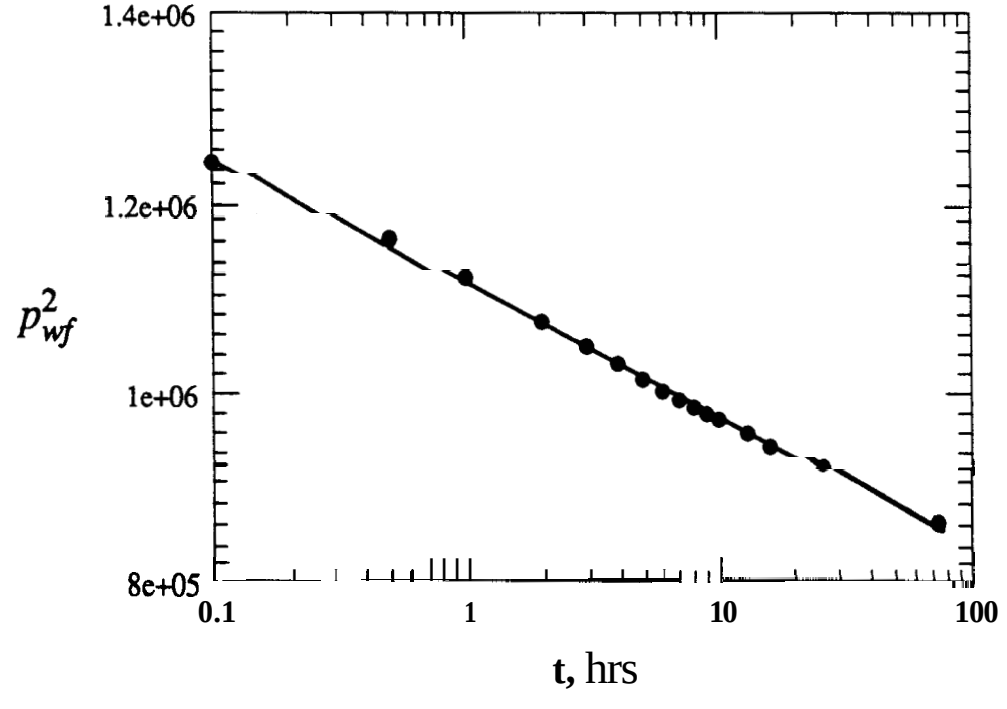

Figure 4.13: **Second drawdown of** small **pressure drop in systems** of **low volatility, Test** No. **2 in Table 4.5**

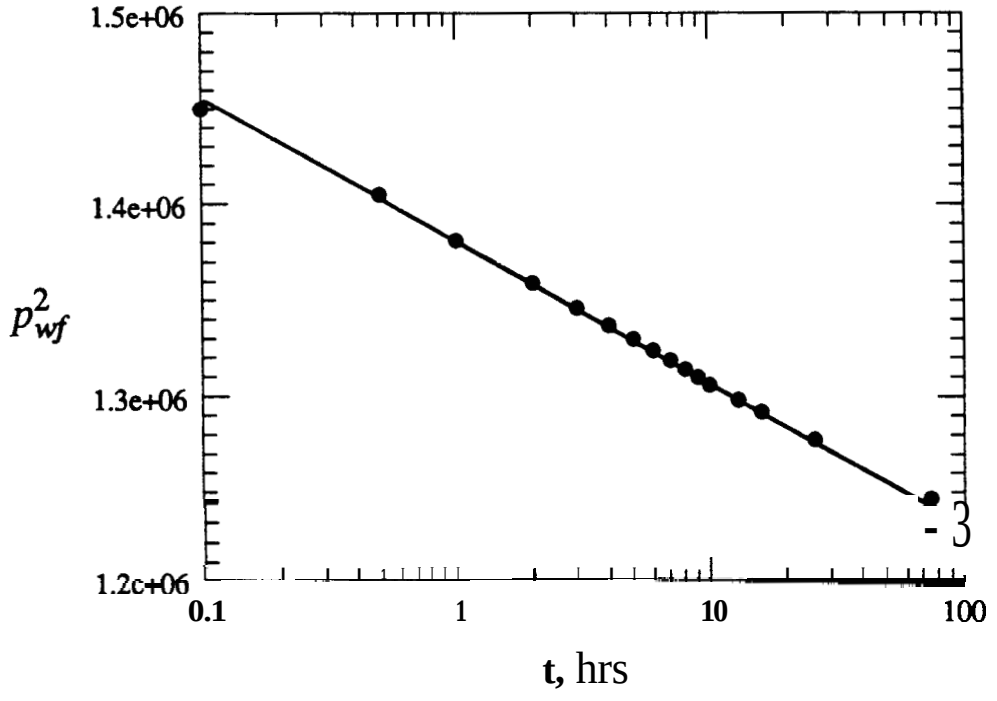

Figure 4.14: Third drawdown test of small pressure drop in systems of low volatility, Test No. 3 in Table 4.5

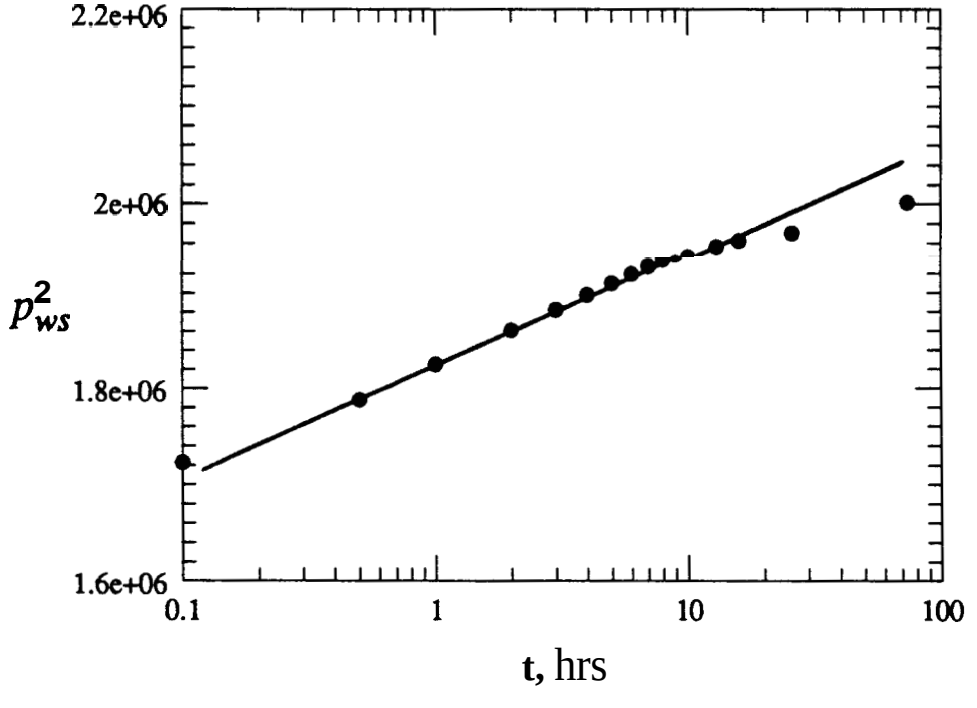

Figure 4.15: A buildup following a drawdown test of small pressure drop in systems of low volatility

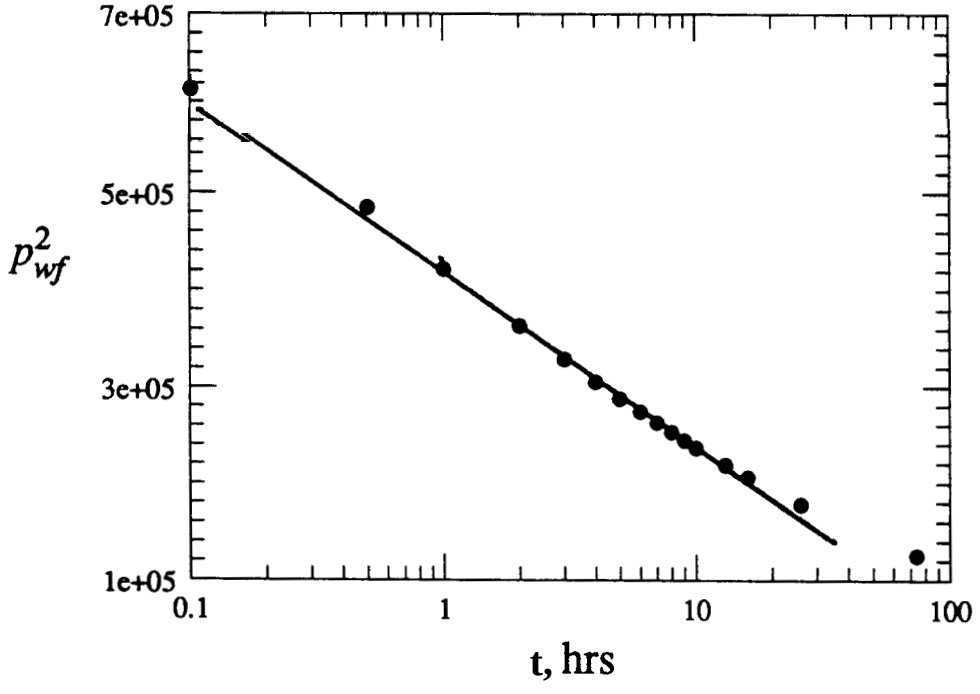

Figure 4.16: **First drawdown of large pressure drop in systems of low volatility, Test No. 1 in Table 4.6**

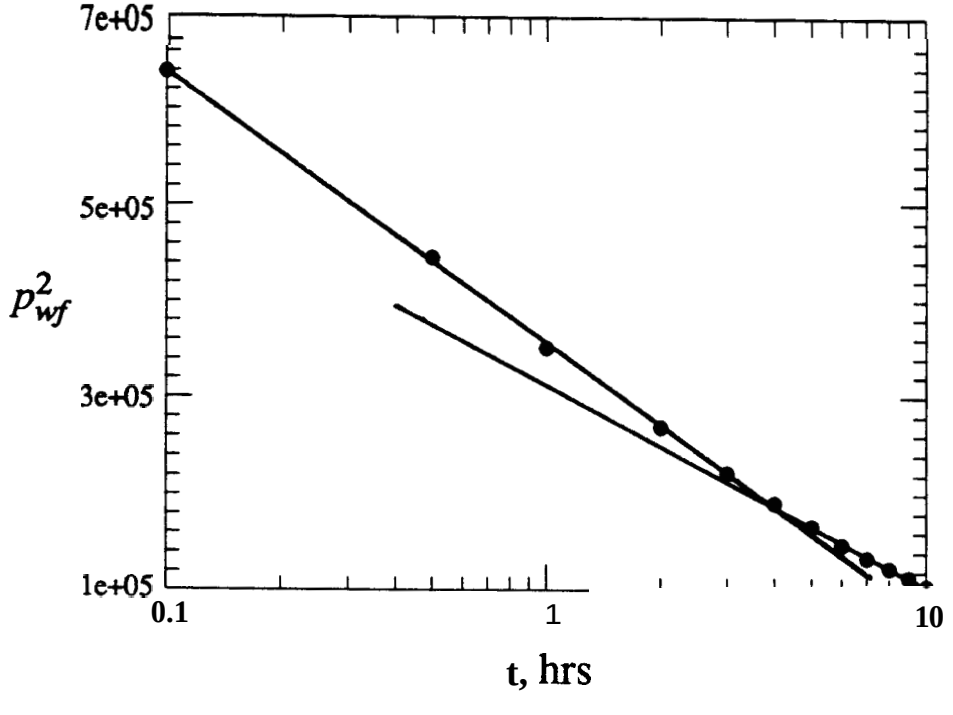

Figure 4.17: Second drawdown of large pressure drop in systems of low volatility, Test No. 2 in Table 4.6

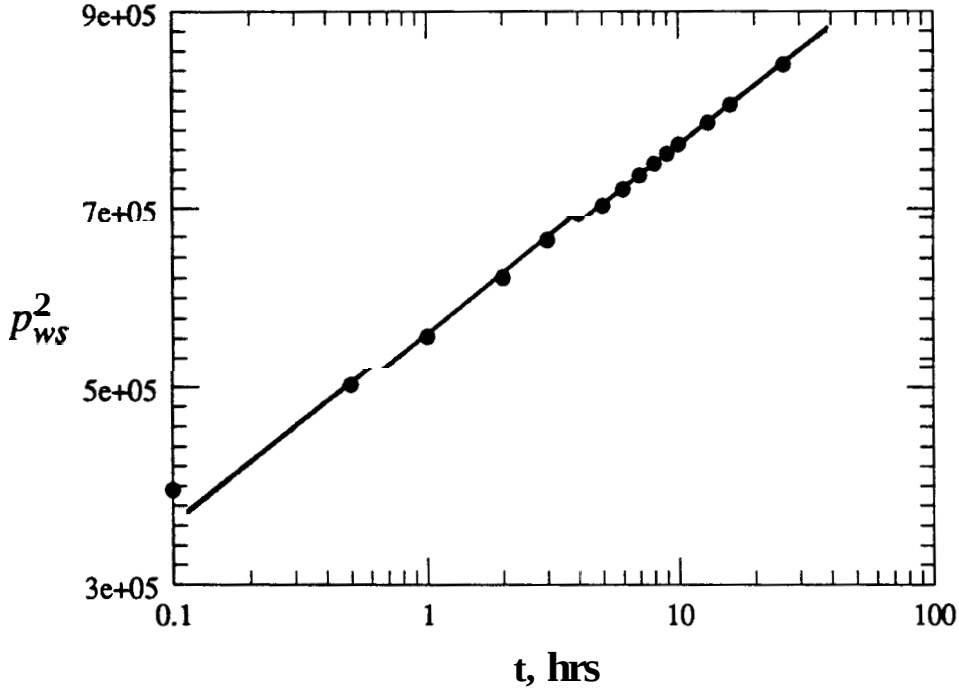

Figure 4.18: First buildup following a drawdown of large pressure drop in systems of low volatility, Test No. 3 in Table 4.6

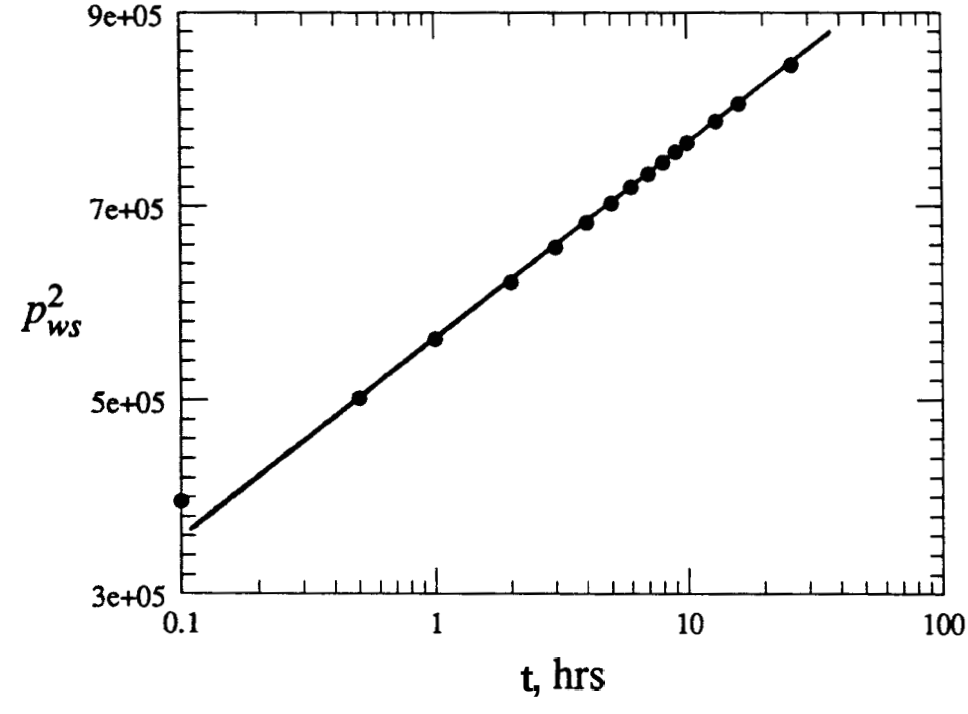

Figure 4.19: Second buildup following a drawdown of large pressure drop in systems of low volatility, Test No. 4 in Table 4.6, Raghavan (1976)

Table 4.7: Effective oil permeabilities for volatile oil systems

Test No.	q_o, STB/D	Input k_o, md	Perrine's Approach k_o, md	New Approach k_o, md
1	1500	5.56	3.50	4.64
2	3000	14.4	11.3	14.42
3	1000	3.66	2.45	3.38
4	2000	5.0	2.92	3.96
5	11000	47.6	37	45.3
6	2000	53	4.16	4.972

Table 4.8: Effective gas permeabilities for volatile oil systems

Test No.	GOR, MSCF/STB	Input k_g, md	Pemne's Approach k_g, md	New Approach k_g, md
1	2.42	0.24	0.5%	0.4 1
2	3.19	4.0	2.29	2.13
3	12.64	0.8	1.01	1.24
4	4.5	0.2	0.429	0.4 1
5	8.5 1	9.6	8.29	9.36
6	1.94	0.24	0.56	0.27

Table 4.9: The wellbore skin for volatile oil systems

Test No.	ϕ	c_t, psi^{-1}	r_w, ft	Input s	Perrine's Approach s	New Approach s
1	0.15	1.19e-04	0.3	0	-0.623	0.00
2	0.2	1.5e-04	0.3	0	-0.37	0.28
3	0.15	4.9e-05	0.3	0	-0.75	0.118
4	0.15	2.3e-05	0.3	0	-1.292	-0.964
5	0.2	1.5e-04	0.3	0	0.83	-1.29
6	0.2	1.16e-04	0.3	0	-0.33	-1.096

Table 4.10 Effective oil permeabilities for drawdowns of small pressure drop and following buildups in systems of low volatiliy

Test No.	q_o, STBP	Input k_o, md	Perrine's Approach k_o, md	New Approach k_o, md
1	400	65	61.09	66.2
2	2000	100	70.01	88.3
3	1000	100	75.64	84.1
4	100	10	8.4	9.18

Table 4.11: Effective oil permeabilities For drawdowns oF large pressure drop and following buildups in systems of low volatility

Test No.	q_o, STBP	Input k_o, md	Perrine's Approach k_o, md	New Approach k_o, md
1	2000	65	45.9	66.3
2	5000	100	46.0	89.5
3	100	3.66	2.9	3.32
4	25	2.8	2.24	2.81

Applications are reported in three categories: (1) tests run in reservoirs of volatile oils, (2) drawdowns of small pressure drop and subsequent buildups in oils of low volatility, and (3) drawdowns of large pressure drop and following buildups in oils of low volatility. Separate tables are presented for each category. These are Tables 4-4, 4-5 and 4-6 respectively. Results from the new method are compared with those from the Penine method and the input values. For volatile oils, Table 4-7 presents oil and Table 4-8 presents gas permeabilities, while Table 4-9 presents the wellbore skin results. For low volatility oils, effective oil permeabilities are given in Table 4-10 for drawdowns of small pressure drop and Table 4-11 for drawdowns of large pressure drop.

Test data were plotted as p^2 versus log t, as shown in Figs. 4.6 to 4.19. The slopes of the semilog straight lines were used in Eqs. 4-39 to 4-42 for effective oil permeabilities, and in Eqs. 4-32 and 4-45 for wellbore skin. Gas permeabilities were evaluated using Eq. 4-43, while water permeabilities were evaluated using Eq. 4-44. For Perrine's approach, oil permeabilities were obtained using Eq. 4-37, while wellbore skins were obtained using Eq. 2-11. For Penine's (1956) approach, the slope used is that of a p versus log t graph.

For all cases studied, the proposed approach seemed to offer a practical way of estimating effective oil pemeabiity to a good accuracy. An improvement over Pemne's approach is evident in Tables 4-9 to 4-11. Figures 4.16 and 4.17, drawdown tests of large pressure drop in oils of low volatility, exhibited more than one semilog slope where the early semilog slope was used here. This behavior of the pressure squared solution was not observed for volatile oil systems, nor for tests of small pressure drop in oils of low volatility. Appendices B and C investigate such behavior in detail.

Based on the cases considered, buildup tests, run in oils of low volatility following large pressure drawdowns exhibited only one semilog slope, Figs. 4.18 and 4.19. These buildup tests seemed to result in more reasonable estimates of effective oil permeabilities than drawdown tests.

4.4.1 Volatility

The volatility defined in this work reflects the amount of gas dissolved in the oil phase. Since oil shrinks as gas comes out of solution, the following parameters are related to volatility:

1) bubble point pressure, p_b

2) solution gas-oil ratio, R_s

3) formation volume factor, B_o.

The two sets of PVT data for volatile oils used in this study had the following values: B_o was 1.806 and 1.85001 RB/STB, R_s was 1.45 and 1.50 MSCF/STB, and p_b was 4514.7 and 5703 psi. The two sets of PVT data for oils of low volatility had the following values: B_o was 1.278 and 1.189 RB/STB, R_s was 0.38 and 0.27 MSCF/STB, and p_b was 1500 and 1275 psi.

Two more sets of PVT data were used, one for the volatile oil given in Table 4.12 and the other for the oil of low volatility given in Table 4.13. The volatile oil has the following properties: B_o is 1.909 RB/STB, R_s is 1.315 MSCF/STB and p_b is 2900 psi. The oil of low volatility has the following properties: B_o is 1.44 RB/STB, R_s is 0.75 MSCF/STB and p_b is 2800 psi. Each of these two data sets was used to simulate two drawdown tests, one with a large and the other with a small pressure drop. These simulated tests were analyzed using Eq. 4-39 for both drawdown tests of volatile oil, Eq. 4-41 for the drawdown of large pressure drop and Eq. 4-39 for the drawdown of small pressure drop in oils of low volatility.

The test data for two drawdown tests, simulated using the first PVT data set, were plotted in Figs. 4.20 and 4.21. The results obtained were compared to the input values in Table 4-14. Similarly, the tests simulated using the second PVT data set were plotted in Figs. 4.22 and 4.23, with results compared to input values in Table 4-15. In general reasonable agreements were achieved using the proposed solutions.

Table 4.12: The *set* of PVT data for the oil of high volatility index

p, psia	B_g, RB/MSCF	μ_g, cp	R_s, MSCF/STB	B_o, RB/STB	μ_o, cp
100.0			0.277	1.331	0.5284
193.14	17.8	0.01 13			
300.0			0.339	1.368	0.5046
622.48	3.38	0.0125			
700.0			0.463	1.442	0.457
1051.8	285	0.0138			
1100.00			0.587	1.5 16	0.4094
1481.17	1.959	0.0152			
1500.0			0.71 1	1.59	0.3618
1910.5	1.46	0.0166			
2100.0			0.927	1.707	0.295
2339.9	1.175	0.0181			
2500.0			1.105	1.7%	0.2639
2769.35	0.997	0.0195			
2900.0			1.315	1.909	0.2403
3100.0			1.315	1.905	0.2405
3198.7	0.873	**0.021**			

Table 4.13: The set of PVT data for the oil of low volatility

p, psi		μ_g, cp	R_s, MSCF/STB	B_o, Rb/STB	μ_o, cp
193.14	17.8	0.01 13			
500.0			0.13	1.12	0.92
622.48	3.38	0.0125			
700.0			0.18	1.14	0.84
1051.8	2.85	0.0 138			
1300.00			0.33	1.23	0.65
1481.17	1.959	0.0 152			
1500.0			0.36	1.25	0.62
1910.5	1.46	0.0166			
2000.0			0.51	1.33	0.52
2339.9	1.175	0.0181			
2500.0			0.68	1.4	0.45
2769.35	0.997	0.0195			
2800.0			0.75	1.44	0.43
3100.0			0.75	1.43	0.44
3198.7	0.873	0.021			

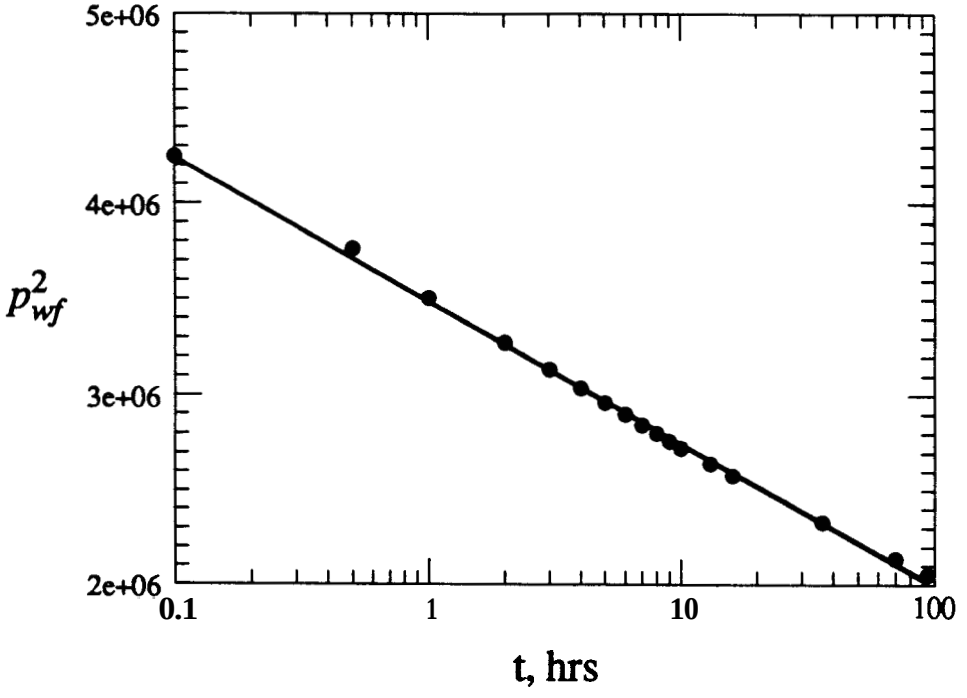

Figure 4.20: A drawdown test of large pressure drop simulated in oils of high volatility

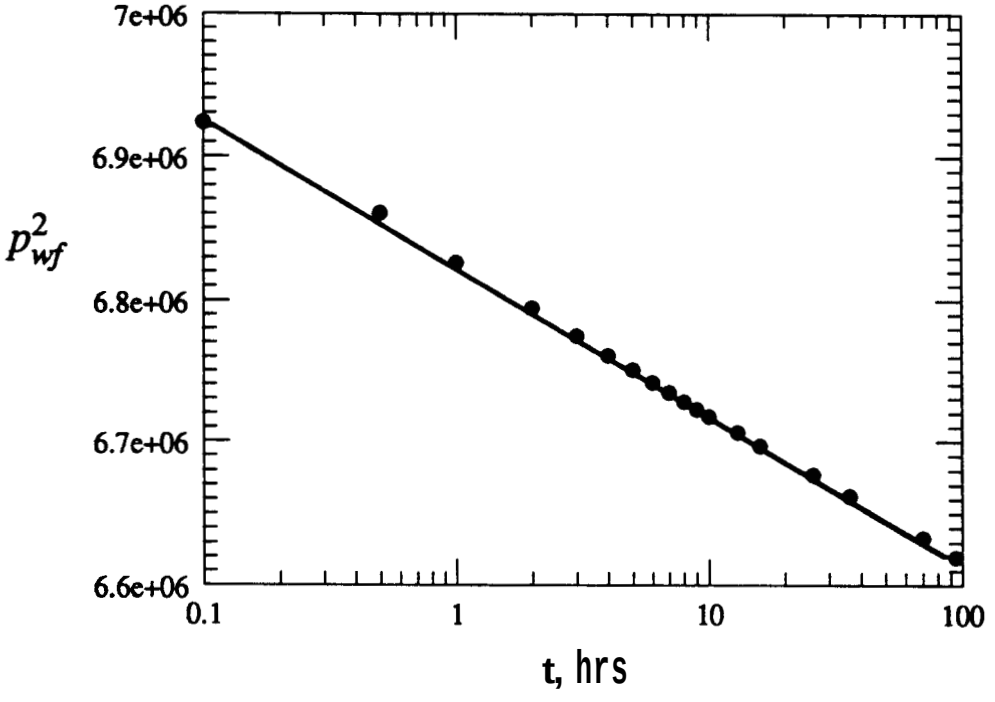

Figure 4.21: A drawdown test of small pressure drop simulated in oils of high volatility

Table 4.14: Effective oil permeabilities for the volatile oil

Test	q_o, STB/D	h, ft	p_i, psi	S_{gi}	Input k_o, md	Resulting k_o, md
high drawdown	8000	100	2700	10%	40	41.8
low drawdown	1000	100	2700.0	10%	40	37.6

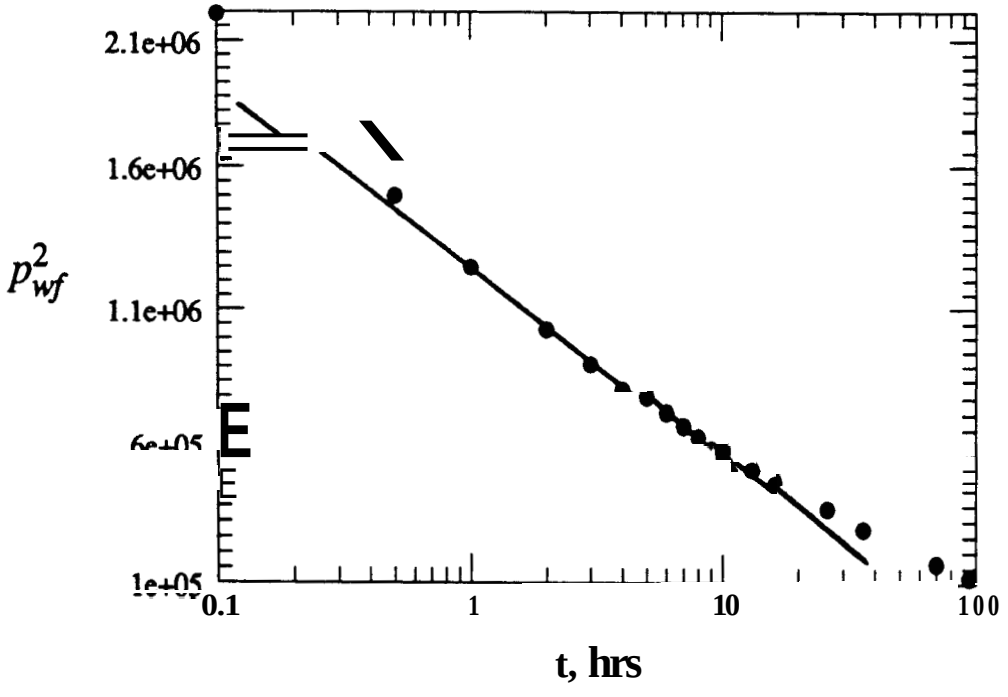

Figure 4.22: **A drawdown test** of **large pressure drop simulated in** oils **of low volatility index**

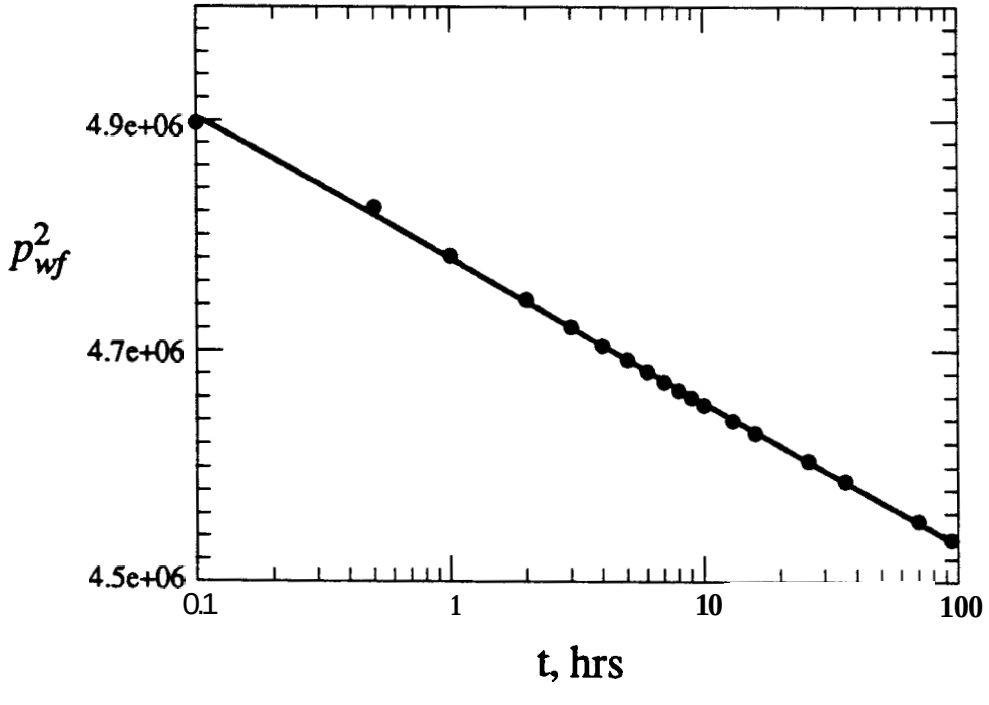

Figure 4.23: **A drawdown test** of small **pressure drop simulated in** oils of **low volatility index**

Table 4.15: Effective oil permeabilities for the oil of low volatility

Test	q_o, STB/D	h, ft	p_i, psi	S_{gi}	Input k_o, md	Resulting k_o, md
high drawdown	8000	100	2300	10 %	40	41.6
low drawdown	1000	100	2300	10 %	40	31.7

The following range of volatility parameters was investigated in this work. The values of p_b ranged from 3100 to 5703 psi for volatile oils and from 1275.0 to 2800.0 psi for oils of low volatility. The values of B_o ranged from 1.806 to 1.909 RB/STB for volatile oils and from 1.189 to 1.44 RB/STB for oils of low volatility. The values of R_s ranged from 1.315 to 1.50 MSCF/STB and from 0.27 to 0.75 MSCF/STB for oils of low volatility. The values of the bubble point pressure were very close in range for both oils, while those of the solution gas-oil ratio, R_s were very wide in range. This may suggest the use of R_s or B_o value at the bubble point pressure as an index value. Such a recommendation needs to be investigated in future work.

4.5 Discussion of Perrine's Approach

Although much of the literature on multiphase well testing deals with Perrine's (1956) approach, an important aspect concerning the inner boundary condition (constant oil rate) has not been considered. Perrine's solutions reported in the literature estimate effective phase permeabiities, using the following equation:

$$k_l = \frac{162.6\, q_l\, \mu_l\, B_l}{m^*\, h} \tag{4-46}$$

Martin (1959) linearized the multiphase diffusivity equation in terms of pressure. However, the linearization of the inner boundary condition, Eq. 4-27, has not been discussed. Assuming $\frac{k_o}{p_o B_o}$ of Eq. 4-27 to be constant throughout a test, the inner boundary condition is linearized as follows:

$$\lim_{r \to r_w} \left[r \frac{\partial p}{\partial r} \right] = \frac{q_o\, \mu_o\, B_o}{2\, \pi\, k_o\, h} \tag{4-47}$$

Martin's difisivity equation can be solved using this linear inner boundary condition to obtain Perrine's solutions, Eq. 4-46.

The assumption that $k_o / (\mu_o B_o)$ is constant through the test holds well for oil-water systems with no gas flowing in the reservoir or water coning into the wellbore. A simulation run in an oil-water system showed a negligible change of this term through the test, see Fig. 4.24. Thus, Penine's approach is applicable to oil-water systems provided no gas is flowing and no water is coning. Figure 4.25 shows a semilog plot of pressure versus time for a drawdown test in an oil-water system. When the semilog slope of Fig. 4.25 was used in Pemne's solution, Eq. 4-46, it resulted in a 395.64 md-ft oil permeability thickness compared to its input value of 388.0 md-ft, The same test is analyzed utilizing the new approach and presented in Section 4.6. Since the new approach only applies to systems with gas phase present, Perrine's approach is superior for application in oil-water systems.

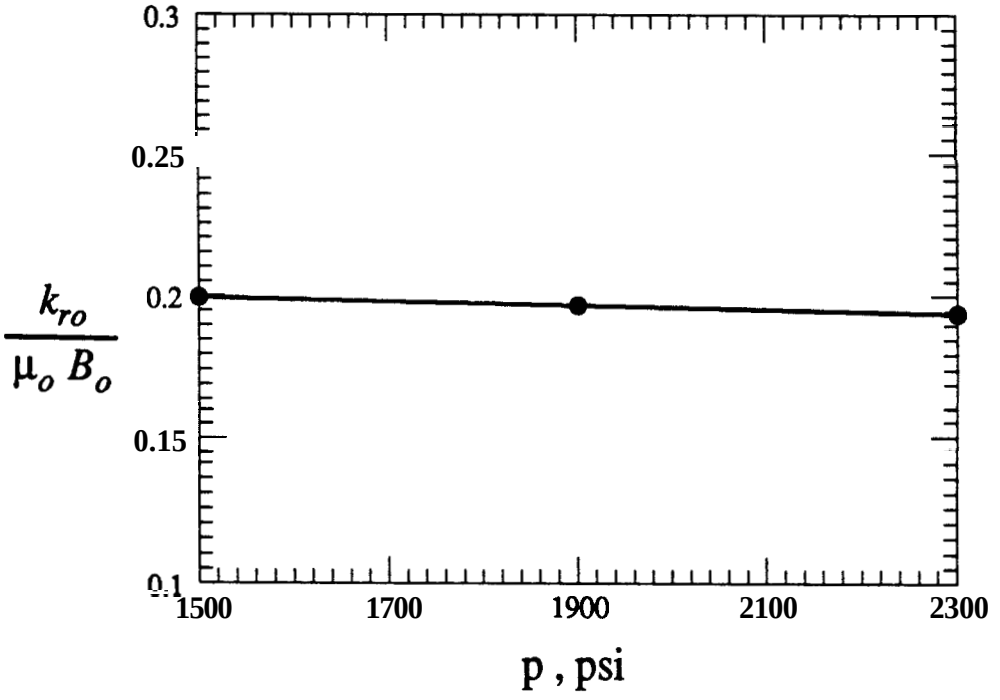

Figure 4.24: k_{ro} / ($\mu_o B$,) vs. p (r_w , t) of a simulated drawdown test for an oil-water system with no flowing gas.

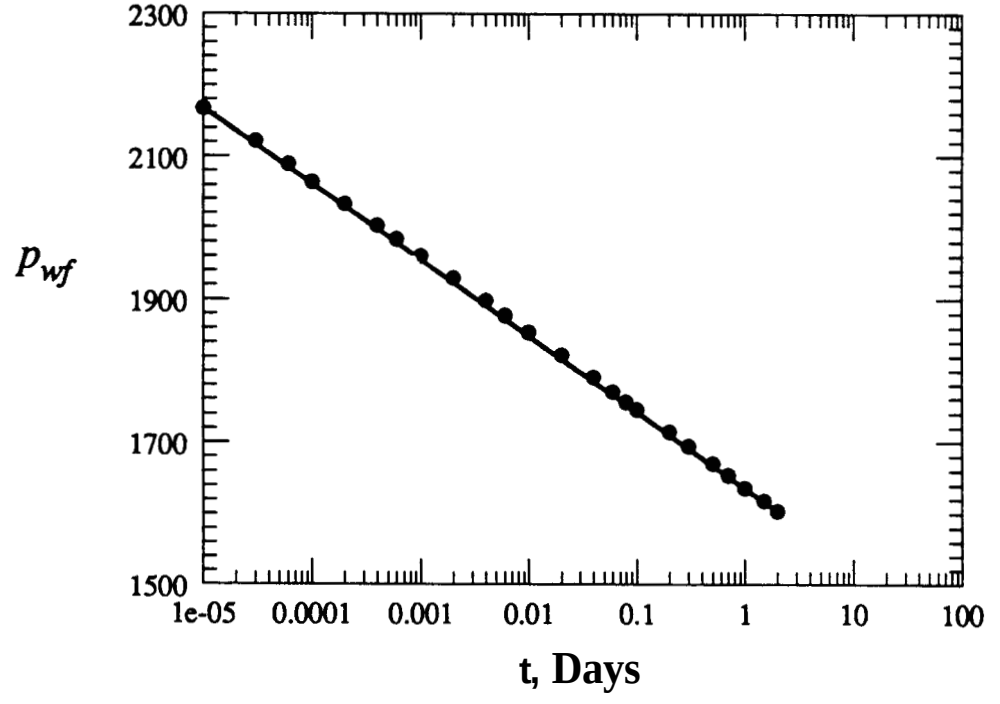

Figure 4.25: A drawdown test for a simulated oil-water system with no flowing gas (p vs. log t).

For systems in which gas phase is present, the necessary assumption for Pemne solution, 4-46, that the $k_o / (\mu_o B_o)$ is constant through the test is invalid. Simulation runs (Figs. 4.3 and 4.4) showed that the change of $\frac{k_o}{p_o B_o}$ is approximately linear with pressure in gas-oil and gas-oil-water systems (Figures in Appendix B show that the highest $k_o / (\mu_o B_o)$ value is at the initial reservoir pressure). The well pressure measured throughout the test is always lower than the initial pressure. Hence, if a constant value of $k_o /(\mu_o B_o)$ is used, the estimated effective oil permeability would be that at a pressure much lower than *the* initial pressure. Such k_o corresponds to the stabilized oil saturation in Fig. 4.2, which is less than the correct k_o that corresponds to the average reservoir saturation. Hence, Pemne's (1956) solution may underestimate effective oil penneabilities, as investigated later.

Perrine's solution for effective oil permeability is a special *case* of the more general approach proposed here. The first approach to evaluate the empirical slope. a, reduces the new solution to Eq. 4-37, which is almost identical to Pemne's solution, Eq. 4-46.

In this work, Penine's (pressure) approach was also tested for flow rate effects. Two drawdown tests were simulated in a gas-oil system. Keeping the system properties identical for both tests, the only difference was the flow rate. The oil rate of the first test was 1000 STB/D, while the oil rate of the second test was 5000 STB/D. The pressure responses are plotted in Figs. 4.26 and 4.27 respectively. Fig. 4.26, for the low rate test, exhibits a single semilog straight line with the correct slope. On the other hand, Fig. 4.27, for the high rate test, exhibits two semilog straight lines with a long transition period, which might be seen to be indicative of a no-flow boundary. Neglecting the first slope, which will probably be masked by wellbore storage, the second slope was used for analysis here. Results from this test were compared to those of the first test as well as with input values in Table 4.16. The results were far from the input values for the high flow rate. These two tests simulated in systems where gas phase was present, as well as many others presented in Appendix C, demonstrates that Pemne's approach is rate sensitive and appears to hold better at low rates.

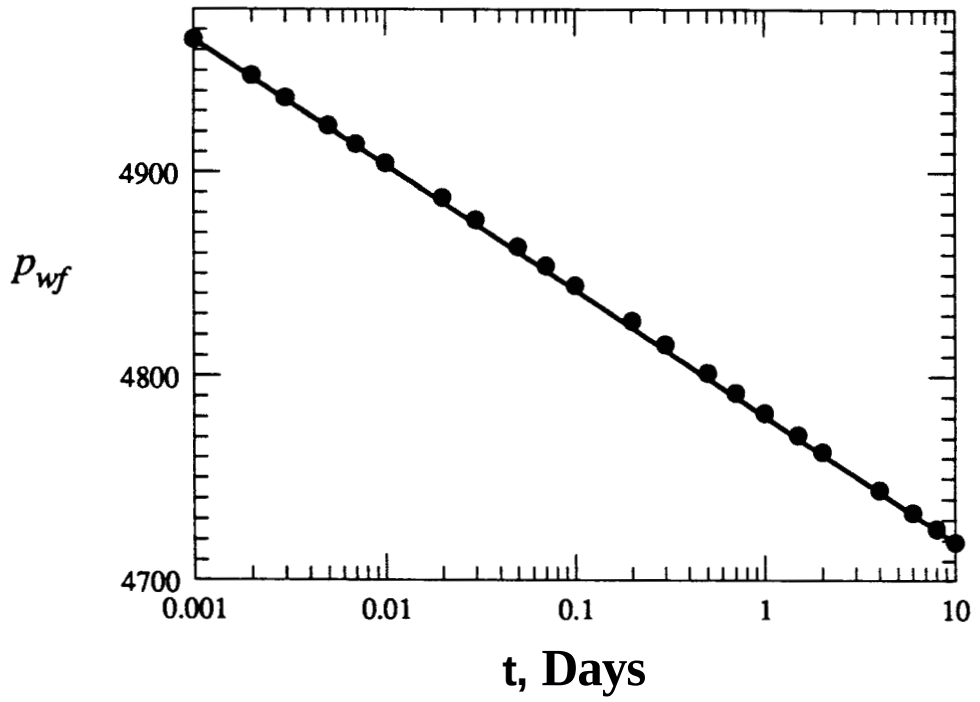

Figure 4.26: A drawdown test with a flow rate of 1000 STB/D.

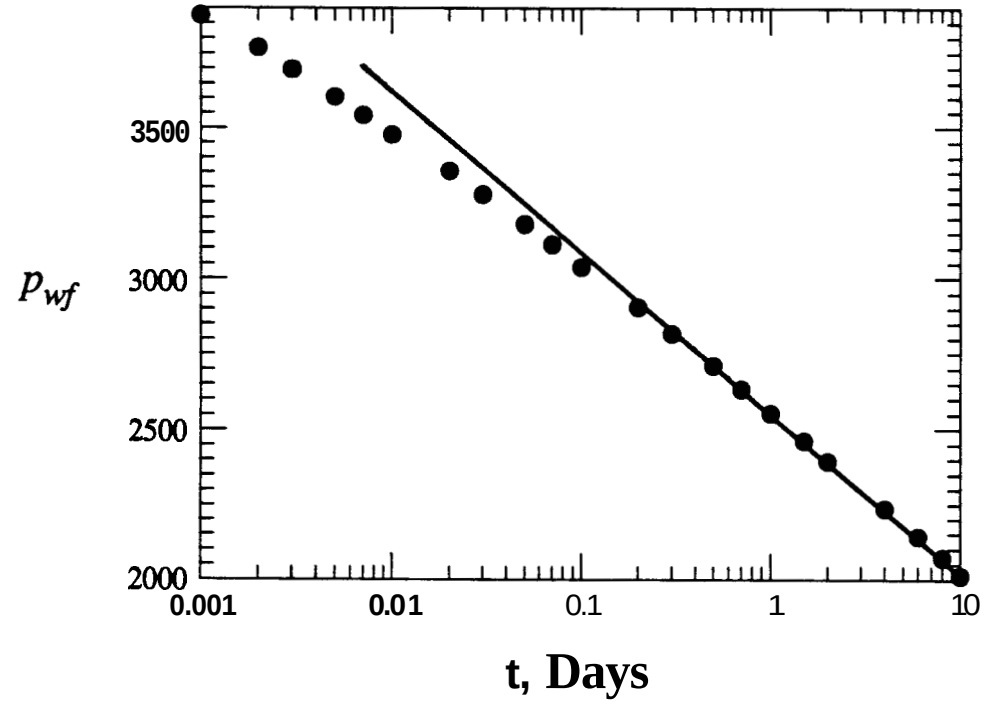

Figure 4.27: A drawdown test with a flow rate of 5000 STB/D.

4.6 Discussion of the new approach

The new approach is based on the assumption that $k_o / (\mu_o B_o)$ changes linearly with pressure. Simulation runs validated this assumption for systems in which gas phase was present (see Figs. 4.3 and 4.4, also Appendix B). For oil-water systems with no gas flowing, simulation runs showed a negligible change of $k_o / (\mu_o B_o)$ with pressure through the test (Fig. 4.24), thus breaking the basis of the new approach. An example test in oil-water systems, plotted in Fig. 4.25 in terms of p, was plotted in Fig. 4.28 in terms of p^2. While Fig. 4.25 exhibited only the correct slope, Fig. 4.28 exhibited two semilog slopes where the first slope resulted in the correct oil permeability thickness product of 382.55 md-ft and the second slope resulted in an overestimated product of 439.4 md-ft. The occurrence of two semilog slopes indicates that the new approach does not represent the physics of flow in oil-water systems for which the change of $k_o / (\mu_o B_o)$ is negligible with pressure. Thus, the Pemne (1956) method is superior for applications in oil-water systems.

The linear change of $k_o / (\mu_o B_o)$ with pressure is pronounced in gas-oil and gas-oil-water systems. As investigated in Section 4.3, there exist several choices for evaluating the empirical slope, a of this linear relation. The first choice applied in Section 4.3 reduced the new solution to Pemne's solution, Eq. 4-37, which may result in an underestimate of effective oil permeability. This underestimation caused by the first choice suggested the need to apply other choices where higher pressures were used to evaluate the empirical slope, a. In order to choose an appropriate pressure, different sets of PVT data for both volatile and low volatile oils were used to simulate several drawdown and buildup tests. When these tests were analyzed, the appropriate pressure at which to evaluate the empirical slope was found to be different for different oils. These different pressures are discussed in the following section.

For volatile oils, the use of initial pressure for drawdowns and average pressure for buildups gave good results. The same pressure was also appropriate for drawdowns of small pressure drop, or following buildups in oils of low volatility. However, use of these pressures was

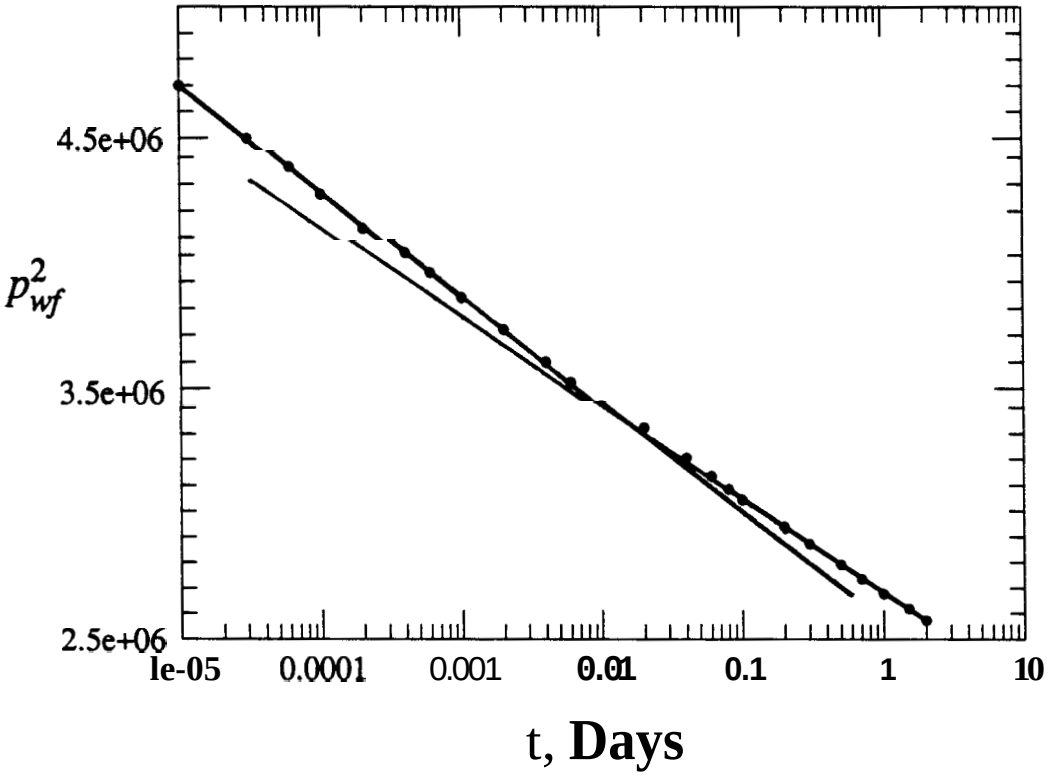

Figure 4.28: A drawdown test fora simulated oil-water system with no flowing gas (p^2 vs. log t), Fig. 4.25.

found to overestimate effective oil permeability for tests with large pressure drops in oils of low volatility. Instead, the following pressures were found to work:

for drawdowns of large pressure drop: p_{wf} ($t = 0.1\ hr$),

for following buildups: p_{ws} ($\Delta t = 10.0\ hr$).

The times at which these pressures were chosen could not be related to the permeability of the system.

The new approach was also tested for flowing rate effects. The two drawdown tests, run in volatile oils and considered in Section 4.5, were also analyzed using the proposed method. The rate of the first test was 1000 STB/D, while the rate of the second test was 5000 STB/D. The responses are plotted in terms of p^2 in Figs. 4.29 and 4.30, respectively. Figure 4.29 corresponds to Fig. 4.26, and exhibits a single semilog straight line with the correct slope. On the other hand, Fig. 4.30 corresponds to Fig. 4.27. Interestingly enough, Fig. 4.30 in terms of p^2, exhibits only a reasonable single slope over most of the test, while Fig. 4.27, in terms of p, showed two semilog straight lines with a long intermediate transition period. Both tests yielded reasonable results when analyzed using the new approach, as can be seen in Table 4-17. Figure 4.30 began to exhibit a slightly lower slope by the end of the test. However, this bending was slight, unlike the continuous bending of the pressure curve in Fig. 4.27.

For systems of low volatility, both the pressure and the pressure squared approaches were found to be rate sensitive and applied better at low flowing rates. The reason behind this behavior is discussed extensively in Appendix B. Illustrative examples are presented in Appendix C.

For all tests studied in gas-oil and gas-oil-water systems, Penine's approach appeared to be flow rate sensitive and applied better at low flow rates, while the new approach was only sensitive to rates in systems of low volatility. The pressure squared approach was insensitive to flowing rate for volatile oil systems. Appendix C elaborates on this observation, and shows a new rate-normalization method in terms of p^2 applicable to multiphase well tests of varying flow rates.

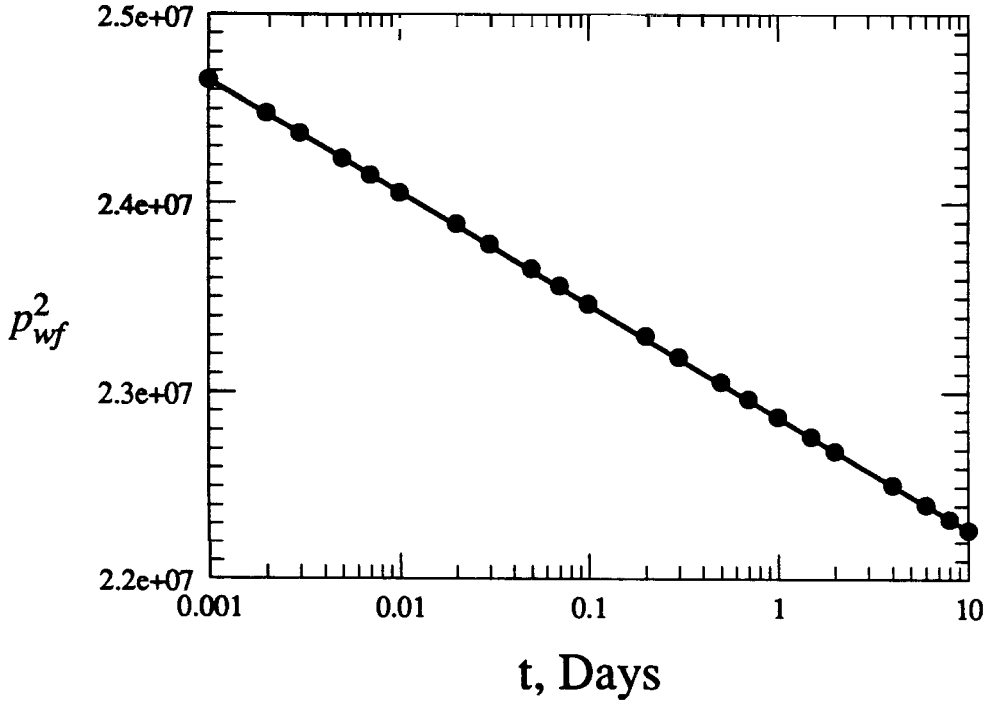

Figure 4.29: A drawdown test with a flow rate of 1000 STB/D, (Fig. 4.26)

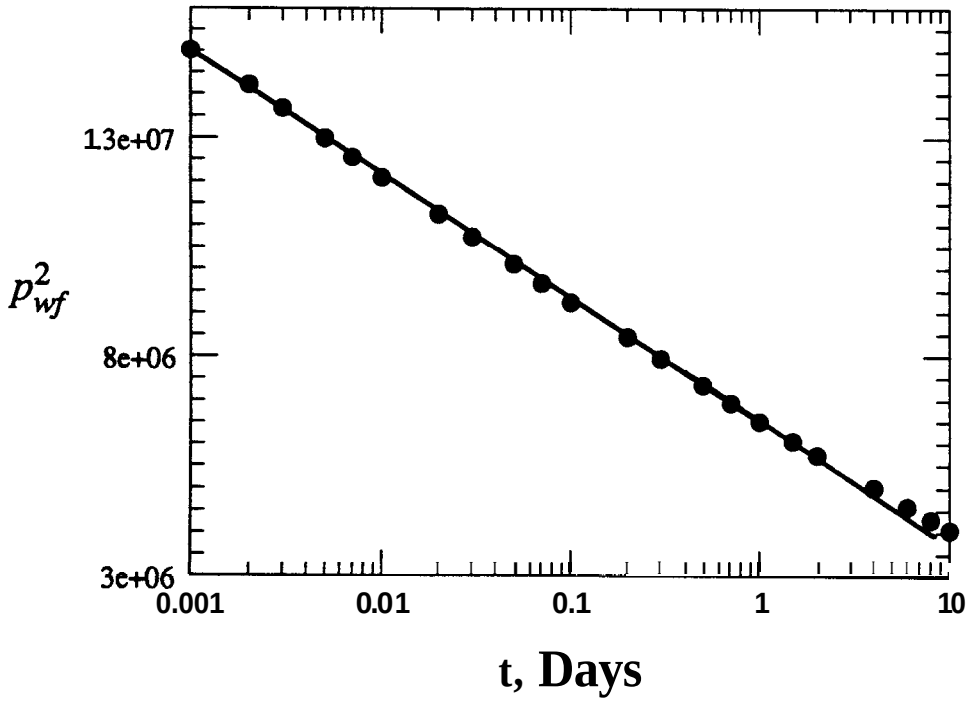

Figure 4.30: A drawdown test with a flow rate of 5000 STB/D, (Fig. 4.27)

Table 4.16: Results of drawdown tests analyzed using Perrine's approach

Input	$k_o h$ = 1542.5 md-ft
Results for q_o = 1000 STBP	$k_o h$ = 1412.7 md-ft
Results for q_o = 5000 STB/D	$k_o h$ = 813.6 md-ft

Table 4.11: Results of drawdown tests analyzed using the new approach

Input	$k_o h$ = 1542.5 md-ft
Results for q_o = 1000 STB/D	$k_o h$ = 1527.0 md-ft
Results for q_o = 5000 STB/D	$k_o h$ = 1632.1 md-ft

initial condition:

$$p^2(r,t) = p_i^2 \qquad \text{for } t = 0, \text{ for all } r, \tag{4-52}$$

outer boundary:

$$\left(\frac{\partial p^2}{\partial r}\right)_{r_e} = 0 \qquad \text{for all } t, \tag{4-53}$$

inner boundary, (constant oil rate):

$$\left[r\left(\frac{k\,k_{ro}}{\mu_o B_o}\right)\frac{\partial p}{\partial r}\right]_{r_w} = \frac{q_o}{2\pi h} \qquad \text{for } t > 0. \tag{4-54}$$

In order to linearize the inner boundary condition, the assumption of a linear $\left(\frac{k_o}{\mu_o B_o}\right)$ versus p relation is made:

$$\left(\frac{k_o}{\mu_o B_o}\right) = a\,p \tag{4-55}$$

Here a is an empirical slope, which can be evaluated at $\bar{p}$ such (hat:

$$a = \left(\frac{k_o}{\mu_o B_o}\right)_{\bar{p}} \frac{1}{\bar{p}} \tag{4-56}$$

Thereafter, the linearized inner boundary condition can be rewritten as:

$$\left[r\,\frac{\partial p^2}{\partial r}\right]_{r_w} = \frac{q_o\,\overline{\mu_o B_o}\,\bar{p}}{\pi\,\bar{k}_o\,h} \tag{4-57}$$

where $\bar{k}_o$ corresponds to $\bar{p}$.

Following the derivation of the pseudosteady state solution in terms of p reported in the literature, Eq. 4-25 was solved for the initial and boundary conditions given in Eqs. 4-52, 4-53 and 4-57. The solution obtained is:

4.7 Fetkovich's Isochronal Testing Approach

This section derives Fetkovich (1973) empirical approach for isochronal oil well testing. Based on empirical results, Fetkovich suggested that the deliverability curve for solution gas-drive systems follows the relation:

$$q_o = J_o' (\bar{p}^2 - p_{wf}^2)^n \tag{4-48}$$

Here J_o' is the back-pressure curve coefficient of a well producing under solution gasdrive, and n is an exponent.

The pseudosteady state behavior may not develop in gas-oil systems. Nevertheless, the pseudosteady state solution of the oil-gas diffusivity equation in terms of p^2 was found necessary to derive the Fetkovich relation, Eq. 4-48. This solution was developed following the pressure solution derivation. reported in the monograph by Matthews and Russell (1967). for a closed reservoir producing at a constant oil rate

The oil-gas diffusivity equation in terns of p^2 is:

$$\nabla^2 p^2 = \frac{\phi c_t}{\lambda_t} \frac{\partial p^2}{\partial t} \tag{4-49}$$

where c_t is the total system compressibility of oil-gas system (from Eq. 4-13):

$$c_t = = - \frac{S_o}{B_o} \frac{dB_o}{dp} + \frac{S_o B_g}{B_o} \frac{dR_s}{dp} - \frac{S_g}{B_g} \frac{dB_g}{dp}$$

$$+ \frac{1}{\phi} \frac{d\phi}{dp} \tag{4-50}$$

and

$$\lambda_t = \frac{k_o}{\mu_o} + \frac{k_g}{\mu_g} \tag{4-51}$$

The initial and boundary conditions for a closed outer boundary system producing at a constant oil rate are:

$$p_{wf}^2 = p_i^2 - \frac{q_o \overline{\mu_o B_o} \bar{p}}{\pi \bar{k}_o h} \left[\frac{2 t_D}{r_{eD}^2} + \ln r_{eD} - \frac{3}{4} \right] \tag{4-58}$$

This pseudosteady state solution applies at the wellbore for $r_e \gg r_w$ and for large t_D. This solution may be expanded to:

$$p_{wf}^2 = p_i^2 - \frac{q_o \overline{\mu_o B_o} \bar{p}}{\pi \bar{k}_o h r_e^2} \frac{2 \lambda_t t}{\phi c_t}$$

$$- \frac{q_o \overline{\mu_o B_o} \bar{p}}{\pi \bar{k}_o h} \ln \left[\frac{0.472 r_e}{r_w} \right] \tag{4-59}$$

In order to reduce Eq. 4-59 to the Fetkovich empirical relation, the term $\bar{p}^2$ has to be introduced in the derivation. This could be done assuming the following equation holds:

$$\bar{p}^2 = p_i^2 - \frac{q_o t}{\pi r_e^2 \phi c_t h} \left[\frac{2 \overline{\mu_o B_o} \lambda_t \bar{p}}{\bar{k}_o} \right] \tag{4-60}$$

Equation 4-60 is a material balance equation for oil-gas systems whose basis is discussed in Section 4.8. To better understand this material balance equation, it may be rewritten as:

$$\left[p_i + \bar{p} \right] = \frac{q_o \overline{B_o} t}{\pi \phi c_t h r_e^2} \frac{\lambda_t}{\bar{\lambda}_o} \frac{2 \bar{p}}{\left[p_i - \bar{p} \right]} \tag{4-61}$$

For single-phase flow reservoirs, the material balance equation is:

$$\left[p_i - \bar{p} \right] = \frac{q_o \overline{B_o} t}{\pi \phi c_t h r_e^2} \tag{4-62}$$

For solution gas-drive reservoirs, the left hand side of Eq. 4-62 will be larger than the right hand side due to the evolution of gas. This evolved gas restricts oil flow, thus consuming additional pressure energy to move the same amount of oil. At the same time the evolved gas increases the total compressibility of the system, c_t. Therefore, the value of the first part of the right hand side term of Eq. 4-61 is less than unity. On the other hand, the $\lambda_t / \bar{\lambda}_o$ term always has a value greater than unity for two-phase reservoirs. If the second part of the right hand

side of Eq. 4-61 is multiplied by the first part, the result may be less, equal to or greater than unity. This value must be greater than unity because $\left[2\,\bar{p}\right]$ on the right side of Eq. 4-61 is less than $\left[p_i + \bar{p}\right]$ on the left side of the same equation. Such a condition will not be satisfied in all cases. Hence, when the material balance equation given by Eq. 4-60 does not hold, the exponent, n, of Fetkovich relation will differ from unity.

Equation 4-60 is substituted in Eq. 4-59 to obtain:

$$p_{wf}^2 = \bar{p}^2 - \frac{q_o \overline{\mu_o B_o}}{2\pi k h}\left[\frac{2\,\bar{p}}{\bar{k}_{ro}}\right] \ln\left(\frac{0.472\, r_e}{r_w}\right) \tag{4-63}$$

Here $\bar{k}_{ro}$ is the relative permeability corresponding to $\bar{p}$.

The rate term can be expressed as:

$$q_o = \frac{2\pi k h}{\ln\left(\frac{0.472\, r_e}{r_w}\right)}\left[\frac{\bar{k}_{ro}}{2\,\overline{\mu_o B_o}\,\bar{p}}\right]\left[\bar{p}^2 - p_{wf}^2\right] \tag{4-64}$$

Equating Eq. 4-64 with the Fetkovich empirical relation, Eq. 448, the following relation is obtained:

$$J_o' = \frac{2\pi k h}{\ln\left(\frac{0.472\, r_e}{r_w}\right)}\left[\frac{\bar{k}_{ro}}{2\,\overline{\mu_o B_o}\,\bar{p}}\right] \tag{4-65}$$

Equation 4-65 defining J_o' is identical to Eq. (A-21) of the Fetkovich paper (1973). The present derivation emphasizes the inherent oil-gas material balance equation given by Eq. 4-60, which was implicit in Fetkovich's approach. When this material balance equation is reasonable, the exponent n becomes unity, provided non-Darcy flow is negligible. On the other hand, if this equation is not appropriate, n will differ from unity, and may also vary with time. This is in agreement with simulation results reported by Camacho and Raghavan (1987) for Darcy flow systems, which demonstrated that the exponent n may be a function of time.

In summary, Fetkovich's empirical relation for solution gas-drive systems was derived in this work using a gas-oil material balance equation. Furthermore, it is intuitive that the same approach may be extended to three-phase reservoirs based on the three-phase diffusivity equation in terms of p^2. The derivation follows exactly the same steps, but with total Compressibility defined by Eq. 4-13, and total mobility defined by Eq. 4-16. The material balance equation, expressed in Eq. 4-60, has to hold for the three-phase derivation in terms of three-phase c_t and λ_t. It appears that this observation has not been reported previously in the literature.

4.8 Fetkovich's Material Balance Relation

The oil-gas material balance equation given by Eq. 4-60, necessary to derive Fetkovich isochronal testing approach, has an empirical basis. Fetkovich (1980) reported an empirical material balance relation for forecasting the performance of solution gas-drive reservoirs. This relation can be written as:

$$\bar{p}^2 = - \left(\frac{\bar{p}_i^2}{N_{p\,i}}\right) N_p + \bar{p}_i^2 \qquad (4\text{-}66)$$

Here $\bar{p}_i$ is the average reservoir pressure at initial condition, which is referred to as p_i in this work; N_p is cumulative oil production; and $N_{p\,i}$ is the cumulative oil production to a reservoir shut-in pressure of zero psia. This relation is identical to Eq. 27 of the Fetkovich paper (1980). Fetkovich empirical relation, Eq. 4-66, can also be expressed as:

$$N_p = Constant \times (p_i^2 - \bar{p}^2) \qquad (4\text{-}67)$$

The material balance equation given by Eq. 4-60 can be related to the empirical relation of Eq. 4-67. Equation 4-60, can be rewritten as:

$$q_o\, t = \frac{(\pi \phi h r_e^2)}{2} \left\{ \frac{\bar{k}_o\, c_t}{\overline{\mu_o B_o}\, \bar{p}\, \lambda_t} \right\} (p_i^2 - \bar{p}^2) \qquad (4\text{-}68)$$

Considering the linear change of $k_o / (\mu_o B_o)$ with pressure, Eq. 4-56, and assuming that c_t / λ_t is constant throughout the production period, Eq. 4-68 reduces to Eq. 4-67. That is the material balance equation given by Eq. 4-60 becomes identical to that proposed by Fetkovich based on empirical observation and given by Eq. 4-67.

4.9 Pressure-Saturation Relations

The pressure-saturation relations, derived by Muskat (1949) and Martin (1959), are rederived here, and their assumptions are explicitly demonstrated. Muskat found that the following pressure-saturation relation applies for tank models:

$$\frac{dS_o}{dp} = \frac{\lambda_o}{\lambda_t} c_t - S_o (c_o + c_f) \tag{4-69}$$

where:

$$c_f = \frac{1}{\phi} \frac{d\phi}{dp},$$

$$c_o = - \frac{1}{B_o} \frac{dB_o}{dp}$$

The same relation was derived by Martin assuming negligible pressure and saturation gradients.

The derivation presented here offers another view of this simple relation. Phase saturations are assumed to be only pressure dependent. Using this assumption, Eq. 4-1 for oil flow can be expanded to:

$$\nabla \left[\frac{k_o}{\mu_o B_o} \right] . \nabla p = - \frac{k}{\mu_o B_o} \nabla^2 p$$

$$+ \left[\frac{S_o}{B_o} \frac{d\phi}{dp} - \frac{\phi S_o}{B_o^2} \frac{dB_o}{dp} + \frac{\phi}{B_o} \frac{dS_o}{dp} \right] \frac{\partial p}{\partial t} \tag{4-70}$$

This equation can be substituted into Eq. 4-18 as:

$$\phi c_t \frac{\partial p}{\partial t} = \lambda_t \nabla^2 p$$

$$+ \frac{B_o \mu_o \lambda_t}{k_o} \left[- \frac{k_o}{\mu_o B_o} \nabla^2 p + \left[\frac{S_o}{B_o} \frac{d\phi}{dp} - \frac{\phi S_o}{B_o^2} \frac{dB_o}{dp} + \frac{\phi}{B_o} \frac{dS_o}{dp} \right] \frac{\partial p}{\partial t} \right]$$

$$+ \frac{k_o}{\mu_o B_o} \left[B_g \left[\nabla p . \nabla \overline{GOR} \right] + B_w \left[\nabla p . \nabla \overline{WOR} \right] \right] \tag{4-71}$$

Considering the linear variation of $k_o / (\mu_o B_o)$ with pressure, given by Eq. 4-21, and assuming that $\nabla p^2 \cdot \nabla \overline{GOR}$ and $\nabla p^2 \cdot \nabla \overline{WOR}$ are negligible, Eq. 4-71 reduces to:

$$\frac{\phi c_t}{\lambda_t} \frac{\partial p}{\partial t} = \nabla^2 p$$

$$+ \frac{\mu_o B_o}{k_o} \cdot \left[- \frac{k_o}{\mu_o B_o} \nabla^2 p + \left[\frac{S_o}{B_o} \frac{d\phi}{dp} - \frac{\phi S_o}{B_o^2} \frac{dB_o}{dp} + \frac{\phi}{B_o} \frac{\partial S_o}{\partial p} \right] \frac{\partial p}{\partial t} \right] \qquad (4\text{-}72)$$

which can be rearranged to :

$$\frac{\phi c_t}{\lambda_t} \frac{\partial p}{\partial t} = \frac{1}{\lambda_o} \left[S_o \frac{d\phi}{dp} - \frac{\phi S_o}{B_o} \frac{dB_o}{dp} + \phi \frac{\partial S_o}{\partial p} \right] \frac{\partial p}{\partial t} \qquad (4\text{-}73)$$

or:

$$\frac{\lambda_o c_t}{\lambda_t} = S_o c_f + S_o c_o + \frac{dS_o}{dp}, \qquad (4\text{-}74)$$

which can be rearranged to obtain Eq. 4-69.

A similar water relation was presented by Martin (1959) as follows:

$$\frac{dS_w}{dp} = \frac{\lambda_w}{\lambda_t} c_t - S_w (c_w + c_f) \qquad (4\text{-}75)$$

The same relation *can* be obtained when Eq. 4-18 is combined with the expanded water equation, utilizing the same assumptions involved in deriving the oil saturation equation.

The pressure-saturation equations derived in this section are simple but limited Throughout the derivation, phase saturations were assumed to be functions of pressure only. This assumption applies only during the infinite acting period, as has been shown by Aanonsen (1985) for solution gas-drive reservoirs. Therefore, Eqs. 4-69 and 4-75 are only applicable during the infinite acting period of a transient test.

5. RELATIVE PERMEABILITY TECHNIQUE FOR SOLUTION GAS-DRIVE RESERVOIRS

This section describes a new method to estimate two-phase relative permeabilities in-situ, using pressure transient analysis. The technique requires a short drawdown test, consisting of a number of steps of increasing flow rates. The resulting relative permeabilities reflect the properties of the entire drainage area, rather than those of a small laboratory core. The proposed technique is an improvement over current historical performance methods. These methods require data over long periods of time, yet yield results for a range of saturation to present conditions. Future projections require extrapolation. By contrast, the new method provides estimates of relative permeabilities at sandface saturations, which cover a range of future reservoir conditions. A well test can then be repeated at a later stage of depletion to forecast further into the future.

The proposed technique applies the solution of a multiphase difisivity equation in terms of the pseudopressure function, $m(p)$. The solution has already been reported for constant-rate tests in solution gas-drive reservoirs, see Raghavan (1976) and Bφe et al. (1981). These solutions were superposed to obtain multiple-rate solutions, which formed the basis for the two-phase relative permeability equations. A saturation equation developed originally by Bφe et al. (1981) for solution gas-drive reservoirs was used to estimate sandface saturations during the test.

Typical well tests were simulated over a 40% range in gas saturation, using the ECLIPSE simulator. Analysis of these tests by the proposed method shows good agreement with input relative permeability curves. In cases where relative permeability is not homogeneous within the drainage area, the resulting estimates of relative permeability curves were representative of in-situ heterogeneities.

This section also explains and demonstrates that the relative permeability technique may be used to estimate the absolute permeability of solution gas-drive reservoirs.

5.1 Methodology

Normally, well tests span a short production time, during which average reservoir saturation can be assumed constant. Well test analysis methods proposed by Perrine (1956), Raghavan (1976). or the new method discussed in Section 4 yield only a single effective permeabiity which corresponds to the average reservoir saturation. Contrary to this, the technique proposed here generates a portion of the relative permeability curve over a range of saturations. This is achieved by calculating the relative permeability at the sandface saturation. The sandface saturation changes significantly during a well test, and more importantly, reaches low oil saturations that will not be reached by the average reservoir oil saturation until much later in the life of the reservoir. The new technique is, therefore, a useful forecasting tool in that it is able to estimate relative permeabilities at saturations that will exist in the future.

The basic approach is to create a pressure drawdown at the wellbore which generates an increasing gas saturation at the sandface. The greater the drawdown below the bubble point pressure. the larger the saturation range. Analytical expressions are derived to describe relative permeability changes over the saturation range developed at the sandface. Such expressions utilize an input absolute permeabiity estimated from prior single-phase tests. If estimates of absolute permeability are not available, only effective permeability-saturation results are obtained. However, these results can be used to estimate reservoir absolute permeability as discussed later.

There are several ways to create a wellbore drawdown. This work investigated two different ways. The first was constant-rate drawdown testing, and the second was multiple-rate testing. The theoretical basis of both tests is presented here. However, as will be discussed in Section 5.2.3, it seems that the analysis of a constant-rate drawdown test is often not practical with available instrumentation for monitoring early rate and pressure changes. On the other hand, multiple-rate testing was found to be practical, and may be useful to estimate relative permeabilities for a 10-15% range in gas saturation. Later in this Section, several simulated two-phase multiple-rate tests are presented. When these tests were analyzed, the resulting rela-

tive permeabilities were found to be in good agreement with the input data

Following is the discussion of both constant- and multiple-rate tests and the analysis procedures proposed for their interpretation.

5.2 Constant-Rate Drawdown Testing

Bøe et al. (1981) derived the logarithmic appmximation of the line source solution in terms of $m(p)$ for solution gas-drive reservoirs. Such approximation of the line source solution can be written, in field units, as:

$$m\left(p_{wf}\right) = m\left(p_i\right) - \frac{141.2\, q_o}{kh}\left[0.5\left[\ln t_D + 0.80907 + 2s\right]\right] \tag{5-1}$$

where :

$$t_D = \frac{0.000264\, k\, t}{\phi\, r_w^2\, (c/\lambda)^*} \tag{5-2}$$

$$\left[\frac{c}{\lambda}\right]^* = \frac{1}{\alpha}\left[\dot{\beta}\,\frac{dS_o}{dp} + \beta'\right] \tag{5-3}$$

where α is defined in Eq. 2-23, and β is defined in Eq. 2-24.

For any parameter of two-phase flow, x_2, the following definitions, given in Eqs. 2-25 and 2-26 respectively, hold:

$$\dot{x}_2 = \left[\frac{\partial x_2}{\partial S_o}\right]_p$$

$$x_2' = \left[\frac{\partial x_2}{\partial p}\right]_{S_o}$$

Super dot defines partial derivative of two-phase parameter to oil saturation at constant pressure, and super prime defines partial derivative of two-phase parameter to pressure at constant oil saturation.

5.2.1 Relative Permeability Equations

From Eq. 5-1, the transient response of a constant-rate drawdown test exhibits a semilog line on a $m(p_{wf})$ vs. log t graph.

The slope of the semilog straight line is defined as :

$$slope = \frac{\partial\, m\left(p_{wf}\right)}{\partial \log t} = - \frac{162.6\, q_o}{k\, h} \tag{5-4}$$

which can be written as:

$$\frac{\partial\, m\left(p_{wf}\right)}{\partial\, p_{wf}} \quad \frac{\partial\, p_{wf}}{\partial \log t} = - \frac{162.6\, q_o}{k\, h} \tag{5-5}$$

Since:

$$\frac{\partial\, m\left(p_{wf}\right)}{\partial\, p_{wf}} = \left[\frac{k_{ro}}{\mu_o\, B_o}\right]_{p_{wf}}$$

Eq. 5-5 can be expressed as:

$$\left(k_{ro}\right)_{p_{wf}} = - \frac{162.6\, q_o}{k\, h} \quad \left[\mu_o B_o\right]_{p_{wf}} \quad [*] \tag{5-6}$$

Eq. 5-6 is the oil relative permeability equation which yields k_{ro} at any flowing pressure in tern of the input absolute permeability, and pressure-rate data for the drawdown test. The producing gas-oil ratio, GOR, monitored at flowing bottomhole pressure, p_{wf}, is related to reservoir and fluid parameters through:

$$GOR = R_s + \frac{k_{rg}}{k_{ro}} \quad \frac{\mu_o\, B_o}{\mu_g\, B_g} \tag{5-7}$$

Therefore, the gas relative permeability, k_{rg}, can be evaluated at any flowing pressure using:

$$\left(k_{rg}\right)_{p_{wf}} = \left(GOR - R_s\right)_{p_{wf}} \left(\frac{\mu_g\, B_g}{\mu_o\, B_o}\right)_{p_{wf}} \left(k_{ro}\right)_{p_{wf}} \tag{5-8}$$

5.23 Saturation Equation

Bøe et al. (1981) derived an analytical expression which relates the change of sandface saturation to the flowing bottom-hole pressure. Their relation applies to solution gasdrive reservoirs as long as boundary effects are negligible, and the Boltzman transformation applies. Bøe et al. (1981) relation for the change of oil saturation with pressure is:

$$\frac{dS_o}{dp} = \frac{(aa' - ua')\frac{N}{y} + (ab' - a\beta')}{(a\dot{\alpha} - \alpha\dot{a})\frac{N}{y} + (a\dot{\beta} - \alpha\dot{b})} \qquad (5\text{-}9)$$

The Bøe et al. notation is used here, and is delined in the nomenclature.

For the early production times, 2 to 5 minutes, they found that Eq. 5-9 reduces to a simplified relation which may be written as:

$$\frac{dS_o}{dp} = \frac{\alpha b' - a\beta'}{a\dot{\beta} - \alpha\dot{b}} \qquad (5\text{-}10)$$

Bøe et al. (1981) demonstrated that both relations were reasonable through simulated drawdown and buildup tests.

A drawdown test starts from known phase saturations, (S_{oi}, S_{gi}), and known relative permeabilities (k_{roi}, k). When the well begins to flow, pressure declines, and relative permeabilities are computed using Eqs. 5-6 and 5-8.

Pressure-saturation relations require two levels of input data. The initial level is at the starting values of pressure, saturations and relative permeabilities. The next level is the monitored pressure at which new relative permeabilities are calculated. Therefore, for solution gasdrive reservoirs the new oil saturation is the only unknown of Eq. 5-9 or 5-10, and is usually obtained through an iterative procedure. In general, as pressure declines, the same procedure can be repeated to calculate new relative permeabilities and the corresponding saturations.

The two-phase derivations, presented in this section, are for solution gasdrive reservoirs. Extension of the derivation to oil-water systems is straightforward. Equation 5-6 will still be the oil phase relative permeability equation. For an oil-water system, the water-oil ratio

measured during the test may be related to reservoir and fluid parameters through:

$$WOR = \frac{k_{rw}}{k_{ro}} \frac{\mu_o B_o}{\mu_w B_w} \tag{5-11}$$

Hence, the following equation allows an estimate of water relative permeability at any flowing pressure:

$$k_{rw} = (WOR)_{p_{wf}} \left(\frac{\mu_w B_w}{\mu_o B_o}\right)_{p_{wf}} (k_{ro})_{p_{wf}} \tag{5-12}$$

The corresponding pressure-saturation relation can be derived from the oil and water flow equations, following the Boe et al. (1981) approach. Sandface saturations change slightly during a test for oil-water reservoirs. Hence, the relative permeabilities are obtained over a small range of phase saturations.

In general, there is a basic assumption in the derivation. It is that the distribution of phase saturations is uniform over the entire reservoir thickness. This work does not include the effect of segregated flow on relative permeability determination.

5.23 Drawdown in Practice

To check the practicality of drawdown testing, several tests were generated using the ECLIPSE simulator. An important observation, common to all tests, was an almost instantaneous adjustment of sandface saturation to the producing rate. Figure 5-1 shows sample sandface saturation-time data graph for a simulated drawdown test. In most of the cases, sandface oil saturation dropped in a few minutes to a reasonably stabilized value until the end of the *test.* This early period is often dominated by wellbore effects and operating conditions. In addition, it is not practical to monitor the rapid change of producing GOR within this short time. Thus, the current state of instrumentation often does not permit estimation of relative permeabilities from a constant-rate test.

Besides this impracticality, other problems are also encountered in attempting to analyze constant-rate tests. The early response, during which most of the k_r vs. S changes occur,

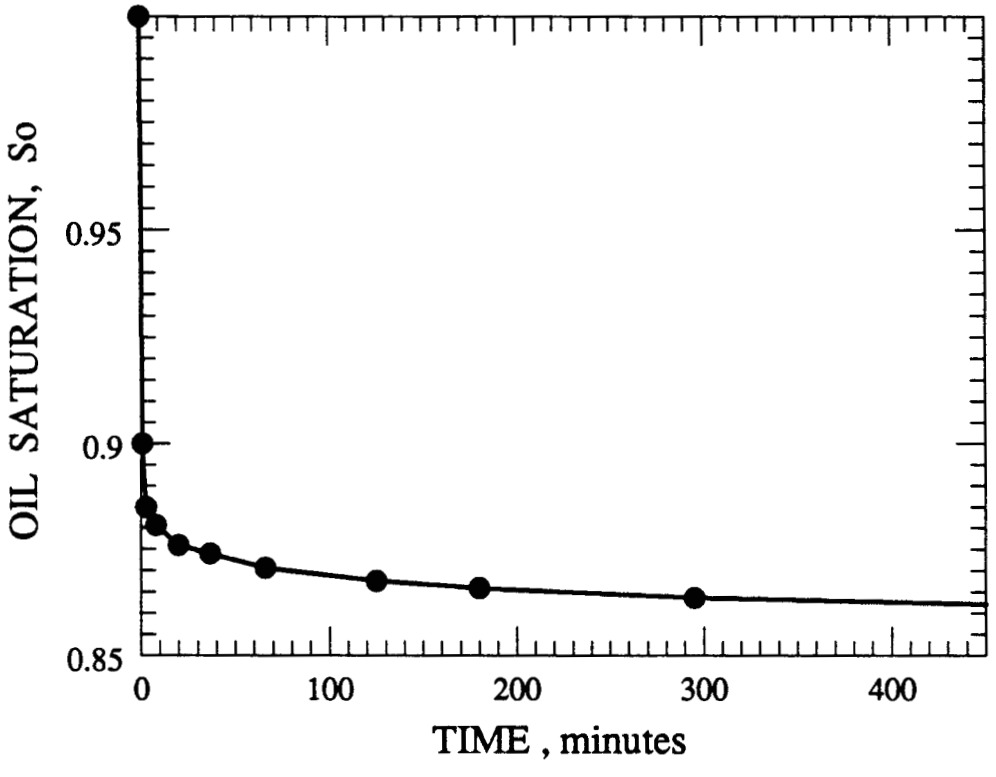

Figure 5.1: **Sandface oil** saturation **vs. time for a simulated constant-rate drawdown test.**

reflects a small area around the wellbore. Hence, the resulting relative permeabilities do not represent a large area of investigation. In cases where the wellbore is damaged, the computed results may be inappropriate because they reflect a skin region of low absolute permeability.

All of these problems suggest that the late time response is better analyzed to represent the bulk of the drainage area, and to minimize the skin and other wellbore effects. Since the late response results in only one stabilized k_r - S value, constant-rate testing results in only such a stabilized value and does not meet the goal of generating several values to construct a curve. This conclusion led to consideration of another option: multiple-rate testing.

5.3 Multiple-Rate Testing

Multiple-rate testing resolves difficulties encountered with constant-rate drawdown testing. Because a change of sandface saturation is dependent on the producing rate, a stepwise increasing oil rate will cause a stepwise increasing gas saturation. Figure 5-2 shows a stepwise decrease in sandface oil saturation for a simulated increasing oil rate steps. Analytical relations were derived to analyze the late time response of each rate step. These relations permit estimation of the stabiied saturation and the comsponding relative permeabilities. A number of data points equal to the number of oil rate steps will be obtained to generate a relative permeability curve.

The proposed multiple rate test starts with a low constant oil rate, and proceeds with increasing oil rate steps as time increases. The highest rate (at the end of the test) should be the maximum possible oil rate expected within operating conditions. The time length of each rate step determines the area of investigation for which the corresponding relative permeabilities are estimated.

53.1 Superposition Principle

The use of the pseudopressure function, $m(p)$, partially linearizes the two-phase flow equations. However, the diffusivity tern was shown by Aanonsen (1985,a) to be a function of the dependent variable, $m(p)$. The diffusivity equation obtained for solution gas-drive

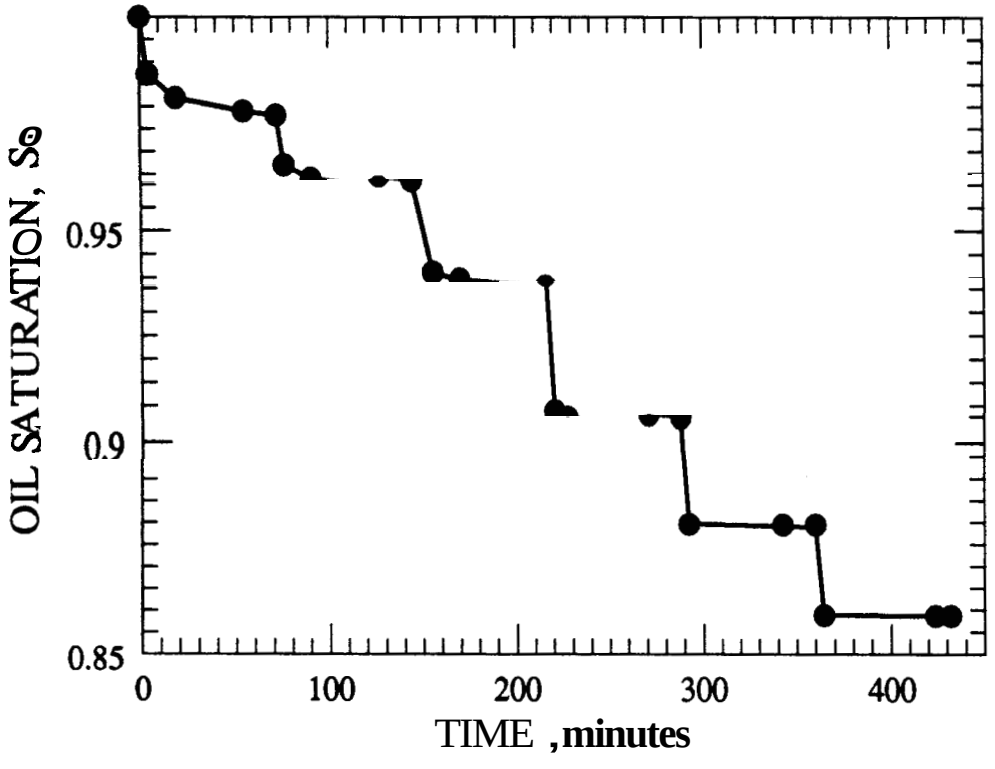

Figure 5.2: **Sandface oil saturation vs. time for a simulated multiple-rate drawdown test.**

reservoirs can be written as:

$$\nabla^2 m(p) = \frac{\phi}{k} \left(\frac{c}{\lambda}\right)^* \frac{\partial m(p)}{\partial t} \qquad (5\text{-}13)$$

Fetkovich (1973) and Bôe et al. (1981) derived the solutions for drawdown and buildup tests run in solution gasdrive reservoirs assuming constant $(c/\lambda)^*$. Raghavan (1976) applied these solutions using different pressure-saturation relations for buildup and for drawdown tests. He concluded that these two tests are not reversible and that superposition *can* not be applied for such systems. Aanonsen (1985,a) showed that $(c/\lambda)^*$ varies with $m(p)$. He also concluded that although superposition applies to pseudosteady state multiple-rate tests reported by Fetkovich (1973) and Whitson (1983). care should be taken in other cases.

The technique proposed in this chapter applies superposition to transient multiple-rate testing based on the following considerations. First, the diffusivity term is assumed constant in order to derive the existing constant-rate solutions. Raghavan (1976). and Bôe et al. (1981) have shown that reasonable accuracy can be obtained with this assumption. Second, the same pressure-saturation relation is used for all steps of the proposed multiple-rate test. Pressure and saturations continue to change monotonically with radius and time during the entire test. As will be shown later, reasonable results were obtained when superposition was applied in this manner.

53.2 Relative Permeability Equations

The multiple-rate solution was prepared by superposition of line source solutions. Derivation of this superimposed form is well documented in the monographs by Matthews and Russell (1967) and by Earlougher (1977) for single phase flow. The same procedure was applied to superpose the line source solution in terms of $m(p)$. The following multiple-rate solution was obtained for solution gasdrive reservoirs:

$$\frac{m(p_i) - m(p_{wf})}{q_n} = \frac{162.6}{k\,h} \sum_{j=1}^{n} \frac{\Delta q_j}{q_n} \log\left[t - t_{j-1}\right]$$

$$+ \frac{162.6}{k\,h}\left\{\log\left[\frac{k}{\phi\, r_w^2}\left(\frac{\lambda}{c}\right)^*\right] - 3.2275 + 0.86895\, s\right\} \qquad (5\text{-}14)$$

where:

q_j : surface rate during step j,

t_{j-1} : starting time of step j, and

q_n : the final rate.

When considering the response of a specific rate step, n, Eq. 5-14 simplifies to:

$$m(p_{wf}) = -\frac{162.6}{k\,h}\left\{\sum_{j=1}^{n} \Delta q_j \log\left[t - t_{j-1}\right]\right\} + C_2 \qquad (5\text{-}15)$$

where C_2 is a constant defined as:

$$C_2 = m\left[p_i\right] - \frac{162.6\, q_n}{k\,h}\left\{\log\left[\frac{k}{\phi\, r_w^2}\left(\frac{\lambda}{c}\right)^*\right] - 3.2275 + 0.86895\, s\right\} \qquad (5\text{-}16)$$

In general, the response of a specific rate step, n, of a transient multiple rate test is a straight line on a plot of:

$$m(p_{wf}) \quad vs. \quad \sum_{j=1}^{n} \Delta q_j \log\left[t - t_{j-1}\right]$$

The slope of the straight line is:

$$slope = \frac{\partial\, m\left[p_{wf}\right]}{\partial\left[\sum_{j=1}^{n} \Delta q_j \log\left[t - t_{j-1}\right]\right]} = -\frac{162.6}{k\,h} \qquad (5\text{-}17)$$

Equation 5-17 can be rewritten as:

$$\frac{\partial\, m\left[p_{wf}\right]}{\partial\, p_{wf}} = -\frac{162.6}{k\,h}\,\frac{1}{\dfrac{\partial\, p_{wf}}{\partial\left[\sum_{j=1}^{n} \Delta q_j \log\left[t - t_{j-1}\right]\right]}} \qquad (5\text{-}18)$$

Since

$$\frac{\partial m\left[p_{wf}\right]}{\partial p_{wf}} = \left[\frac{k_{ro}}{\mu_o B_o}\right]_{p_{wf}},$$

Eq. 5-18 becomes:

$$= - \frac{162.6}{k h} \frac{\left[\mu_o B_o\right]_{p_{wf}}}{\dfrac{\partial p_{wf}}{\partial\left[\sum_{j=1}^{n} \Delta q_j \log\left[t - t_{j-1}\right]\right]}} \qquad (5\text{-}19)$$

This relation allows an estimate of oil relative permeability at any flowing pressure in terms of input absolute permeability and rate-pressure data for a multiple-rate test.

The pressure-summation derivative can be evaluated by choosing a short time interval within the rate step *n*. This time interval is chosen late enough to represent a large area of investigation and to minimize wellbore and skin effects. The instantaneous pressure-summation derivative may be approximated by the slope of a line over this short time interval. For example, if $(t1 - t2)$ is a short interval within the rate step *n*, then:

$$\left[\frac{\partial p_{wf}}{\partial \sum term}\right] = \frac{p_{wf}\left[t1\right] - p_{wf}\left[t2\right]}{\left[\sum_{j=1}^{n} \Delta q_j \log\left[t1 - t_{j-1}\right]\right] - \left[\sum_{j=1}^{n} \Delta q_j \log\left[t2 - t_{j-1}\right]\right]} \qquad (5\text{-}20)$$

Both *t1* and *t2* are within the specific rate step, *n*, for which the stabilized oil relative permeability is to be estimated. Also the $\left[\mu_o B_o\right]$ tern in Eq. 5-19 is to be estimated at:

$$\left[\frac{p_{wf}(t1) + p_{wf}(t2)}{2}\right] \qquad (5\text{-}21)$$

Choosing the (t1 - t2) interval late in step *n*, results in a large area of investigation, and, hopefully, minimal wellbore effects. Gas relative permeability, k_{rg}, may be computed using *Eq.* 5-8, which requires the stabilized producing GOR measured for the rate step, *n*. All other parameters in Eq. 5-8 should be evaluated at the mean flowing pressure defined by Eq. 5-21.

5.3.3 Saturation Equations

The stepwise decrease in sandface oil saturation corresponds to a stepwise increase in producing oil rate. All simulated multiple-rate tests showed that adjustment of the sandface saturation takes less than a few minutes, after which sandface saturation nearly stabilizes until the next rate step. The stabiition might take as long as ten or twenty minutes for low flow rates, but takes less and less time as the flow rate gets higher. Figure 5-2 presents sandface saturation vs. time for a simulated multiple-rate test.

The pressure-saturation relations, Eqs. 5-9 and 5-10, were applied here, but differently from the approach used by Bφe et al. (1981). In their work, they used laboratory relative permeability curves to compute a continuous change in sandface saturatio with flowing bottomhole pressure. In this work, a single relative permeabiity value was determined for each rate step using Eqs. 5-19 and 5-8. This estimate of phase relative permeability cornsponds to an unknown stabilized saturation for each rate step. No relative permeabii information is obtained in the saturation range between rate steps. Therefore, the Bφe et al. relation can not be used as such to compute the continuous change in saturation from previous to current stabilized saturations. Rather, their relation may be used to compute only the stabilized saturation of each rate step using the corresponding relative permeability obtained.

Simulated multiple-rate tests showed a rapid change in sandface saturation with a change in oil rate, as shown in Fig. 5-2. Since the saturation change is almost instantaneous (less than five minutes for the cases simulated), Eq. 5-10 was assumed to apply for solution gasdrive reservoirs. Equation 5-9 is applicable as well. Such presswe-saturation relations are used only to compute the stabilized oil saturation values at which the relative permeabilities have been obtained using Eqs. 5-19 and 5-8.

The pressure-saturation relation, Eq. 5-10, may be used to compute the stabilized phase saturations of any step, n, using two levels of input data. The first data level is the stabilized relative permeabilities-saturation values for step $n-1$, together with the flowing bottomhole pressure just before the start of step n, and the second data level is the stabilized relative

permeabilities for step *n*, with the flowing bottomhole pressure soon after the start of step *n*. The pressure drops just after the instantaneous saturation change. The simulation runs showed that for low starting rates, an appropriate time at which to take this pressure is between 0.5 and 3 minutes after the rate change. For high rates, the pressure may be taken at less than 0.5 minute after the rate change. In most of the applications reported in this work, 0.5 minute was used for the early low rates and 5 to 10 seconds was used for the late high rates. This early pressure response prevents possible underestimation of Eq. 5-10 that could happen if the late pressure response was to be used, see Bϕe et al. (1981).

As discussed in Section 5.2.2 for drawdown testing, simple iteration with Eq. 5-10 yields a new stabilized oil saturation. The same process is repeated for step $n+1$. The two levels of input data are now those for steps n and $n+1$, and the unknown is the stabilized saturation for step $n+1$.

The saturation relations, Eq. 5-9 or 5-10, can be used to obtain an estimate of stabilized saturation for each rate step. Each of these stabilized saturations has its own estimated stabilized relative permeability. Therefore, the resulting relative permeability curves are made up of a number of data points equal to the number of rate steps.

5.4 Test Procedure

Figure 5-3 presents a typical pressure and rate data during a multiple-rate test. The main aspects of the test are:

1) The well is produced at a series of constant oil rates increasing in steps with time. The length of each rate step is determined based on the radius to be investigated and the time needed to minimize afterflow.

2) Stabilized oil and gas rates are measured at the surface for each rate step.

3) Pressure versus time is monitored throughout the entire test.

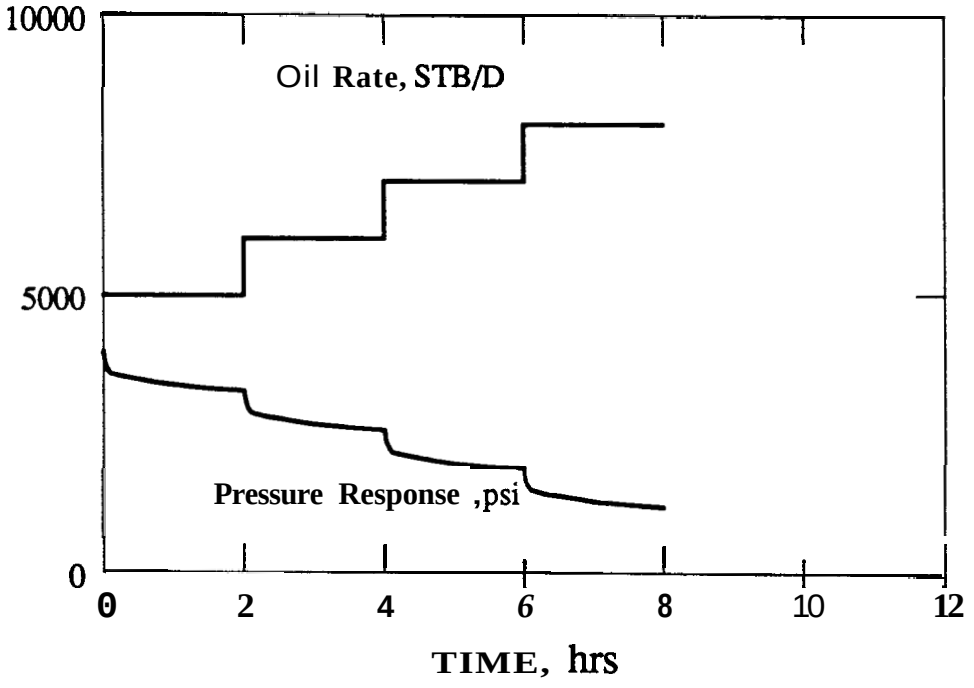

Figure 5.3: **Pressure and flow** rate **for a multiple-rate** *test*

5.5 Test Analysis

The proposed approach was derived for solution gas-drive reservoirs assuming a uniform saturation distribution at the start of the test. The effects of coning, fingering and segregated flow on the proposed technique were not investigated in this work.

Initial input parameters required for the method are the initial average pressure, initial average saturations, initial relative penneabiities and the absolute penneability. If an estimate of the absolute permeabiity is not available from single-phase tests, the proposed technique results in estimates of the effective permeabiities versus saturation. These values can be used to estimate the absolute permeability, as will be discussed in a later section.

Some of the initial input parameters can be obtained with the help of other types of well tests, e.g. a buildup test run after a pseudosteady state flow period. Such a buildup test, when analyzed using the proposed approach discussed in Section 4, results in estimates of average drainage area effective oil permeability. An average effective gas permeabii can also be obtained, using the pseudosteady state producing GOR before shutin, and average reservoir pressure in Eq. 5-8. The effective phase permeabilities can be used to produce average relative permeabilities when divided by the absolute permeabiity. The average values of relative permeabilities can then be used with the $k_r - S$ results of a previous multiple-rate test to estimate the corresponding average reservoir saturation (average reservoir saturation can also be obtained through material balance). The average v lues of saturation and relative penneabilities can then be used as initial input parameters for a following multiple-rate test covering another range in phase saturations.

Investigation showed that values of saturations obtained were relatively insensitive to the initial relative permeability values required to estimate the phase saturations for the first rate step. Hence, laboratory relative permeability values may be used to obtain the saturation value of the first rate step, if reservoir values are not available.

The proposed analysis can be used to produce a single k_r-S data point for each rate step. This data point represents stabilized conditions after an early adjustment period. To summarize

the method, the following procedure is recommended for each rate step, *n:*

1) Stabilized relative permeabilities are estimated using: *Eq.* 5-19 for stabilized k_{ro}, and Eq. 5-8 for stabilized k_{rg},

2) The corresponding stabilized sandface saturation is estimated using Eq. 5-9, or Eq. 5-10.

5.6 Numerical Applications

The validity of the proposed technique was investigated for several two-phase multiple-rate tests. These tests were simulated for both homogeneous and composite systems. For the homogeneous case, a single set of relative penneabiity curves represented the entire drainage area. The composite system had two sets of relative permeability curves applying for different regions of the drainage area. *All* other rock properties were considered homogeneous.

5.6.1 Discretization

An oil reservoir is usually considered a physically continuous entity. However, numerical modeling represents discrete volumes over increments of time.

The proposed analysis technique uses the derivative of the pressure response. *An* objective of this work was to reduce discretization errors to a degree where practical accuracy could be obtained. In all the simulation runs, short time steps were chosen. The time step started with 10^{-2} minute and ended within the range of *0.25* to 1.25 minutes. When longer time steps of around 15 to *20* minutes were used, results were found to be sensitive to the time interval used in Eq. 5-20.

5.62 Homogeneous System

A one-dimensional, 40-block radial model was constructed using the ECLIPSE simulator. This model was then used to verify the proposed approach. All simulation runs used the PVT properties reported by Bφe et al.(1981).

In homogeneous systems, multiple-rate tests were generated using a single set of relative permeabii curves describing the whole drainage area. Following is a detailed analysis of the applications.

Case 1 : Corey-Type Relative Permeability

The following Corey-type (1954) relative permeability relations were used:

$$k_{ro} = (S_o^*)^{3.3} \tag{5-22}$$

$$k_{rg} = 0.9\,(1 - S_o^*)^{2.0} \tag{5-23}$$

where :

$$S_o^* = \frac{(S_o - S_{or})}{(1 - S_{or})}$$

and:

$$S_{or} = 0.20$$

Each multiple rate test covered a range of 8-15% change in sandface saturation. Therefore, three multiple-rate tests were simulated at different stages of depletion to cover a total range of 35% in gas saturation. Input data common to all three tests are given in Table 5-1.

Following is a demonstration of the test analysis explained in Section 5.5. Relative permeabilities and the corresponding saturation are calculated for one rate step of the first multiple-rate test.

Table 5.1: General input data for the three tests (Case 1)

Parameter	Input value
Wellbore Radius	0.3 ft.
Porosity	0.15
Rock Compressibility	3.0×10^{-6} psi-'
Oil Density	45.0 Lb/SCF
Gas Density	0.068735 Lb/SCF.
Absolute Permeability	10 md.
Thickness	150 ft.

Relative Permeabilities:

Rate-pressure data from the first test, as well as the starting conditions, are presented in Table 5-2. Oil relative permeability is evaluated using Eq. 5-19 expressed as:

$$\left(k_{ro}\right)_{p_{wf}} = - \frac{162.6}{k\,h} \frac{\left(\mu_o B_o\right)_{p_{wf}}}{\partial p_{wf}} \Big/ \partial \left[\sum_{j=1}^{n} \Delta q_j \log\left(t - t_{j-1}\right)\right]$$

The pressure-summation derivative was evaluated by choosing a short time interval within the considered rate step. For example, the time interval was taken to be (0.044 to 0.05 day) within the first rate step which extended to 0.05 day. Using Eq. 5-20 expressed as:

$$\left[\frac{\partial p_{wf}}{\partial \sum term}\right] = \frac{p_{wf}(t1) - p_{wf}(t2)}{\left[\sum_{j=1}^{n} \Delta q_j \log\left(t1 - t_{j-1}\right)\right] - \left[\sum_{j=1}^{n} \Delta q_j \log\left(t2 - t_{j-1}\right)\right]}$$

where $t1$ was 0.044 day and $t2$ was 0.05 day, the following was obtained:

$$\left(\frac{\partial p_{wf}}{\partial \sum term}\right) = 0.06413$$

The $(\mu_o B_o)$ term in Eq. 5-19 is estimated at $[\,p_{wf}(t1) + p_{wf}(t2)\,] / 2 = 5546.85$ psi to be 0.53798 cp RB/STB. Substituting this value and others (k and h given in Table 5.2) in Eq. 5-19, the relative permeability at 5546.85 psi flowing pressure was found to be:

$$k_{ro} = - \frac{162.6}{10 \times 150} \frac{0.53798}{0.06413} = 0.9093$$

Using this calculated oil relative permeability, gas relative permeability may be obtained using Eq. 5-8 expressed as:

$$\left(k_{rg}\right)_{p_{wf}} = \left(GOR - R_s\right)_{p_{wf}} \left[\frac{\mu_g B_g}{\mu_o B_o}\right]_{p_{wf}} \left(k_{ro}\right)_{p_{wf}}$$

Table 5.2: Data of first test (Case 1)

Step No.	q_o, STB/D	GOR, MSCF/STB	t, D	p, psia
1	500	1.47	0.0007	5604.46
			0.003	5584.79
			0.008	5571.32
			0.013	5564.69
			0.0 18	5560.21
			0.038	5549.78
			0.044	5547.74
			0.05	5545.96
2	1000	1.46	0.0507	5435.99
			0.053	5414.66
			0.058	5401.08
			0.063	5392.08
			0.068	5386.39
			0.088	5312.46
			0.094	5368.92
			0.10	5366.12
3	2000	1.48	0.1007	5119.23
			0.103	5065.42
			0.108	5033.22
			0.113	5015.84
			0.1 18	5003.50
			0.138	4974.82
			0.144	4967.71
			0.15	4961.5 1
4	4000	1.66	0. 1500289	5119.23
			0.1507	4334.07
			0.153	4201.99
			0.158	4111.01
			0.163	4053.58
			0.168	4024.40
			0.188	3957.57
			0.194	3941.87
			0.20	3926.93
5	6000	2.12	0.2000289	3474.51
			0.2007	2893.69
			0.203	2657.27
			0.208	2483.17
			0.2 13	2414.32
			0.218	2357.89
			0.238	2250.56
			0.244	2235.28
			0.25	2218.36

Initial Pressure = 5703 psi
Initial Oil Saturation = 100 %

Table 5.3: Relative permeabilities for first test (Case 1)

Data used in Eq. 5-19					Results	
Step No.	$t1$, D	$p(t1)$, psia	$t2$, D	$p(t2)$, psia	k_{ro}	k_{rg}
1	0.044	5547.74	0.05	5545.96	0.90934	9.466e-04
2	0.094	5368.92	0.10	5366.12	0.8598	2.544e-03
3	0.144	4967.71	0.15	4961.51	0.7474	6.133e-03
4	0.194	3941.87	0.20	3926.93	0.6886	1.5214e-02
5	0.244	2235.28	0.25	2218.36	0.6053	2.532e-02

Table 5.4 Oil saturations for first test (Case 1)

Data used in Eq. 5-10								Results
Step No.	$p(t1)$, psia	k_{ro1}	k_{rg1}	S_{o1}	$p(t2)$, psia	k_{ro2}	k_{rg2}	S_{o2}
1	5703.0	1.0	0.0	1.0	5604.97	0.909	9.47e-04	0.986
2	5545.96	0.909	9.47	0.986	5435.99	0.859	2.54e-03	0.97
3	5366.12	0.859	2.54e-03	0.97	5119.23	0.747	6.13e-03	0.936
4	4961.99	0.747	6.13e-03	0.936	4651.85	0.6886	1.52e-02	0.894
5	3926.93	0.6886	1.52e-02	0.894	3474.57	0.6053	2.53e-02	0.834

For first rate step, GOR was 1.47 MSCF/STB, and other PVT data were taken at 5546.85 psi flowing pressure and substituted as follows:

$$k_{rg} = (1.47 - 1.438)\left(\frac{0.01774}{0.53798}\right)(0.9093) = 9.466 \sim 10^{-4}$$

For the first rate step, the resulting estimate of the oil relative permeability was 0.9093 and that for the gas relative permeability was 9.466×10^{-4}. The same calculations were repeated for other rate steps whose pressure-rate data are given in Table 5-2. Test data used in Eqs. 5-19 and 5-8 as well as the resulting estimates of relative permeabilities are summarized in Table 5-3 for all rate steps.

Phase Saturations:

After calculating the relative permeabilities for any rate step, the comsponding phase saturations may be calculated using Eqs. 5-9 or simply Eq. 5-10. Equation 5-10 is:

$$\frac{dS_o}{dp} = \frac{ab' - a\beta'}{up - ad}$$

which can be written in expanded form as:

$$\frac{dS_o}{dp} = \frac{\left(\frac{k_{ro}}{\mu_o B_o}\right)\frac{\partial}{\partial p}\left(\frac{\phi S_g}{B_g} + \frac{\phi R_s S_o}{B_o}\right) - \left(\frac{k_{rg}}{\mu_g b_g} + \frac{R_s k_{ro}}{\mu_o B_o}\right)\frac{\partial}{\partial p}\left(\frac{S_o}{B_o}\right)}{\left(\frac{k_{rg}}{\mu_g b_g} + \frac{R_s k_{ro}}{\mu_o B_o}\right)\frac{\partial}{\partial S_o}\left(\frac{S_o}{B_o}\right) - \left(\frac{k_{ro}}{\mu_o B_o}\right)\frac{\partial}{\partial S_o}\left(\frac{\phi S_g}{B_g} + \frac{\phi R_s S_o}{B_o}\right)}$$

Such an equation requires two levels of input data. The initial level is at the starting values of pressure, oil and gas saturations and oil and gas relative penneabilities. The next level is the very early flowing pressure of the rate step together with its calculated relative penneabilities. The only unknown is the stabilized oil saturation during the rate step, which can be obtained through an iterative procedure. An initial guess of the oil saturation change, ΔS_o during the rate step is used. If the two sides of Eq. 5-10, equate to each other, then the guess is correct Otherwise, this guess is either increased or decreased and the iteration is repeated until Eq. 5-10 is satisfied.

The following is a demonstration of the iterative process applied to the first rate step of the first test. The initial pressure was 5703.0 psi and the early flowing pressure was 5604.97 psi. The starting relative permeabilities were 1.0 for the oil and 0.0 for the gas, while the relative permeabilities calculated for this first rate step were 0.909 for the oil and 9.47×10^{-4} for the gas. The initial oil saturation was 100%, and the stabilized saturation of this first rate step was to be determined iteratively using Eq. 5-10. Using these values along with a porosity value of 0.15 (given in Table 5-1), an initial guess for ΔS_o was taken to be 0.002. The convergence criteria for the iteration was that the two sides of Eq. 5-10 equate to each other within a tolerance of 2×10^{-6}. When an iteration did not converge, ΔS_o was increased by another 0.002. A total of seven iterations were needed to m e r g e in the first rate step, with a total saturation change of 0.014. Therefore, the stabilized oil saturation for the first rate step of the first test was 0.986.

The oil saturation obtained for the first step along with corresponding relative permeabilities were then used as starting values for the second step. The starting pressure of the second step was 5545.96 psi, and the early flowing pressure was 5435.99. The relative permeabiities calculated for the second step are also given in Table 5.3. A similar iterative process was also performed for this rate step as well as the others. The data used in the iteration process of Eq. 5-10 together with the resulting saturations are presented in Table 5-4.

Results:

The other two tests were also analyzed following the same steps. Tables 5-5 through 5-7 present results for the second test, and Tables 5-8 through 5-10 present results for the third test. The relative pemeability-saturation results of the three tests are shown in Fig. 5-4, as well as the reservoir simulation input data curves. A good comparison between input and calculated results was obtained over the entire saturation range.

Table 5.5 Data of second test (Case 1)

Step No.	q_o STB/D	*GOR* MSCF/STB	*t* D	*P* psi
1	500	3.32	0.000347	4534.32
			0.0007	4515.67
			0.003	4475.55
			0.008	4449.0
			0.013	4436.57
			0.018	4427.57
			0.038	4406.52
			0.044	4402.42
			0.05	4398.86
2	1000	3.90	0.050347	4201.85
			0.0507	4178.61
			0.053	4129.63
			0.058	4095.84
			0.063	4076.61
			0.068	4062.98
			0.088	4030.93
			0.094	4024.40
			0.10	4018.58
3	2000	5.56	0.1000289	3751.61
			0.1007	3408.49
			0.103	3300.84
			0.108	3196.31
			0.113	3143.21
			0.118	3104.80
			0.138	3025.15
			0.144	3008.96
			0.15	2994.49
4	3000	9.72	0.1500289	2585.02
			0.1507	1796.0
			0.157	1266.50
			0.162	1056.91
			0.167	955.46
			0.187	666.77
			0.193	608.34
			0.1990	560.54

Initial pressure = 4700 psi,
Initial gas saturation = 14 %.
Initial oil saturation = 86 %.

Table 5.6: Relative permeabilities for second test (Case 1)

Data used in Eq. 5-19					Results	
Step No.	$t1$ D	$p(t1)$ psi	$t2$ D	$p(t2)$ psi	k_{ro}	k_{rg}
1	0.044	4402.31	0.05	4398.75	0.4903 0.4903	3.381e-02 3.381e-02
2	0.094	4024.48	0.10	4018.66	0.4685	4.035e-02
3	0.144	3009.28	0.15	2994.81	0.42597	5.435e-02
4	0.194	606.12	0.20	557.20	0.278	0.1126

Table 5.7: Oil saturations for second test (Case 1)

Data used in Eq. 5-10								Results
	$p(t1)$	k_{ro1}	k_{rg1}	S_{o1}	$p(t2)$	k_{ro2}	k_{rg2}	S_{o2}
1	4700	0.53	2.75e-03	0.86	4573.08	0.49	3.38e-02	0.844
2	4398.75	0.49	3.38e-02	0.844	4255.02	0.468	4.0e-02	0.8276
3	4018.66	0.468	4.0e-02	0.8276	3751.27	0.426	5.44e-02	0.798
4	3751.27	0.426	5.44e-02	0.798	2585.02	0.278	1.226e-01	0.763

Table 5.8: Data of the third test (Case 1).

step No.	q_o STB/day	GOR Mscf/STB	t days	P psia
1	500	22.50	0.000349	3756.86
			0.0007	3696.25
			0.003	3590.93
			0.008	3528.23
			0.013	3493.02
			0.018	3467.07
			0.038	3407.08
			0.044	3395.91
			0.05	3386.25
2	1000	39.69	0.05003	2916.77
			0.050347	2408.67
			0.0507	2302.52
			0.053	2214.23
			0.058	2045.03
			0.063	1908.22
			0.068	1823.50
			0.088	1653.18
			0.094	1573.36
			0.10	1540.77

Initial Pressure = 4200 psi

Initial gas saturation = 28 %

Initial oil saturation = 72 %

Table 5.9: Relative permeabilities for third test (Case 1)

Data used in Eq. 5-19					Results	
Step No.	rl D	p (tl) psi	t2 D	p (t2) psi	k_{ro}	k_{rg}
1	0.044	3395.91	0.05	3386.25	0.2105	1.23e-01
2	0.094	1573.36	0.10	1540.77 1540.77	0.1376 0.1376	1.558e-01 1.558e-01

Table 5.10: Oil saturations for third test (Case 1)

	Data used in Eq. 5-10							Results
	$p1$	k_{ro1}	k_{rg1}	S_{o1}	$p2$	k_{ro2}	k_{rg2}	S_{o2}
1	4200.0	0.249	1.063e-01	0.86	3756.86	0.21	1.226e-01	0.6886
2	3756.86	0.29	1.226e-01	0.6886	3386.25	0.1376	1.52e-01	0.6549

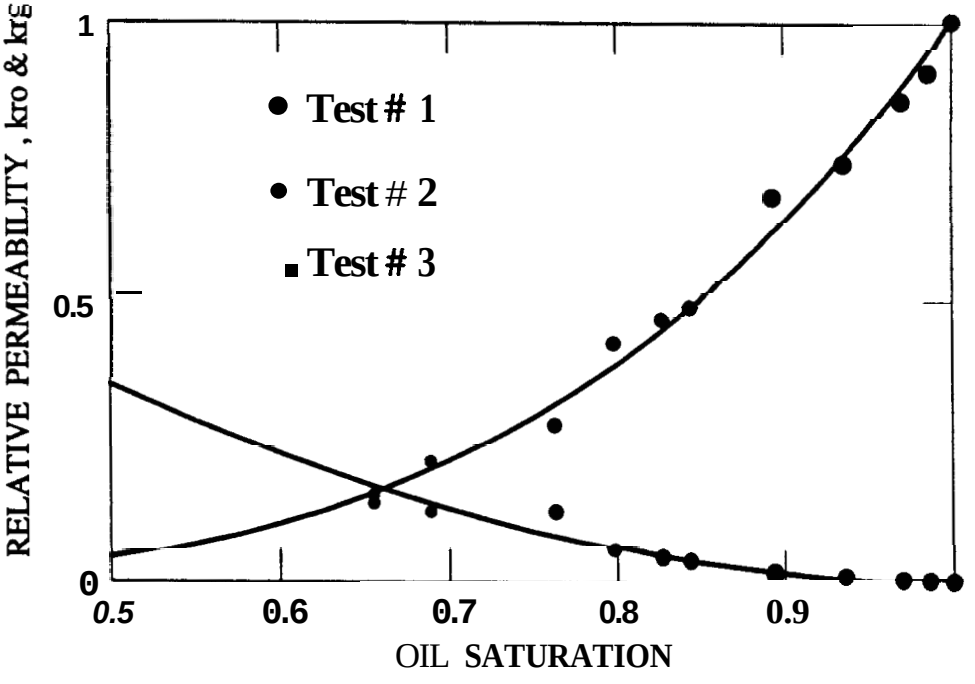

Figure 5.4: **Relative permeabilities from the three tests (Case 1)**

Case 2: Straight Line Relative Permeability

Exploring the limits of the technique, the following set of relative permeability curves was used to simulate a multiple-rare *test*

$$k_{rl} = S_l \tag{5-24}$$

Here *l* stands for both oil and gas phases.

The input data for the model in this *case* is given in Table 5-11. Results are presented in Tables 5-12 through 5-14, and graphed in Fig. 5-5, which shows good agreement with the input relative penneabilities.

Sensitivity of the proposed analysis technique to a possible error in the value of initial reservoir saturation was tested. Analysis of this test was repeated using an input value of 97 % for the initial oil saturation, that is 3 % less than the correct value. Such an error did not introduce any change in estimated relative permeabilities. The reason was that saturation is not used in Eqs. 5-8 and 5-19 to calculate relative permeabilities On the other hand, it resulted in approximately 3 % constant shifts for all saturations obtained using Eqs. 5.9 or 5.10 *(see* Fig. 5-6). This shift was equal to the error introduced in initial oil saturation.

Case 3: Quadratic Relative Permeability

Another attempt to test the technique was to consider the *case* when:

$$k_{rl} = S_l^2 \tag{5-25}$$

Here *l* stands for both oil and *gas* phases.

The general input data for the model for this case is given in Table 5-15. The test started at the bubble point pressure, $p_b = 5703$ psia. Test data and results are given in Tables 5-16 through 5-18. Figure 5-7 presents the resulting relative permeability-saturation CURVES. Again reasonable agreement was obtained.

Table 5.11: Input data (Case 2)

Parameter	In ut value
	10 md.

Table 5.12: Data of the test (Case 2)

Step No.	q_o STB/D	GOR MSCF/STB	t D	P psi
1	500	2.33	0.000029	5472.75
			0.0007	5310.3
			0.003	5240.86
			0.008	5189.4
			0.013	5165.85
			0.018	5149.78
			0.038	5112.99
			0.044	5105.44
			0.05	5099.23
2	1000	3.90	0.050029	4855.58
			0.0507	4654.65
			0.053	4565.30
			0.058	4494.16
			0.063	4459.62
			0.068	4436.33
			0.088	4376.93
			0.094	4365.02
			0.10	4354.60
3	2000	5.56	0.100029	3749.36
			0.1007	3196.78
			0.103	2935.83
			0.108	2745.02
			0.113	2633.42
			0.118	2562.68
			0.138	2379.31
			0.144	2344.13
			0.15	2312.83

Initial pressure = 5703 psi,
Initial oil saturation = 100 %.

Table 5.13: Relative permeabilities for the test (Case 2)

Data used in Eq. 5-19					Results	
Step No.				p ($t2$) psi	k_{ro}	k_{rg}
1	0.044	5105.44	0.05	5099.23	0.9897	3.371e-02
2	0.094	4365.02	0.10	4354.60	0.9366	6.33e-02
3	0.144	2344.13	0.15	2312.83	0.8467	1.145e-01

Table 5.14: Oil saturations for the test (Case 2)

Data used in Eq. 5-10								Results
	p ($t1$)	k_{ro1}	k_{rg1}	S_{o1}	p ($t2$)	k_{ro2}	k_{rg2}	S_{o2}
1	5703.0	1.0	0.0	1.0	5472.75	0.989	3.37e-02	0.97
2	5472.75	0.989	3.37e-02	0.97	4855.58	0.936	6.33e-02	0.94
3	4855.58	0.936	6.33e-02	0.94	3749.36	0.847	1.15e-01	0.868

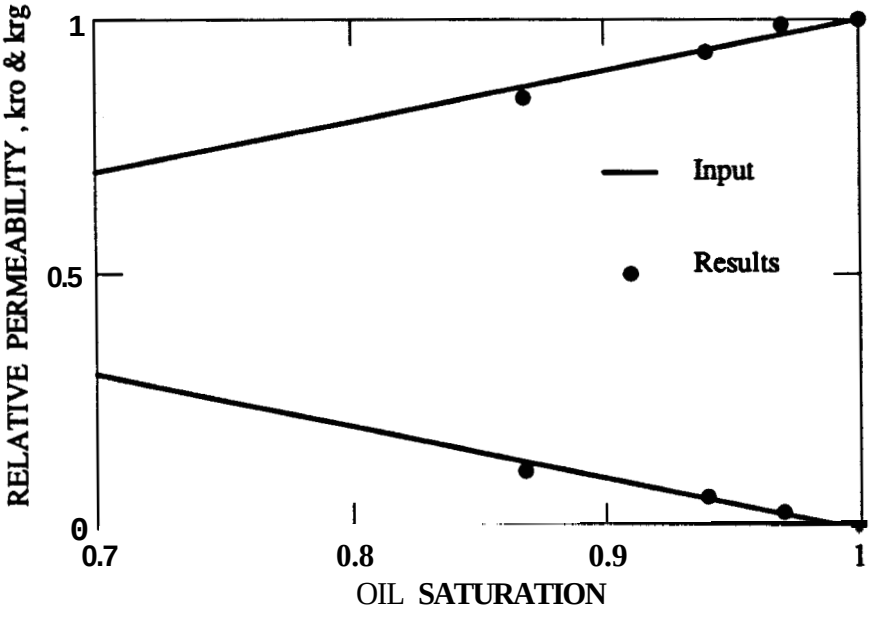

Figure 5.5: Relative permeability vs. oil saturation (Case 2)

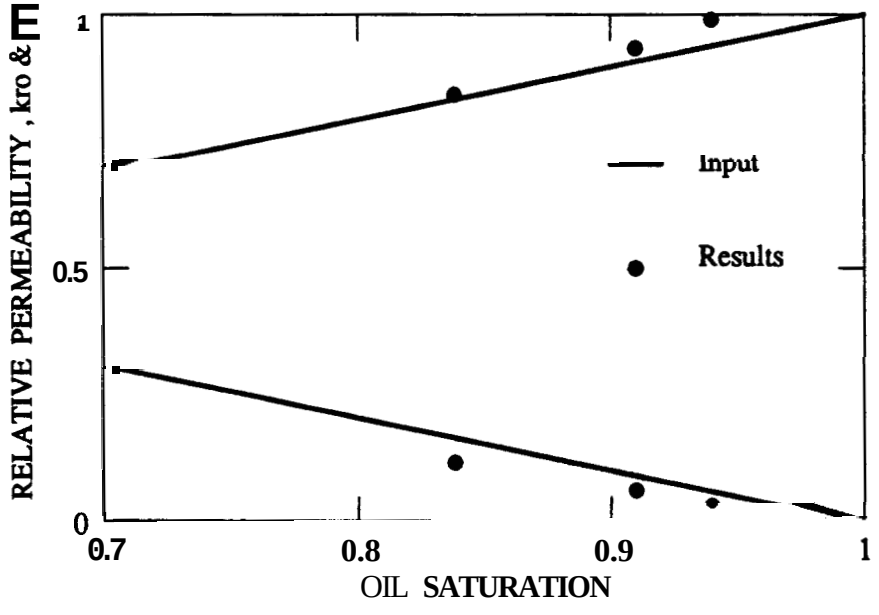

Figure 5.6: The test of Case 2 repeated with a 3 % error in starting oil saturation

Table 5.15: Input data *(Case* 3)

Table 5.16: Data of the test *(Case* 3)

Step No.	q_o STB/D	*GOR* MSCF/STB	*t* D	*P* psi
1	500	1.47	0.000349	5637.26
			0.003	5616.33
			0.008	5606.7
			0.013	5602.06
			0.018	5598.88
			0.038	5591.56
			0.044	5590.12
			0.05	5588.85
2	1000	1.46	0.050349	5519.44
			0.053	5498.67
			0.063	5483.01
			0.088	5468.61
			0.094	5466.51
			0.10	5464.64
3	2000	1.44	0.100349	5317.24
			0.103	5270.55
			0.113	5239.55
			0.138	5212.78
			0.144	5208.51
			0.15	5204.75
4	4000	1.47	0.150349	4896.74
			0.1507	4861.57
			0.153	4787.85
			0.163	4709.63
			0.188	4650.18
			0.194	4641.25
			0.20	4633.02
5	6000	1.54	0.2000289	4443.46
			0.2007	4230.39
			0.203	4150.11
			0213	4053.16
			0.238	3968.78
			0.244	3956.07
			0.25	3944.58
6	8000	1.69	0.2500289	3727.04
			0.2507	3463.25
			0.253	3358.08
			0.263	3231.14
			0.268	3204.21
			0.294	3105.54
			0.30	3088.74

Table 5.17: Relative permeabilities for the test (Case3)

Data used in Eq. 5-19					Results	
Step No.	tl D	p ($t1$) psi	$t2$ D	p ($t2$) psi	k_{ro}	k_{rg}
1	0.044	5590.12	0.05	5588.85	0.963	4.83e-04
2	0.094	5466.51	0.10	5464.64	0.9648	1.67e-03
3	0.144	5208.51	0.15	5204.75	0.9078	3.899e-03
4	0.194	4641.25	0.20	4633.02	0.8535	9.55e-03
5	0.244	3956.07	0.25	3944.6	0.849	1.58e-02
6	0.294	3105.54	0.30	3088.74	0.773	2.09e-02

Table 5.18: Oil saturations for the test (Case3)

Data used in Eq. 5-10								Results
	P ($t1$)	k_{ro1}	k_{rg1}	S_{o1}	P ($t2$)	k_{ro2}	k_{rg2}	S_{o2}
1	5703.0	1.0	0.0	1.0	5637.26	0.963	4.83e-04	0.988
2	5585.85	0.963	4.83e-04	0.988	5519.44	0.964	1.67e-03	0.976
3	5464.64	0.964	1.67e-03	0.976	5317.24	0.908	3.9e-03	0.952
4	5204.75	0.908	3.9e-03	0.952	4896.74	0.855	9.55e-03	0.91
5	4633.02	0.855	9.55e-03	0.91	4443.46	0.849	1.58e-02	0.88
6	3944.58	0.849	1.58e-02	0.88	3727.04	0.773	2.09e-02	0.85

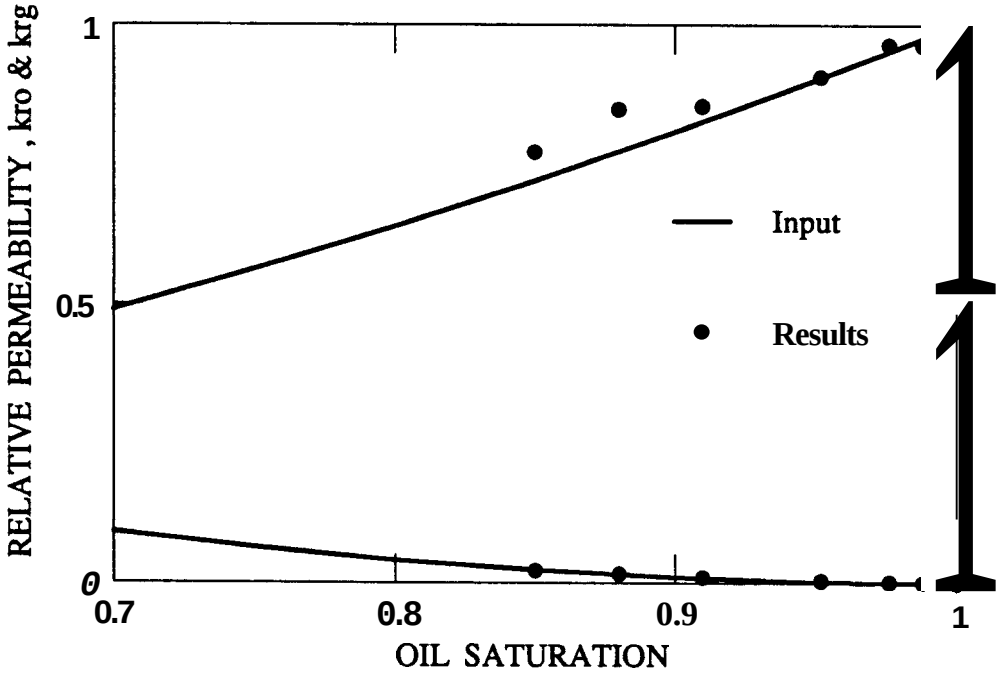

Figure 5.7: **Relative permeability vs. oil saturation (Case 3)**

5.63 Composite System

The relative permeabiity technique developed in this section implicitly assumes the following two conditions:

1) the entire drainage area is described by a single set of relative permeability curves, and

2) fluid properties are uniform over the entire drainage area.

While the second condition may be reasonably correct in many cases, the first condition may fail because of rock heterogeneity and wettabiity changes. Heterogeneities cause variation in relative permeability, and can be divided into small scale and large-scale heterogeneities. Relative permeability changes noticed in a laboratory using different cores from the same well are typical examples of the influence of small-scale heterogeneities. Examples of large-scale heterogeneities are composite, or layered reservoirs. with completely different relative permeabiity behavior in each of the regions or layers.

Single-phase homogeneous models average small scale changes of absolute permeability. However, for large-scale heterogeneities, different models have been developed for more complex systems, such as composite, layered, or fractured reservoirs as reviewed by Earlougher (1977). The same overall approach can be extended to non-uniform relative permeabiity within well drainage area. This is the type of heterogeneity considered in this section. As a test of the proposed technique to a more complex problem, the model presented earlier was used used to analyze two multiple-rate tests in simulated composite relative permeability reservoirs.

The theory of single-phase well testing in reservoirs with composite absolute permeability is well documented in the literature. For example, Ambastha and Ramey (1987) reported that the early pressure response reflects inner region properties, while the late response reflects outer region properties. The same rule was found here to apply to the case of composite relative permeability systems.

Simulated Examples

The proposed relative permeability technique works well for both small and large inner regions. For small inner region, the effects of the outer region quickly dominate the response, resulting in outer region relative permeabilities. For large inner region, the outer region may not be felt until much later in the test, resulting in inner region relative permeabilities. Following are two examples simulated in composite relative permeability systems. The first was run for a system with a 2.5 ft radius inner region, and the second was run for a system with a 600 ft radius inner region. For both examples, the total reservoir radius was 3300 ft.

Example 1 - 2.5 ft Inner Region

The one-dimensional, radial, two-phase model, discussed before was divided into two regions with two different sets of relative permeabilities. The inner 2.5 ft radius region was represented by Corey-type relative permeability relations, as in Eqs. 5-22 and 5-23. The outer region was described by a quadratic relative permeability relation, defined by Eq. 5-25. All other rock properties were the same for both regions.

The average gas saturation at the start of the test was 10 %, and increased at the sandface to 20 % by the end of the test. Table 5-19 presents the relative permeability calculations, while Table 5-20 shows the saturation results from each of the flow rate steps. The resulting estimates of the relative permeabilities graphed in Fig. 5-8 were found to match the quadratic relative permeabilities of the outer region. This indicates that the response of the outer region quickly dominated the response of the small inner region. Hence, the effects of such small regions die quickly, and do not prevent the use of the relative permeability interpretation technique. This application demonstrates one of the advantages of the proposed technique over laboratory methods. When the inner region extends further in the reservoir, but is still small, the rate step could be made longer to allow the effects of the inner region to die.

Table 5.19: Relative permeabilities for the composite system

Parameter	Input value
p_i	5202.3 psi
S_{gi}	10%

Data used in Eq. 5-19						Results	
Step No.	q_o STB/D	tl D	p ($t1$) psi	$t2$ D	p ($t2$) psi	k_{ro}	k_{rg}
1	500.0	0.14584	4996.31	0.15	4995.93	0.794%	1.385e-02
2	1000.0	0.29584	4762.94	0.30	4762.33	0.7515	1.688e-02
3	2000.0	0.44584	4246.30	0.45	4245.01	0.7115	2.346e-02
4	3000.0	0.59584	3618.47	0.60	3616.67	0.7099	3.009e-02
5	4000.0	0.74584	2930.90	0.75	2925.38	0.6666	3.61e-02 3.61e-02

Table 5.20: Oil saturations for the composite system

	Data used in Eq. 5-10							Results
	p ($t1$)	k_{ro1}	k_{rg1}	S_{o1}	p ($t2$)	k_{ro2}	k_{rg2}	S_{o2}
1	5202.3	0.81	0.01	0.9	5086.07	0.795	1.385e-02	0.885
2	4995.93	0.795	1.385e-02	0.885	4883.50	0.752	1.688e-02	0.87
3	4762.33	0.752	1.688e-02	0.87	4639.74	0.711	2.346e-02	0.854
4	4245.01	0.711	2.346e-02	0.854	4101.44	0.7099	3.009e-02	0.835
5	3616.67	0.7099	3.009e-02	0.835	3440.66	0.666	3.609e-02	0.812

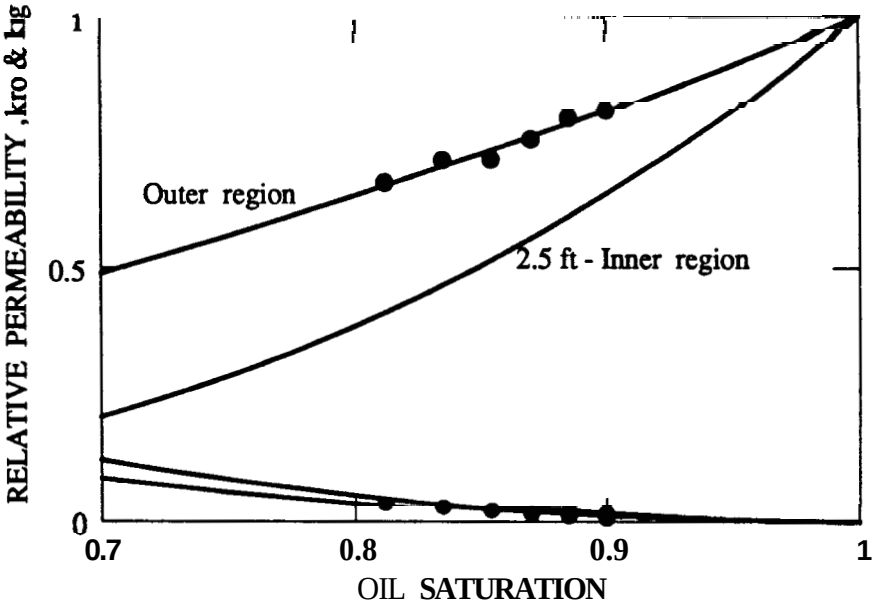

Figure 5.8 : **Relative permeability vs.** oil **saturation for** the **composite system, Example** 1

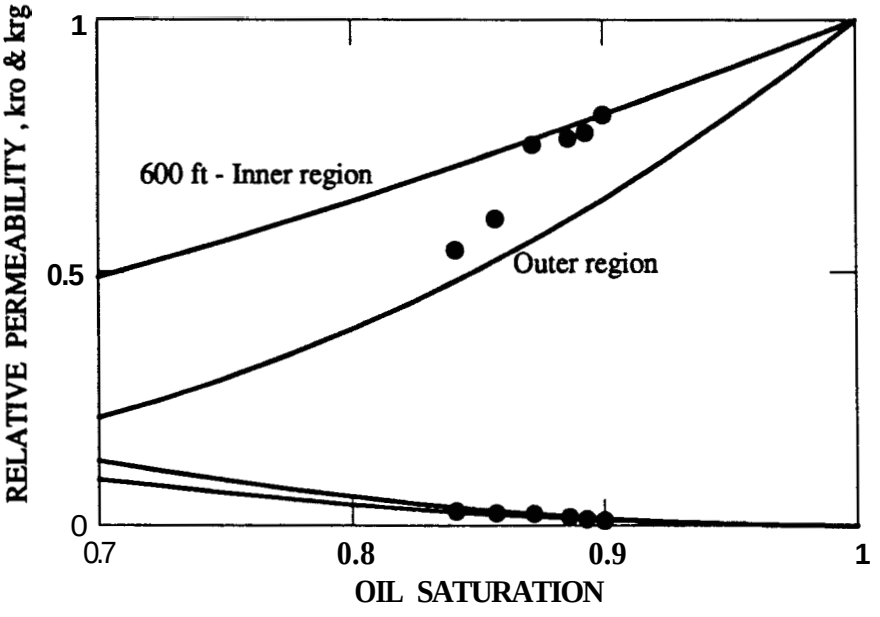

Figure 5.9 : **Relative permeability vs.** oil **saturation for** the **composite system, Example 2**

Example 2 - 600 ft Inner Region

The one-dimensional, radial two-phase model used to simulate Example 1, was also used for this example with the following changes. The inner region was 600 ft radius, and had the quadratic relative permeability relations defined by *Eq.* 5-25. For this example, the outer region relative permeabilities were represented by Corey-type relative permeabiiity relations, as in Eqs. 5-22 and 5-23.

The multiple-rate test was repeated at the same starting saturation and pressure of Example 1. The resulting relative permeability curves are shown in Fig. 5.9. As can be seen, the effects of the outer region did not *appear* until late in the test. Such a test could be repeated with shorter rate step periods in order to reduce the outer region effects.

5.7 Estimation of the Absolute Permeability

Both the pressure and pressure-squared methods described in Section 4 result in estimates of effective phase permeabiities. If the reservoir average saturation is known, and the corresponding resewoir relative permeability is available, an estimate of the absolute pemeability can be obtained. Raghavan's method for solution gas-drive reservoirs, extended in Section 6 to three-phase flow reservoirs, is reasonable if reservoir relative permeabilities are used. Therefore, unless single-phase tests are available, estimation of absolute permeability will require the (yet to be found) reservoir relative permeability.

The relative permeability technique yields effective permeabilities as functions of saturation if absolute permeability is not known. When the technique is applied to a multiple-rate test, the effective permeabilities can be obtained for a 10 - 15% change in the sandface saturation. At a later stage of depletion, the test can be repeated to cover further saturation ranges. Results of one or more tests can be used to estimate the absolute permeability. The wetting phase effective permeabilities for the saturation range tested can be matched by the following relation:

$$k_w = k\,(S_w)^{n'} \qquad (5\text{-}26)$$

Here, w refers to the wetting phase.

A regression match of the data with Eq. 5-26 can be obtained for the wetting phase effective permeabilities over the entire range of tested saturation. This match should result in both the absolute permeability, k, and an exponent, n'. Since the saturation in Eq. 5-26 is not normalized, the exponent obtained is not the same as that in the Corey-type equation (Eq. 5.22). In general, the absolute permeability obtained falls in a range of acceptable accuracy, as will be seen in the following two examples.

Results of this approach can be improved as more multiple-rate tests are analyzed to cover large saturation ranges. If a long segment of the wetting phase effective permeability

curve is available, more representative relations would result from the match. It may also be possible to use other relative permeability relations (e.g. Chierici, 1984). This kind of match may yield both the absolute permeability and the residual wetting phase saturation.

The absolute permeability obtained is sensitive to the accuracy of multiple-rate test results. Nevertheless, this application of the relative permeability technique offers a direct method to estimate reservoir absolute permeability.

Example 1

Table 5-21 shows the results of the first test (Case 1) previously reported. This test started at the bubble point pressure which declined to form an oil-gas region around the wellbore. Therefore, normal (pressure or pressure squared approaches) analysis may result in underestimated absolute permeability. The wetting phase (oil) relative permeability curve used to generate the test data was:

$$k_{rw} = (S_w^*)^{3.3}$$

where:

$$S_w^* = \frac{(S_w - 0.20)}{(1 - 0.20)}$$

Therefore, the input wetting phase effective permeability curves used to generate the first test were:

$$k_w = 10.0\ (S_w^*)^{3.3}$$

Where, the input absolute permeability is 10.0 md.

A regression fit by Eq. 5-26 results in both k and n', but here. In this example, approximate results were obtained using only two points in Eq. 5-26. When the first two points of Table 5-21 were used, the following was obtained:

$$n' = 3.458$$

k = 9.544 md.

The resulting absolute permeability is in good agreement with the input value of 10.0 md.

Example 2

Table 5-22 shows the results from the second test (Case 1) previously discussed. The wetting phase (oil) relative permeability curve used in Test 1 was also used to generate this test.

When a regression fit was performed using all points in Table 5-22, the following values for the parameters were obtained:

$n' = 4.925$

k = 11.71 md.

The estimate obtained for absolute permeability compared reasonably with the 10 md input value. This application of the proposed technique demonstrates a way to estimate the absolute permeability of multiphase reservoirs.

Table 5.21: Effective permeability - saturation results for the first test (Case 1)

S_o	k_o, md
0.986	9.09
0.97	8.59
0.936	7.47

Table 5-22: Effective permeability - saturation results for the second test (Case 1)

S_o	k_o, md
0.844	4.90
0.8276	4.68
0.798	4.26
0.763	2.78

6. RELATIVE PERMEABILITY TECHNIQUE FOR THREE-PHASE FLOW RESERVOIRS

Simultaneous flow of oil and gas in the presence of mobile water can be described by three-phase relative permeabilities. Three-phase flow occurs during carbon dioxide injection, steam drive, in-situ combustion, and other EOR processes. Three-phase flow also occurs for reservoirs producing by simultaneous gas and water drive. When produced by water drive, solution gasdrive reservoirs encounter three-phase flow.

This Section describes an extension of the relative permeability technique (discussed in Section 5 for two-phase flow) to three-phase flow reservoirs. The three-phase diffusivity equation was derived in terms of the pseudopressure function, $m(p)$. This equation was then solved and superposed to obtain the multiple-rate transient solution in terms of $m(p)$, the basis of the three-phase relative pexmeabiity equations. Following an approach similar to that of Bϕe et al. (1981), equivalent three-phase pressure-saturation equations were derived to permit calculations of the sandface saturations.

The proposed approach was investigated with several multiple-rate tests generated using the ECLIPSE simulator. These tests covered a range of 30 96 in both oil and gas saturations.

6.1 Pseudopressure Solution for Three-phase Flow

The three-phase flow equations, given in Eqs. 4-1 to 4-3, may be expressed as:

for oil:

$$\nabla \cdot [a_{vp}] = \frac{\phi}{k} \frac{\partial \beta}{\partial t} \tag{6-1}$$

for gas:

$$\nabla \cdot [a \nabla p] = \frac{\phi}{k} \frac{\partial b}{\partial t} \tag{6-2}$$

and for water.

$$\nabla \cdot \left[\gamma \nabla p\right] = \frac{\phi}{k} \frac{\partial \zeta}{\partial t} \tag{6-3}$$

where:

a, β, a, b were defined in Eqs. 2-27, 2-28, 2-30 and 2-39 respectively. Other parameters are defined as follows:

$$\gamma = \frac{k_{rw}}{\mu_w B_w} \tag{6-4}$$

and

$$\zeta = \frac{S_w}{B_w} \tag{6-5}$$

These flow equations neglect both gravity and capillary effects. It was also assumed that oil does not evaporate into the gas phase, and that gas does not dissolve in the water phase. The resewoir was assumed to be homogeneous and isotropic.

Following a treatment simiiar to that of Bϕe et al. (1981) for a solution gas-drive reservoir, the three-phase pseudopressure function, $m(p)$, can take any of the following definitions:

$$m_o(p) = \int_0^p \alpha \, dp \tag{6-6}$$

$$m_l(p) = \int_0^p (\alpha + \gamma) \, dp \tag{6-7}$$

$$m_t(p) = \int_0^p (\alpha + a + \gamma) \, dp \tag{6-8}$$

Equation 6-6 represents constant oil rate, Eq. 6-7 applies for constant liquid rate, and Eq. 6-8 applies for constant total rate. In the following derivation, Eq. 6-6 constant oil rate, is used for the inner boundary condition For simplicity, $m_o(p)$ will be written as $m(p)$.

The Boltzman transformation was applied to the flow equations in terns of $m(p)$. The

Boltzman transform variable, y, is defined as:

$$y = \frac{\phi r^2}{4kt} \tag{6-9}$$

Equation 6-1 can be written for radial flow as:

$$\frac{1}{r}\frac{\partial}{\partial r}\left[\alpha r \frac{\partial p}{\partial r}\right] = \frac{\phi}{k}\frac{\partial \beta}{\partial t}, \tag{6-10}$$

which can be expressed using the Boltzman transform, as:

$$\frac{1}{r}\frac{\partial y}{\partial r}\frac{\partial}{\partial y}\left[\alpha r \frac{\partial p}{\partial r}\right] = \frac{\phi}{k}\frac{\partial y}{\partial t}\frac{\partial \beta}{\partial y} \tag{6-11}$$

and reduced to:

$$\frac{d}{dy}\left[\alpha y \frac{dp}{dy}\right] = -y\frac{d\beta}{dy} \tag{6-12}$$

However, from Eq. 6-6:

$$\alpha \frac{dp}{dy} = \frac{dm}{dy} \tag{6-13}$$

The variable β is a function of pressure and any two of the three saturations. Hence:

$$\frac{d\beta}{dy} = \beta' \frac{dp}{dy} + \dot{\beta}\frac{dS_o}{dy} + \beta^* \frac{dS_g}{dy} \tag{6-14}$$

where the following definitions apply for any three phase parameter, x_3:

$$x_3' = \left[\frac{\partial x_3}{\partial p}\right]_{S_o,S_g} \tag{6-15-a}$$

$$\dot{x}_3 = \left[\frac{\partial x_3}{\partial S_o}\right]_{p,S_g} \tag{6-15-b}$$

$$x_3^* = \left[\frac{\partial x_3}{\partial S_g}\right]_{p,S_o} \tag{6-15-C}$$

Substituting Eqs. 6-13 and 6-14 in Eq. 6-12 results in:

$$\frac{d}{dy}\left[y\,\frac{dm}{dy}\right] = -y\left[\beta' + \dot{\beta}\,\frac{dS_o}{dp} + \beta^*\,\frac{dS_g}{dp}\right]\frac{dp}{dy} \qquad (6\text{-}16)$$

which can be rewritten as:

$$\frac{d}{dy}\left[y\,\frac{dm}{dy}\right] = -y\left[\beta' + \dot{\beta}\,\frac{dS_o}{dp} + \beta^*\,\frac{dS_g}{dp}\right]\alpha^{-1}\,\frac{dm}{dy} \qquad (6\text{-}17)$$

Using the following definition:

$$\left[\frac{c}{\lambda}\right]^{**} = \left[\beta' + \dot{\beta}\,\frac{dS_o}{dp} + \beta^*\,\frac{dS_g}{dp}\right]\alpha^{-1} \qquad (6\text{-}18)$$

Equation 6-17 can be written as:

$$\frac{d}{dy}\left[y\,\frac{dm}{dy}\right] = -\left[\frac{c}{\lambda}\right]^{**} y\,\frac{dm}{dy} \qquad (6\text{-}19)$$

The term $(c/\lambda)^{**}$ is the three-phase compressibility-mobility ratio, which corresponds to $(c/\lambda)^{*}$ for solution gas-drive reservoirs. When $(c/\lambda)^{**}$ is assumed constant, Eq. 6-19 becomes a linear equation in terms of $m(p)$.

Equation 6-19 can be solved using standard procedures for single-phase pressure equations. The line source solution can be written, in field units, as:

$$m(p_{wf}) = m(p_i) + \frac{70.6\,q_o}{k\,h}\,E_i\left[-\frac{56900\,\phi\,r_w^2}{k\,t}\left(\frac{c}{\lambda}\right)^{**}\right] \qquad (6\text{-}20)$$

If the logarithmic appmximation applies, Eq. 6-20 reduces to:

$$m(p_w) = m(p_i) - \frac{141.2\,q_o}{k\,h}\left[0.5\,(\ln t_D + 0.80907)\right] \qquad (6\text{-}21)$$

where

$$t_D = \frac{0.000264\,k\,t}{\phi\,(c/\lambda)^{**}\,r_w^2} \qquad (6\text{-}22)$$

When Eq. 6-22 replaces Eq. 5-2, Eq. 6-21 derived for three-phase flow becomes identical to Eq. 5-1 derived by Bøe et al (1981) for solution gas-drive reservoirs.

6.2 Relative Permeability Equations

The following multiple-rate solution can be obtained for three-phase flow reservoirs:

$$\frac{m(p_i) - m(p_{wf})}{q_n} = \frac{162.6}{k\,h} \sum_{j=1}^{n} \frac{\Delta q_j}{q_n} \log\left[t - t_{j-1}\right] + \frac{162.6}{k\,h}\left\{\log\left[\frac{k}{\phi\, r_w^2}\left(\frac{\lambda}{c}\right)^{**}\right] - 3.2275 + 0.86895\, s\right] \quad (6\text{-}23)$$

where:

q_j : surface rate during step j,

t_{j-1} : starting time of step j,

q_n : the final rate.

When considering the response of a specific rate step, n, Eq. 6-23 simplifies to:

$$m(p_{wf}) = -\frac{162.6}{k\,h}\left\{\sum_{j=1}^{n} \Delta q_j \log\left[t - t_{j-1}\right]\right\} + C_3 \quad (6\text{-}24)$$

where C_3 is a constant defined as:

$$C_3 = m(p_i) - \frac{162.6\, q_n}{k\,h}\left\{\log\left[\frac{k}{\phi\, r_w^2}\left(\frac{\lambda}{c}\right)^{**}\right] - 3.2275 + 0.86895\, s\right\} \quad (6\text{-}25)$$

Equation 6-24 is similar to Eq. 5-15 with C_3 defined by Eq. 6-25 replacing C_2 defined by Eq. 5-16. Based on this, the oil relative permeability equation is identical to that for two-phase systems and given by Eq. 5-19. Similarly, gas and water relative permeability equations are identical to Eqs. 5-8 and 5-12 respectively.

6.3 Saturation Equations

The three-phase saturation equations were derived, following a procedure similar to that applied by Bøe at al. (1981) in deriving the two-phase saturation equations for solution gas-drive reservoirs (which are Eqs. 5-9 and 5-10).

The Boltzman transformation permits to write the oil flow equation as (Eq. 6-12):

$$\frac{d}{dy}\left[\alpha\, y \frac{dp}{dy}\right] = -\,y\,\frac{d\beta}{dy} \quad (6\text{-}26)$$

Similarly the gas and water flow equations may be written as:

$$\frac{d}{dy}\left[a\,y\,\frac{dp}{dy}\right] = -\,y\,\frac{db}{dy} \tag{6-27}$$

$$\frac{d}{dy}\left[\gamma\,y\,\frac{dp}{dy}\right] = -\,y\,\frac{d\zeta}{dy} \tag{6-28}$$

Any three-phase parameter, x_3, is a function of the pressure and any two of the three phases saturations. Hence, the total derivative is:

$$dx_3 = \left[\frac{\partial x_3}{\partial p}\right]_{S_o,\,S_g} dp + \left[\frac{\partial x_3}{\partial S_o}\right]_{p,\,S_g} dS_o + \left[\frac{\partial x_3}{\partial S_g}\right]_{p,\,S_o} dS_g \tag{6-29}$$

or:

$$dx_3 = x_3'\,dp + \dot{x}_3\,dS_o + x_3^*\,dS_g \tag{6-30}$$

The following definitions are also used in the derivation:

$$N = y\,\frac{dp}{dy} \quad ; \quad K = y\,\frac{dS_o}{dy} \quad ; \quad L = y\,\frac{dS_g}{dy} \tag{6-31}$$

Equation 6-27 can be rearranged to:

$$y\,\frac{dp}{dy}\,\frac{da}{dy} + a\,\frac{d}{dy}\left[y\,\frac{dp}{dy}\right] = -\,y\,\frac{db}{dy} \tag{6-32}$$

which can be written as:

$$N\,\frac{da}{dy} + a\,\frac{dN}{dy} = -\,y\,\frac{db}{dy} \tag{6-33}$$

The derivatives of a and b in Eq. 6-33 may be expanded, using Eq. 6-30:

$$N\left[a'\,\frac{dp}{dy} + \dot{a}\,\frac{dS_o}{dy} + a^*\,\frac{dS_g}{dy}\right] + a\,\frac{dN}{dy}$$

$$= -\,y\left[b'\,\frac{dp}{dy} + \dot{b}\,\frac{dS_o}{dy} + b^*\,\frac{dS_g}{dy}\right] \tag{6-34}$$

which *can* be simplified, applying the definitions of Eq. 6-31, to:

$$N\left[a'\frac{N}{y} + \dot{a}\frac{K}{y} + a^*\frac{L}{y}\right] + a\frac{dN}{dy} = -y\left[b'\frac{N}{y} + \dot{b}\frac{K}{y} + b^*\frac{L}{y}\right] \tag{6-35}$$

Grouping the terms of this equation, it reduces to:

$$a\frac{dN}{dy} + N\left[a'\frac{N}{y} + b'\right] + K\left[\dot{a}\frac{N}{y} + \dot{b}\right] + L\left[a^*\frac{N}{y} + b^*\right] = 0 \tag{6-36}$$

Similarly for the oil phase, Eq. 6-13 leads to:

$$\alpha\frac{dN}{dy} + N\left[\alpha'\frac{N}{y} + \beta'\right] + K\left[\dot{\alpha}\frac{N}{y} + \dot{\beta}\right] + L\left[\alpha^*\frac{N}{y} + \beta^*\right] = 0 \tag{6-37}$$

Also for water, Eq. 6-28 yields:

$$\gamma\frac{dN}{dy} + N\left[\gamma'\frac{N}{y} + \zeta'\right] + K\left[\dot{\gamma}\frac{N}{y} + \dot{\zeta}\right] + L\left[\gamma^*\frac{N}{y} + \zeta^*\right] = 0 \tag{6-38}$$

The term $\frac{dN}{dy}$ can be evaluated, using Eq. 6-38:

$$\frac{dN}{dy} = -\frac{N}{\gamma}\left[\gamma'\frac{N}{y} + \zeta'\right] - \frac{K}{\gamma}\left[\dot{\gamma}\frac{N}{y} + \dot{\zeta}\right] - \frac{L}{\gamma}\left[\gamma^*\frac{N}{y} + \zeta^*\right] \tag{6-39}$$

Substitution of Eq. 6-39 into Eq. 6-36 yields:

$$-\frac{N a}{Y}\left[\gamma' \frac{N}{Y} + \zeta'\right] - \frac{K a}{\gamma}\left[\gamma \frac{E}{Y} + \dot{\zeta}\right] - \frac{L a}{\gamma}\left[\gamma^* \frac{N}{y} + \zeta^*\right]$$
$$+ N\left[a \frac{\dot{N}}{y} + b'\right] + K\left[\dot{a} \frac{N}{y} + b\right] + L\left[a^* \frac{N}{y} + b^*\right] = 0 \qquad (6\text{-}40)$$

which can be multiplied by $\frac{\gamma}{N}$ and factored to yield:

$$\frac{K}{N}\left\{\left[\dot{a}\gamma - a\dot{\gamma}\right]\frac{N}{y} + \left[\gamma \dot{b} - a\dot{\zeta}\right]\right\}$$
$$+ \frac{L}{N}\left\{\left[a^*\gamma - a\gamma^*\right]\frac{N}{y} + \left[\gamma b^* - a\zeta^*\right]\right\}$$
$$+ \frac{N}{y}\left\{\left[\gamma a' - a\gamma'\right]\right\} + \left[\gamma b' - a\zeta'\right] = 0 \qquad (6\text{-}41)$$

From the definitions of Eq. 6-31, the following hold:

$$\frac{K}{N} = \frac{dS_o}{dp} \qquad (6\text{-}42)$$

and

$$\frac{L}{N} = \frac{dS_g}{dp} \qquad (6\text{-}43)$$

If these relations are substituted into Eq. 6-41, the following results:

$$\frac{dS_o}{dp} = \frac{\left[a\gamma^* - \gamma a^*\right]\frac{N}{y} + \left[a\zeta^* - \gamma b^*\right]}{\left[\dot{a}\gamma - \dot{\gamma}a\right]\frac{N}{y} + \left[\gamma \dot{b} - a\dot{\zeta}\right]} \frac{dS_g}{dp}$$
$$+ \frac{\left[a\gamma' - \gamma a'\right]\frac{N}{y} + \left[a\zeta' - \gamma b'\right]}{\left[\gamma \dot{a} - a\dot{\gamma}\right] + \left[\gamma \dot{b} - a\dot{\zeta}\right]} \qquad (6\text{-}44)$$

Similarly, if Eq. 6-39 is substituted into Eq. 6-37 the result is:

$$-\frac{Na}{Y}\left[\gamma' \frac{N}{y} + \zeta'\right] - \frac{Ka}{\gamma}\left[\dot{\gamma} \frac{N}{y} + \dot{\zeta}\right] - \frac{L\alpha}{\gamma}\left[\gamma^* \frac{N}{y} + \zeta^*\right]$$
$$+ N\left[\alpha' \frac{N}{y} + \beta'\right] + K\left[\dot{\alpha} \frac{N}{y} + p\right] + L\left[\alpha^* \frac{N}{y} + p\right] = 0 \qquad (6\text{-}45)$$

which, if multiplied by $\frac{\gamma}{N}$ and factored, yields:

$$\frac{K}{N}\left\{\left[\gamma\dot{\alpha}-\alpha\dot{\gamma}\right]\frac{N}{y}+\left[\gamma\dot{\beta}-\alpha\dot{\zeta}\right]\right\}$$
$$+\frac{K}{N}\left\{\left[\gamma\alpha^{*}-\alpha\gamma^{*}\right]\frac{N}{y}+\left[\gamma\beta^{*}-\alpha\zeta^{*}\right]\right\}$$
$$+\frac{N}{\gamma}\left[\gamma\alpha'-a\gamma'\right]+\left[\gamma\beta'-\alpha\zeta'\right]=0 \qquad (6\text{-}46)$$

This equation *can* be written as:

$$\frac{dS_o}{dp}=\frac{\left[\alpha\gamma^{*}-\gamma\alpha^{*}\right]\frac{N}{y}+\left[\alpha\zeta^{*}-\gamma\beta^{*}\right]}{\left[\dot{\alpha}\gamma-\dot{\gamma}\alpha\right]\frac{N}{y}+\left[\gamma\dot{\beta}-\alpha\dot{\zeta}\right]}\frac{dS_g}{dp}$$
$$+\frac{\left[\alpha\gamma'-\gamma\alpha'\right]\frac{N}{y}+\left[\alpha\zeta'-\gamma\beta'\right]}{\left[\gamma\dot{\alpha}-\alpha\dot{\gamma}\right]\frac{N}{y}+\left[\gamma\dot{\beta}-\alpha\dot{\zeta}\right]} \qquad (6\text{-}47)$$

Equating Eqs. 647 and 6-44 yields the following pressure-saturation relation for gas phase :

$$\frac{dS_g}{dp}=\frac{II}{I} \qquad (6\text{-}48)$$

where:

$$II=\left\{\frac{\left[a\gamma'-\gamma a'\right]\frac{N}{y}+\left[a\zeta'-\gamma b'\right]}{\left[\dot{a}\gamma-\dot{\gamma}a\right]\frac{N}{y}+\left[\gamma\dot{b}-a\dot{\zeta}\right]}\right.$$
$$\left.-\frac{\left[\alpha\gamma'-\gamma\alpha'\right]\frac{N}{y}+\left[\alpha\zeta'-\gamma\beta'\right]}{\left[\gamma\dot{\alpha}-\alpha\dot{\gamma}\right]\frac{N}{y}+\left[\gamma\dot{\beta}-\alpha\dot{\zeta}\right]}\right\} \qquad (6\text{-}49)$$

and:

$$I=\left\{\frac{[a\gamma^{*}-y\,a^{*}]\frac{N}{\gamma}+[a\zeta^{*}-y\,\beta^{*}]}{\left[\gamma\dot{\alpha}-\alpha\dot{\gamma}\right]\frac{N}{\gamma}+\left[\gamma\dot{\beta}-\alpha\dot{\zeta}\right]}\right.$$
$$\left.-\frac{\left[a\gamma^{*}-\gamma a^{*}\right]\frac{N}{\gamma}+\left[a\zeta^{*}-y\,b^{*}\right]}{\left[\gamma\dot{a}-a\dot{\gamma}\right]\frac{N}{y}+\left[\gamma\dot{b}-a\dot{\zeta}\right]}\right\} \qquad (6\text{-}50)$$

Equation 6-48 may be substituted into Eq. 6-47 to obtain the following pressure-saturation relation for the oil phase:

$$\frac{dS_o}{dp} = \frac{\left[\alpha\gamma^* - \gamma\alpha^*\right]\frac{N}{y} + \left[\alpha\zeta^* - \gamma\beta^*\right]}{\left[\dot{\alpha}\gamma - \dot{\gamma}\alpha\right]\frac{N}{y} + \left[\gamma\dot{\beta} - \alpha\dot{\zeta}\right]}\ \frac{II}{I} + \frac{\left[\alpha\gamma' - \gamma\alpha'\right]\frac{N}{y} + \left[\alpha\zeta' - \gamma\beta'\right]}{\left[\gamma\dot{\alpha} - \alpha\dot{\gamma}\right]\frac{N}{y} + \left[\gamma\dot{\beta} - \alpha\dot{\zeta}\right]} \tag{6-51}$$

Equations 6-48 and 6-51 for three-phase flow are equivalent to Eq. 5-9 for solution gasdrive reservoirs. While there is only one variable saturation for two-phase flow in Eq. 5-9, there are two variable saturations for three-phase flow described by Eqs. 6-48 and 6-51. Simultaneous iteration of both equations is necessary to yield the two unknowns (S_o and S_g).

6.3.1 Early Time Period

At very early times, as t tends to zero, the Boltzman transform variable, y, tends to infinity. Since N is bounded, the term $\frac{N}{Y}$ tends to zero for the early producing times.

Therefore, Eq. 6-48 reduces to:

$$\frac{dS_g}{dp} = \frac{IV}{III} \tag{6-52}$$

where:

$$IV = \frac{a\zeta' - \gamma b'}{\gamma b - a\dot{\zeta}} - \frac{\alpha\zeta' - \gamma\beta'}{\gamma\dot{\beta} - \alpha\dot{\zeta}} \tag{6-53}$$

and:

$$III = \frac{\alpha\zeta^* - \gamma\beta^*}{\gamma\dot{\beta} - \alpha\dot{\zeta}} - \frac{a\zeta^* - \gamma b^*}{\gamma b - a\dot{\zeta}} \tag{6-54}$$

Similarly, Eq. 6-51 reduces to:

$$\frac{dS_o}{dp} = \frac{\alpha\zeta^* - \gamma\beta^*}{\gamma\dot{\beta} - \alpha\dot{\zeta}}\ \frac{IV}{III} + \frac{\alpha\zeta' - \gamma\beta'}{\gamma\dot{\beta} - \alpha\dot{\zeta}} \tag{6-55}$$

Equations 6-52 and 6-55 provide three-phase pressure-saturations relations that apply at early times. Such equations may be used to estimate rapid changes in sandface saturations that occur within the first few minutes of a well test.

6.4 Numerical Applications

A one-dimensional, 40-block radial model was constructed using the ECLIPSE simulator. This model was then used to test the proposed approach for a homogeneous system. Multiple-rate tests were generated using a single set of relative permeability curves describing the entire drainage area. All simulation runs used the PVT properties reported by Bøe et al. (1981).

In general, the proposed approach allows any phase relative permeability to be a function of any pair of phase saturations. This can be seen in the definition of the total derivative of Eq. 6-30. Hence, this approach is likely to be more applicable than probability models which consider gas and water relative permeabilities to depend only on their individual saturations.

Three multiple-rate tests were simulated using the following oil and gas relative permeability relations, defined as :

$$k_{ro} = S_o^2 \tag{6-56}$$

$$k_{rg} = S_g^2 \tag{6-57}$$

Water relative permeabilities are presented in Table 6-1.

For all of the simulated tests, water saturation changed only slightly during each multiple-rate test. Water saturation change should be more pronounced for situations where gas is allowed to dissolve in the water phase. All three multiple-rate tests were simulated at the same starting water saturation, $S_w = 30\%$. This mobile water saturation changed only within the range of 28 - 30% at the sandface, during each test. The same initial water saturation was used for all three tests to simplify the demonstration which covered a considerable range of gas and oil saturations at the sandface.

Three multiple-rate tests were simulated at different stages of depletion, but all were at the Same initial water saturation. These three tests covered a range of 30% gas and oil saturation changes.

Relative permeabilities were evaluated using Eqs. 5-19, 5-8, and 5-12. Sandface saturations were estimated by a simultaneous iteration on Eqs. 6-52 and 6-55.

Input data for all three tests is given in Table 6-2. The relative permeability results for the first test are presented in Table 6-3, while the saturation results are shown in Table 6-4. The corresponding tables for the second test are Tables 6-5 and 6-6, and those for the third test are Tables 6-7 and 6-8. The resulting estimates of oil relative permeabilities for all the three tests are plotted in Fig. 6-1, and compared with the input, "reservoir", data (curves). A reasonable match was obtained. Oil relative permeability is normally plotted on a ternary saturation diagram. However, for this simple demonstration, water saturation was almost constant for all three tests. Therefore, oil relative permeability was plotted against oil saturation only. In general, oil relative permeability obtained by the proposed approach should contribute a part of the oil relative permeability ternary diagram.

The resulting estimates of gas relative permeabilities are presented in Fig. 6-2, and found to be in good agreement with the input data curves. Water relative permeability was equal to a reasonably constant value of 0.018 throughout the tests. The obtained water relative permeability was in good agreement with the input value of 0.02, and was constant because water saturation did not change much during these simulated tests.

The proposed technique produced three-phase relative permeabilities of reasonable values. A transient multiple-rate test may be run at any stage of depletion to cover a range of 10-15% in future gas saturation. Neither long production data, nor extrapolation is required for this method.

Table 6.1: Water relative permeability data for the three phase runs.

S_w	k_{rw}
0.2	0.0
0.3	0.02
0.4	0.06
0.5	0.15
0.6	0.25

Table 6.2 : Input data for all three phase runs.

Item	Input value
r_w	0.3 ft
ϕ	0.15
c_r	3.0×10^{-6} psi^{-1}
k	20 md.
h	100 ft.
B_w	1 Rb/STB
μ_w	1 cp.

Table 63: Relative permeability for the first test

Data used in Eqs. 5-19 and 5-8						Results	
Step No.	q_o STBD	t1 D	$p(t1)$ psi	$t2$ D	$p(t2)$ psi	k_{ro}	k_{rg}
1	500	0.044	5477.75	0.05	5475.03	0.447	0.000714
2	1000	0.094	5221.01	0.10	5217.18	0.472	0.00211
3	2000	0.144	4663.03	0.15	4654.77	0.43	0.00486
4	3000	0.194	3992.18	0.20	3980.34	0.413	0.0079
5	4000	0.244	3170.83	0.25	3155.92	0.416	0.0133
6	4500	0.294	2609.02	0.30	2594.23	0.352	0.0138

Table 6.4: Oil saturation for the first test

Data used in *Eqs.* 6-52 and *6-55*								Results
Step No.	P $(t1)$ psi	k_{ro1}	k_{rg1}	S_{o1}	P $(t2)$ psi	k_{ro2}	k_{rg2}	S_{o2}
1	5703.0	0.49	0.0	0.7	5560.0	0.447	7.14e-04	0.687
2	5474.83	0.447	7.14e-04	0.687	5342.5	0.472	2.11e-03	0.6773
3	5216.71	0.472	2.11e-03	0.6773	4940.18	0.43	4.86e-03	0.651
4	4653.97	0.43	4.86e-03	0.651	4333.31	0.413	7.9e-03	0.62
5	3978.29	0.413	7.9e-03	0.62	3786.28	0.416	1.33e-02	0.602
6	3152.92	0.416	1.33e-02	0.602	3044.74	0.352	1.38e-02	0.591

Table 6.5: Relative permeability for the second test

Data used in Eqs. 5-19 and 5-8						Results	
Step No.	q_o STB/D	$t1$ D	$p(t1)$ psi	$t2$ D	$p(t2)$ psi	k_{ro}	k_{rg}
1	500	0.044	4895.7	0.05	4892.11	0.347	0.0131
2	1000	0.094	4539.16	0.10	4533.44	0.334	0.0158
3	2000	0.144	3714.74	0.15	3702.17	0.321	0.0215
4	3000	0.194	2592.07	0.20	2571.90	0.314	0.0277
5	4000	0.244	778.03	025	741.40	0.304	0.0529

Table 6.6: Oil saturation for the second test

Data used in Eqs. 6-52 and 6-55								Results
Step No.	$p(t1)$, psi	k_{ro1}	k_{rg1}	S_{o1}	$p(t2)$, psi	k_{ro2}	k_{rg2}	S_{o2}
1	5202.0	0.36	0.01	0.6	5101.35	0.347	1.31e-02	0.59
2	4891.44	0.347	1.31e-02	0.59	4796.32	0.334	1.58e-02	0.582
3	4530.53	0.334	1.58e-02	0.582	4317.89	0.321	2.15e-02	0.564
4	3691.07	0.321	2.15e-02	0564	3433.60	0.314	2.77e-02	0.543
5	2544.87	0.314	2.77e-02	0.543	2229.81	0.304	5.29e-02	0.523

Table 6.7: Relative permeability for the third test

Data used in Eqs. 5-19 and 5-8						Results	
Step No.	q_o STB/D	$t1$ D	$p(t1)$ psi	$t2$ D	$p(t2)$ psi	k_{ro}	k_{rg}
1	500	0.044	4064.7	0.05	4058.9	0.236	0.0493
2	1000	0.094	3449.45	0.10	3439.28	0.221	0.05166
3	2000	0.144	1659.66	0.15	1629.79	0.209	0.0753

Table 6.8: Oil saturation for the third test

Data used in Eqs. 6-52 and 6-55								Results
Step No.	$p(t1)$, psi	k_{ro1}	k_{rg1}	S_{o1}	$p(t2)$, psi	k_{ro2}	k_{rg2}	S_{o2}
1	4502.0	0.25	0.04	0.5	4282.62	0.236	4.93e-02	0.48
2	4056.65	0.236	4.93e-02	0.48	3732.79	0.221	5.166e-02	0.4597
3	3428.26	0.221	5.166e-02	0.4597	3024.62	0.209	7.53e-02	0.43

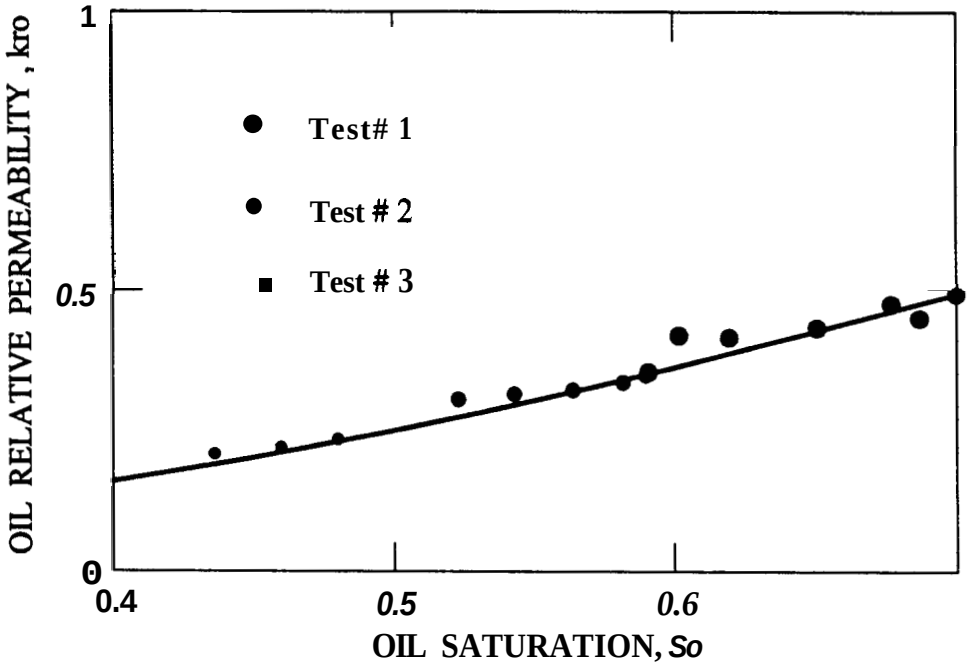

Figure 6.1: **Oil relative permeability vs. oil saturation for the three phase tests**

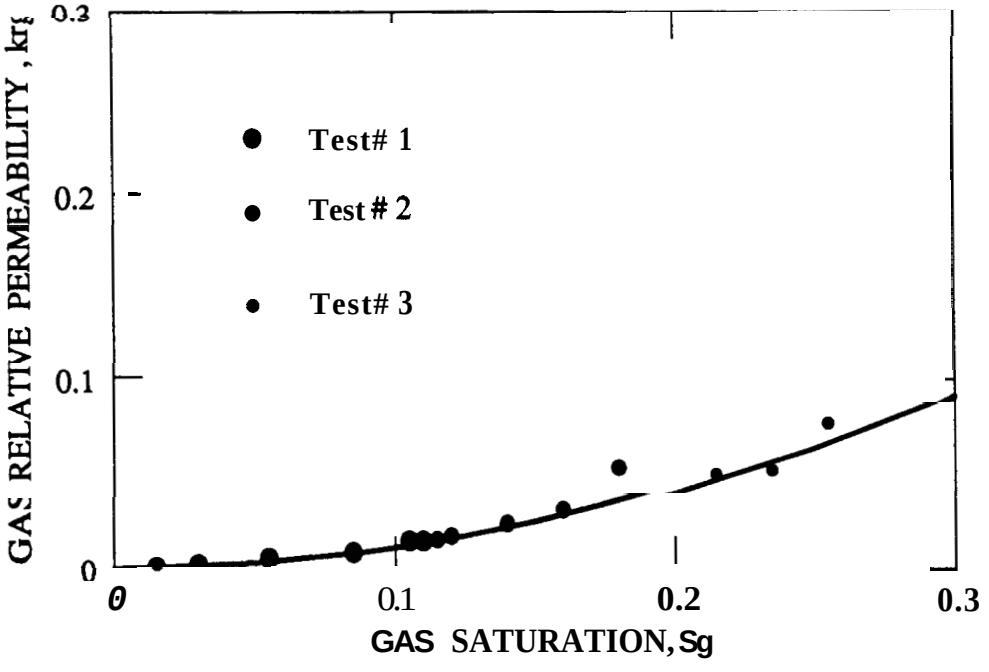

Figure 6.2: Gas relative permeability vs. gas saturation for the three phase tests

7. CONCLUSIONS AND RECOMMENDATIONS

7.1 Conclusions

This work can be divided into two parts. The first part is the new approach to analyze multiphase well tests. The second part is the technique to estimate the absolute and the relative permeabilities.

The New Approach to Multiphase Well Test Analysis

In this work, a practical approach to analyze multiphase well tests has been presented. This approach applies to systems in which a gas phase is present (i.e. gas-oil and gas-oil-water systems). Such an approach may be used to obtain estimates of effective phase permeabilities and wellbore skins. The multiphase flow equations were simplified to a diffusivity equation in terms of p^2. Line source solutions were applied to both simulated and published multiphase data. Semiempirical observation was used to account for different volatilities of oils. This resulted in three different forms of the solution. One of the forms was shown to reduce to Perrine's (1956) approach. However, other forms were different and they provided better estimates of effective oil permeabilities.

1. Multiphase flow was modelled by a diffusivity equation in terms of p^2. This equation was linearized assuming a constant total compressibility-mobility ratio. The inner boundary condition was also linearized based on the physical behavior of the system. The linear diffusivity equation was then solved with its linear boundary conditions to obtain the line source solution in terms of p^2. In general, pressure solutions reported in the literature can be followed to solve the diffusivity equation in terms of p^2 for any reservoir and testing condition.

2. Linearization of the inner boundary condition allowed different solutions to be considered. One of the solutions was found to reduce to Perrine's (1956) approach. Since Pemne's solution underestimates effective oil permeability, other solutions were also investigated. A generally applicable solution was found for volatile oils. For oils of low volatility two

solutions were chosen: the first was the same as that for volatile oils and was valid for drawdowns of small pressure drop and the following buildups, while the second was different and held for drawdowns of large pressure drop and their subsequent buildups. These solutions were found to estimate effective oil permeability more accurately than Penine's approach for all cases considered. Estimates of wellbore skin obtained by the new approach were accurate for drawdown tests, and slightly low for buildup tests, compared to those obtained by Perrine's approach.

3. Perrine's approach was found superior for application in two-phase, oil-water systems. For gas-oil and gas-oil-water systems, Perrine's approach was found to be rate sensitive and better applies at low flowing rate?. The rate normalization method, based on Penine's approach and currently used in the oil industry, applies only at low rates. Its sensitivity to rates is due to the terms neglected in deriving Perrine's approach and most importantly the improper linearization of the inner boundary condition. Such normalization requires that the total rate (oil and gas rates) be monitored throughout the test. It results in Underestimated values for the total system mobility and yields no individual phase permeability.

4. The new approach was found to apply for all rates in volatile oil systems. Based on this approach, a new rate normalization method was proposed for volatile oil systems. This method suggests that the test response in terms of p^2 be normalized using surface oil rates. Such a method is relatively insensitive to rates due to the proper linearization of the inner boundary condition and the proper treatment of the nonlinear terms when deriving the line source solution in terms of p^2. Moreover, it results in accurate estimates of individual phase permeabilities and thereby an accurate value for total system mobility.

5. The relation of $k_o / (\mu_o B_o)$ with pressure was assumed to have a constant slope and a zero intercept. This assumption facilitated the practical use of the pressure squared approach which was found applicable to all rates in volatile oil systems. On the other hand, the new approach was found to be rate-sensitive in oils of low volatility.

6. Martin's total compressibility was derived from basic principles. Martin's original assumption of negligible pressure and saturation gradients was avoided in this derivation. This demonstrates that Martin's relation is valid for any flow condition, provided thermodynamic equilibrium is reached and PVT properties reflect interphase mass transfer in the reservoir.
7. The Fetkovich empirical approach for isochronal oil-well testing was derived using the pseudosteady state solutions in terms of p^2. This approach, originally developed for solution gasdrive reservoirs, may be applicable to three-phase systems.

The Relative Permeability Technique

This work also developed a technique to estimate two- and three-phase relative permeabilities in-situ, using constant or multiple-rate tests. The proposed technique applies the solutions of the multiphase diffusivity equation in terms of a pseudopressure function, $m(p)$, which is defined by Eq. 2-17. The saturation equation of Bøe et al. (1981) was extended to three-phase systems and applied to estimate the sandface saturations during the test. Several two- and three-phase multiple-rate tests were simulated and analyzed to demonstrate the validity of the proposed technique.

The proposed technique is an improvement over current laboratory and historical performance methods. The resulting relative permeability curves reflect the in-situ reservoir heterogeneity, wettability and fluid composition, rather than those of a small core. The existing historical performance methods *need* data over long periods, yet only cover a range of saturation prior to present conditions - all future projections require extrapolation. By contrast, the proposed technique estimates relative permeabilities at values of sandface saturations that will not be reached by the average reservoir saturation until much later in the life of the field. The new technique is therefore a good forecasting tool in that it estimates the relative permeabilities at saturations that will exist far into the future. Based on the work done, the following conclusions are warranted:

1. The proposed technique estimates two- and three-phase relative pemeabilities to a good practical accuracy. A transient multiple-rate test may be run at any stage of depletion, to cover a range of 10-15% in future gas saturation Neither long term production data, nor extrapolations are needed for the approach.
2. The proposed technique was found applicable to reservoirs with composite relative pemeability regions. When the inner region is very small, this technique yields the relative permeability curves of the outer region On the other hand, when the inner region is very large, the obtained curves represent the inner region. The proposed method seems to be the most direct approach available to estimate relative permeabilities over a representative drainage area.
3. The relative permeability technique was also applied to estimate the absolute pemeabiity of multiphase reservoirs. An effective pemeability-saturation relation, with both the absolute permeability and an exponent as unknowns, was used to fit the results. Such a fit resulted in reservoir absolute permeability to a reasonable accuracy.

7.2 Recommendations

Extension of the pseudopressure solutions to three-phase reservoirs will have several other applications, besides the one reported here. Drawdown tests, run in three-phase reservoirs, may be analyzed using the pseudopressure approach to obtain an estimate of the reservoir absolute permeability. The three phase saturation equations may be coupled with the pseudopressure solutions to facilitate the analysis of these drawdown tests.

In general, multiphase well testing is very hard to tackle rigorously, thus simplifying assumptions have been used to facilitate the analytical treatment of the problem. This implies that there may be room for improvement in seeking a better, more accurate, way of simplifying the problem. Physical understanding of the multiphase flow will be essential for significant achievements in the future. Following are some of the pending problems in this field:

1. Applications of these techniques to both gas condensate and geothermal reservoirs,
2. Field applications of the relative penneabiiity technique. The resulting curves could then be compared to core relative permeabilities, thus suggesting a scaling procedure.
3. Application of the relative penneabiity technique to other types of heterogeneities, i.e. layered systems or randomly distributed sets of relative permeability curves,
4. Effect of wellbore storage on the relative permeabiity technique,
5. An index or a correlation for oil volatility.

NOMENCLATURE

$a = \frac{k_{rg}}{\mu_g B_g} + \frac{R_s k_{ro}}{\mu_o B_o}$

$b = \frac{\phi S_g}{B_g} + \frac{R_s \phi S_o}{B_o}$

B_l = formation volume factor of phase l, RB/STB, RB/MSCF

$\bar{B}_l$ = formation volume factor of phase l at $\bar{p}$

c = compressibility, psi–'

c_f = rock compressibility, psi–'

c_l = compressibility of phase l, psi–'

c_t = total system compressibility **(Eq. 9),** psi–'

$(\frac{c}{\lambda})^*$ = **compressibilityhnobility** ratio for solution gas-drive reservoir (Eq. **5-3)**

$(\frac{c}{\lambda})^{**}$ = **compressibilityhnobility** ratio for three-phase reservoir (Eq. 6-12-a)

C_2 = two-phase constant

C_3 = three-phase constant

GOR = producing gas-oil ratio, **MSCF/STB**

$\overline{GOR}$ = **GOR** at any (r,t), MSCF/STB

h = thickness, feet

J_o' = back-presswe curve coefficient, **STB/D/psi^{2n}**

k = absolute permeability, md

k_l = effective permeability of phase *1*, md

$\bar{k}_l$ = effective permeability of phase l **at** $\bar{p}$, md

k_{lj} = effective permeability at S_{lj}, md

k_{rl} = relative permeability of phase l

$\bar{k}_{rl}$ = relative permeability of phase l at $\bar{p}$

m = slope of **the** semilog **straight** line in p^2 plot, **psi^2/log**

m^* = slope of the semilog straight line in p plot, psi/log

$m(p)$ = pseudopressure function (Eq. 2-17), (psi/cp)/(RB/STB)

n = exponent of Fetkovich relation

n' = exponent of Corey's relative permeability relation for the wetting phase

N_p = cumulative oil production, STB

N_{pi} = cumulative oil production to a reservoir pressure of 0 psi, STB

$\frac{N}{y} = \frac{40\ t}{13.44\ r_w^2\ h\ \phi\ \alpha}$ in field units

p = pressure, psi

$p1$ = pressure at t1, psi

$p2$ = pressure at $t2$, psi

p_i = initial pressure, psi

p_{wf} = flowing bottom hole pressure, psi

p_{wfs} = flowing bottom hole pressure at $\Delta t = 0.0$, psi

p_{ws} = shutin bottom hole pressure, psi

$\bar{p}$ = average pressure, psi

Δp = $p_i - p_{wf}$ for drawdown, psia

= $p_{ws} - p_{wf,s}$ for buildup, psia

Δp^2 = $p_i^2 - p_{wf}^2$ for drawdown, psi'

= $p_{ws}^2 - p_{wf,s}^2$ for buildup, psia^2

q = flow rate, STB/D

q_j = flow rate of step j, STB/D

q_n = last flow rate which affects the pressure, STB/D

$q_{o,v}$ = varying oil flow rate, STB/D

q_{sf} = sandface flow rate, STB/D

q_t = total voidage rate, RB/D

Δq_j = $q_j - q_{j-1}$, STB/D for multiple-rate test

Δq = $q(\Delta t) - 4(\Delta t = 0.0)$, STB/D for oil rate or RB/D for total rate

r = radial distance, feet

r_D = dimensionless radius

r_e = external radius, feet

r_w = wellbore radius, feet

R_s = solution gas/oil ratio, MSCF/STB

s = skin

S_l = saturation of phase l

S_{lj} = saturation of phase l at rate step j

S_{or} = residual oil saturation

$S_o^* = \frac{(S - S_{or})}{(1 - S_{or})}$

t = time, hrs

$t1$ = start of the time interval

$t2$ = end of the time interval

t_D = dimensionless time based on wellbore radius (Eq. 5-2 for solution gas-drive, and Eq. 6-22 for three-phase reservoirs)

Δt = shutin time, hrs

WOR = water/oil ratio, BBL/STB

$\overline{WOR}$ = WOR at any (r,t), BBL/STB

x_2 = any two-phase parameters

x_3 = any three-phase parameters

y = Boltzman transform variable (Eq. 6-9)

$\alpha = \frac{\text{SO}}{\mu_o B_o}$

$\beta = \frac{\phi S_o}{B_O}$

$\gamma = \frac{k_{rw}}{\mu_w B_w}$

X = mobility of phase 1, $\frac{k_l}{\mu_l}$, md/cp

$\lambda_t = \lambda_o + \lambda_g + \lambda_w$, md/cp

μ_l = viscosity of phase *1*, cp

$\bar{\mu}_l$ = viscosity of phase *l* at $\bar{p}$, cp

ϕ = porosity

$\zeta = \frac{\phi S_w}{B_w}$

∇ = gradient operator

∇^2 = Laplacian operator

Subscripts

g = gas

i = initial

j = index

1 = liquid or phase

o = oil

t = total

w = water or wetting

REFERENCES

Aanonsen, S.I.: *Nonlinear Effects During Transient Fluid Flow in Reservoirs as Encountered in Well Test Analysis,* Dissertation - Dr. Scient., Univ. of Bergen, Norway, 1985-a.

Aanonsen, S.: "Application of Pseudotime to Estimate Average Reservoir Pressure," Paper SPE 14256 presented at the 60th Annual Technical Conference and Exhibition, Las Vegas, Nevada, Sept. 22-25, 1985-b.

Al-Hussainy, R., Ramey, H. J., Jr. and Crawford, P.B.: "The Flow of Real Gases Through Porous Media," *J. Pet. Tech.* (May 1966), 624-636.

Al-Khalifah, A.A., Al-Hashim, H.S., Al-Marhoun, M.A., and Menouar, H.K.: "Revised Pulse Testing Correlation Charts," Paper SPE 14253 presented at the 60th Annual Technical Conference and Exhibition, Las Vegas, NV, Sept. 22-25, 1985.

Al-Khalifah, A.A., *Aziz,* K. and Home, R.N.: "New Approach to Multiphase Well Test Analysis," Paper SPE 16743 presented at the 62nd Annual Technical Conference and Exhibition, Dallas, Texas, Sept. 27-30, 1987.

Al-Khalifah, A.A., Home, R.N. and Aziz, K.: "In-Place Determination of Reservoir Relative Penneability Using Well Test Analysis," Paper SPE 16774 presented at the 62nd Annual Technical Conference and Exhibition, Dallas, Texas, Sept. 27-30, 1987.

Al-Khalifah, A.A.: *Two Phase Pulse Testing,* Master thesis, Univ. of Petroleum and Minerals, Dhahran, Saudi Arabia, 1985.

Ambastha, A.K. and Ramey, H.J.,Jr.: "Thermal Recovery Well Test Design and Interpretation," Paper SPE 16746 presented at the 62nd Annual SPE Meeting, Dallas, Texas, Sept. 27-30, 1987.

Amyx, J.M., Bass, D.M. and Whiting, R.L.: *Petroleum Reservoir Engineering* (1960) McGRAW-HILL, New York, 184-210.

Ayan, C. and Lee, W.J.: "The Effects of Multiphase Flow on the Interpretation of Buildup Tests," paper SPE 15537 presented at the 61st Annual Technical Conference and Exhibition held in New Orleans, LA October 5-8, 1986.

Aziz, K. and Settari, A.: *Petroleum Reservoir Simulation.* Applied Science Publishers, London (1979) 16.

Bilhartz, H.L. and Ramey, H.J.,Jr.: 'The Combined Effects of Storage, Skin, and Partial Penetration on Well Test Analysis," Paper SPE 6753 presented at the 52nd Annual Fall Technical Conference and Exhibition, Denver, Colorado, Oct. 9-12, 1977.

Bøe, A., Skjaeveland, S.M. and Whitson, C.S.: "Two-Phase Pressure Transient Test Analysis," Paper SPE 10224 presented at the 56th Annual Fall Technical Conference and Exhibition, San Antonio, Texas, Oct. 5-7, 1981.

Camacho, R.G. and Raghavan, R.: "Inflow Performance Relationships for Solution Gas-Drive Reservoirs," Paper SPE 16204 presented at the 1987 Production Symposium.

Chierici, G.L.: "Novel Relations for Drainage and Imbibition Relative Permeabilities," *Soc. of Pet. Eng. J.* (June 1984) 275-276.

Chu, W.C., Reynolds, A.C., Jr. and Raghavan, R: "Pressure Transient Analysis of Two-Phase Flow Problems," ***SPE Formation Evaluation*** (April, 1986).

Corey, A.T.: "The Interrelation Between Gas and Oil Relative Permeabilities," ***Producers Monthly,*** (Nov. 1954) 38-41.

Corey. A.T. and Rathjens, C.H.: "Effect **of** Stratification on Relative Permeability," ***Trans.,*** AIME (1956). ***207,*** 349-351.

Dake, L.P.: ***Fundamentals*** Of ***Reservoir Engineering*** (1978) 67-70.

Darcy, H.(1856). Les Fontaines Publiques de la Vie de Dijon, Dalmount, Paris (reprinted in Hubbert, 1969).

Dodson, C.R., Goodwyn, D., and Mayer, E.H.: "Application **of** Laboratory PVT Data to Reservoir Engineering problems," ***JPT*** (Dec. 1953) 287-298; ***Trans., AIME,*** 198.

Earlougher, R.C., Miller, F.G. and Mueller, T.D.: "Pressure Buildup Behavior in a Two-Well Gas-Oil System," ***Soc. Pet. Eng. J.,*** (June 1967) 195-204.

Earlougher, R.C., **Jr.:** ***Advances in Well Test Analysis,*** Monograph Series, Society of Petroleum Engineers **of** AIME, Dallas, **TX,** (1977) ***5.***

ECLIPSE: ***Reference Manual,*** Version 84/11, Exploration Consultants Limited (November, 1984).

ERCB (1975). ***The Theory and Practice of the Testing of Gas Wells,*** 3rd Edn.. Energy Resources Conservation Board.

Evinger, H.H. and Muskat, M.: "Calculation **of** Theoretical productivity Factor **,"** ***Trans., AIME*** (1942) *146*, 126-139.

Fetkovich, M.D., Guerrero. E.T., Fetkovich, M.J. and Thomas, L.K.: "**Oil** and Gas Relative Permeabilities Determined from Rate-Time Performance Data," Paper SPE 15431 presented at the SPE 61st Annual Meeting, New Orleans, October 5-8, 1986.

Fetkovich, M.J.: "The **Isochronal** Testing **of** Oil Wells," Paper SPE 4529 presented at the 48th Annual Fall Meeting, **Las** Vegas, Nevada, Spet. 30 - October 3, 1973. (SPE Reprint Series No. 14, 265.)

Fetkovich, M.J.: "Decline Curve **Analysis** Using Type Curves," ***J. Per. Tech.*** (June 1980) 1065-1077.

Fetkovich, M.J.: Personal Discussion (Dec. 1986).

Fetkovich, M.J. and Vienot, M.E.: "Rate Normalization of Buildup Pressure by Using Afterflow Data," ***J. Pet. Tech.*** **(Oct. 1980)** 1813-1824.

Firoozabadi, A.R, and Aziz, K.: "Relative Permeability From Centrifuge Data," Paper **SPE** 15059 presented at the 56th California Regional Meeting, Oakland, CA April 2-4, 1986.

Firoozabadi, A., Nuttaki, R., Wong, T. and Aziz, K.: "EOS Predictions of Compressibility and phase Behavior in Systems Containing Water, Hydrocarbons, and CO_2," Paper SPE 15674 presented at the 61st Annual Technical Meeting, New Orleans, LA October 5-8, 1986.

Gladfelter, R.E., Tracy, G.W., and Wilsey, L.E.: "Selecting Wells Which Will Respond to Production-Stimulation Treatment," *Drill. and Prod. Pruc.*, API, Dallas (1955) 117-128.

Handy, L.L.: "Effect of Local High Gas Saturations on productivity Indices," *Drill. and Prod. Pruc.*, API (1957).

Honarpour, M., Koederitz, L. and Harvey, A. H.: *Relative Permeability of Petroleum Reservoirs* (1986) CRC Press, Boca Raton, 1-134.

Homer, D.R.: "Pressure Build-up in Wells," *Proc.*, Third World Pet. Cong., The Hague (1951) II, 503-521.

Huppler, J.D.: "Numerical Investigation of the Effects of Core Heterogeneities on Water Flood Relative Permeability," *Soc. Per. Eng. J.*, 10, 381, 1970.

Hurst, W.: "Establishment of the Skin Effect and its Impediment to Fluid Flow into a Wellbore," *Per. Eng. (Oct.* 1953) B6-B16.

Johnson, C.E., Jr. and Sweeney, S.A.: "Quantitative Measurement of Flow Heterogeneity in Laboratory Core Samples and its Effect on Fluid Flow Characteristics," Paper SPE 3610 presented at the SPE 46th Annual Meeting, New Orleans, October 3, 1971.

Jones, R and Raghavan, R.: "Interpretation of Flowing Well Responses in Gas Condensate Wells," Paper SPE 14204 presented at the 60th Annual Technical Conference and Exhibition of the SPE of AIME, Las Vegas, Nevada, Sept. 22-25, 1985.

Kazemi, H.: "A Reservoir Simulator for Studying Productivity Variation and Transient Behavior of a Well in a Reservoir Undergoing Gas Evolution," *Trans.* AIME (1975) 259, 1401-1412.

Kimbler, O.K. and Caudle, B.H.: "New Technique for Study of Fluid Flow and Phase Distribution in Porous Media," *Oil and Gas J.*, (1957),

Kucuk, F.: "Gladfelter Deconvolution," Paper SPE 16377 presented at the 57th Annual California Regional Meeting held in Ventura, California, April 8-10, 1987.

Lee, W. J., Harrel, R.R.. and McCain, W.D.: "Analysis Procedure for Variable-Rate Pressure Drawdown Data," *J. Pet. Tech.*, (Jan. 1975) 115-116.

Lee, W. J.: *Well Testing,* Textbook Series, Society of Petroleum Engineers of AIME, Dallas, (1982) *1*, 45-50.

Levine, J.S. and Prats, M.: "The Calculated Performance of Solution Gas-Drive Reservoirs," *Soc. Pet. Eng. J.* (Sept. 1961) 222, 142-152.

Macias, L.C. and Ramey, H.J.: "Multiphase, Multicomponent Compressibility in Petroleum Reservoir Engineering," Paper SPE 15538 presented at the 61st Annual Technical Conference and Exhibition of the SPE, New Orleans, LA October 5-8, 1986.

Marle, C.M.: ***Multiphase Flow in Porous Media*** (1981) **EDITIONS TECHNIP,** Paris, 23-34. Vol. 55. **85.**

Martin, J.C.: "Simplified Equations of Flow in Gas Drive Reservoirs **and the Theoretical** Foundation of Multiphase **Pressure** Buildup Analysis," ***Trans.*** *AIME* (1959) 216, 309-311.

Matthews, C.S. and Russell, D.G.: ***Pressure Buildup and Flow Tests in Wells,*** Monograph **Series,** Society of Petroleum Engineers of AIME, Richardson, TX, (1967) *I*, 130-133.

Meunier, D., Wittman, M.J., and Stewart, G.: "Interpretation of Pressure Buildup Test Using In-Situ Measurement of Afterflow," Paper SPE 11463 presented at the 1983 SPE Middle East **Oil** Technical Conference and Exhibition, Manama, Bahrain, March 14-17.

Miller, C.C., Dyes, A.B. and Hutchinson, C.A., Jr.: "The Estimation of Permeability and Reservoir Pressure from Bottom-Hole Pressure Build-up Characteristics," ***Trans.*** **AIME** (1950) **189,** 91-104.

Moses, **P.L.:** "Engineering Applications of Phase Behavior of Crude **Oil** and Condensate Systems," ***J. Pet. Tech.*** (July 1986) 715-723.

Mueller, **T.D.,** Warren, J.E. and West, W.J.: "Analysis of Reservoir Performance k_g/k_o Curves **and a** Laboratory k_g/k_o Curve Measured on a Core Sample," ***Trans.*** **AIME** (1955) 204, 128-131.

Muskat, M.: ***Physical Principles of Oil Production.*** International Human Resources Development Corporation (1949) 404-431.

Muskat. M. and Meres. M.W.: 'The Flow of Heterogeneous Fluids Through Porous Media," ***Physics*** (Sept. 1936) ***Vol. 7,*** 346-363.

Nygård, R.: ***Calculating Relative Permeabilities From Two-Phase Drawdown Tests,*** thesis for the Cand. Techn. Degree. Rogaland Regional College, Stavanger (1982) (In Norwegian).

Penine, **R.L.:** "Analysis of **Pressure** Buildup Curves," ***Drill*** *and* ***Prod. Prac.***, **API** (1956), 482-509.

Rafigul-Islam, **M.** and Bentsen, R.G.: "A Dynamic Method for Measuring Relative Permeability," ***J. Can. Pet. Tech.,*** (Jan-Feb. 1986) 39-50.

Raghavan, R.: "Well Test Analysis: Wells Producing by Solution Gas Drive Wells," Soc. Pet. Eng. J. (Aug. 1976) 196-208.

Raghavan, R.: "Well Test Analysis for Multiphase Flow," paper SPE 14098 presented at the SPE 1986 International Meeting on Petroleum Engineering held in Beijing, China March 17-20, 1986.

Ramey, H.J. Jr.: Personal communication (Dec. 1987).

Ramey, H.J. Jr.: "Non-Darcy **Flow** and Wellbore Storage Effects in Pressure Build-Up and Drawdown of Gas wells," ***J. Pet. Tech.,*** (Feb. 1965) 223-233; ***Trans.,*** **AIME, 234.**

Ramey, H.J. Jr.: "Verification of the Gladfelter-Tracy-Wilsey Concept for Wellbore Storage-Dominated Transient Pressures During production," *J. Cdn. Per. Tech.* (April-June 1976) 84-85.

Rapoport, L.A. and Leas, W.J.: "Relative Permeability to Liquid in Liquid-Gas Systems," *Trans.* AIME, (1951), *192,* 83-98.

Scheidegger, A.: *The Physics of Flow Through Porous Media,* Third Edition, Canada: University of toronto Press, 1974.

Stone, H. L.: "Probability Model for Estimating Three-phase relative Permeability," *Truns.* AIME, (1970) *249,* 214-218.

Uraiet, A.A. and Raghavan, R.: "Pressure Buildup Analysis for a Well produced at Constant Bottomhole Pressure," *J. Per. Tech.* (Oct. 1980) 1813-1824.

van Everdingen, A.F.: "the Skin Effect and its Influence on the Productive Capacity of a Well," J. Pet. Tech. (June 1953) 171-176; *Trans.,* AIME, 198.

Verbeek, C.M.J.: "Analysis of Production Tests of Hydraulically Fractured Wells in a Tight Solution Gas-Drive Reservoir," Paper SPE 11084 presented at the 1982 SPE annual Technical Conference and Exhibition, New Orleans, Sept. 26-29.

Weller, W.T.: "Reservoir Performance During Two-Phase Flow," *J. Per. Tech.* (Feb. 1966) 240-246.

Whitson, *C.S.: Topics on Phase Behavior and Flow of Petroleum Reservoir Fluids,* Dissertation - Doctor of Technical Sciences, University of Trondeim, Norway, (Aug. 1983).

Winestock, A.G. and Colpitis, G.P.: " Advances in Estimating Gas Well Deliverability," *J. Cdn. Per. Tech.* (July-Sept. 1965) 111-119.

Wyckoff, R.D. and Botset, H.G., *Physics,* 7, 325 (1936).

APPENDIX A

ECLIPSE SIMULATOR

ECLIPSE is a fully implicit, three phase, three dimensional black oil simulator. Its program is written in Fortran 77. Therefore, ECLIPSE may operate on any computer with enough storage and standard Fortran 77 compiler, i.e. CRAY, IBM 3081 and VAX 11/780.

Fully Implicit Procedure

ECLIPSE is a fully implicit simulator. Hence, it has no problem of instability. Newton's method is applied to solve the nonlinear equations with the Jacobian fully expanded in all its variables. In order to accelerate the convergence, Nested Factorization is utilized to solve simultaneously the linear equations resulting after each Newton's iteration. Nested Factorization helps solving large problems implicitly and with very small residual sums, material balance errors.

Three-phase Relative Permeability

ECLIPSE uses an effective simple model to obtain the three-phase oil relative permeability of the two sets of two-phase relative permeabilities. The model can be expressed as such:

$$k_{ro} = \frac{S_g\, k_{rog} + (S_w - S_{wco})\, k_{row}}{S_g + S_w - S_{wco}} \qquad (1)$$

where:

k_{rog} is the oil relative permeability for the oil-gas system,

k_{row} is the oil relative permeability for the oil-water system,

S_{wc} is the connate water saturation.

Well Control

There is a wide spectrum of options that ECLIPSE allows to control the well. Some options are for the well individually, while others are either for a group of wells or for the

whole field. The set of options for controlling individual wells include: specified oil rate, water rate, gas rate, liquid rate, reservoir voidage rate, and bottom hole or tubing head pressures. In all the runs that I did, I specified a constant oil rate which when not satisfied the well control changed automatically to a constant bottom hole pressure and reported that in the output file.

Input File

Two choices are available for ECLIPSE users. First is the special **ECLIPSE EDIT** screen with its help facility. Second is the free format input through keyword systems using any standard screen editor. A copy of one of my input files is shown at the end of *this* section. As can be seen, the main sections of input data are as follows:

RUNSPEC: has several flags for dimension, phases, storage and others,

GRID: defines the geometry and the various rock properties for each grid block,

PROPS: includes the tables of rock and fluid properties as functions of saturation and pressure,

SOLUTION: initializes the model with the values of pressure, saturation and gas/oil ratio for each grid block,

SUMMARY: states the variables whose values are to be reported in each *summary* tile,

SCHEDULE: specifies the type of process to be simulated, i.e. production or injection, and also the times for which the output report is needed,

END: indicates the end of the data file.

```
                INPUT FILE FOR THE ECLIPSE SIMULATOR
                      THREE-PHASE RUN

RUNSPEC  ================================================
NDIVIX  NDIVIY ndiviz qrdral numres qnncon mxnaqn  mxnaqc  qdporo  qdperm
  40       1      1       T       1      F       0        0       F       F /
 OIL      WATER   GAS     DG      VG
   T        T       T       T       F       /
  UNITS
  'FIELD'  /
  NRPVT   NPPVT    NTPVT    NTROCC   QROCKC   QRCREV
   20      20       1        1        F        T    /
  NSSFUN     NTSFUN     QDIRKR      QREVKR      QVEOPT     QHYSTR
    20         1          F           T           F          F   /
  NDRXVD    NTEQUL     NDPRVD      QuieSC     Qthprs  Qrevth
    20         1          10          F          F       T     /
  NTFIP      QPAIR
    1          F     /
  NWMAXZ    NCWMAX    NGMAXZ     NWGMAX
    1         1         2          1    /
  QIMCOL      NWCOLC      NUPCOL
    F           0           4     /
  mxmflo  mxmthp  mxmwfr  mxmgfr  mxmalq   nmmvft
  /
  mxsflo mxsthp  nmsvft
    /
  naqfet    ncamax
    /
    DAY   MONTH   YEAR
    1     JAN'    1983 /
    QSOLVE      NSTACK     QPMTOU     QFMTIN
                  T          8          T          T   /
  GRID   ==================================
  DRV
  0.05 0.1 0.2 0.5 1.0  3.0 5.0 8.0 10.0 15.0 7*18.0 5*30.0 5*40.0
  2*60.0 4*80.0 2*120 150 2*250.0 500.0 1000.0/
  INRAD
  0.3 /
  DYV
  360.0/
  DZ
  40*100. /
  PERMR
  40*20.  /
  COPY
    'PERMR'    'PERMTHT' 1  40   1  1    1  1   /
  /
  PERMZ
    40*20.  /
  PORO
     40*0.15  /
  TOPS
  40*00  /
  RPTGRID
  5*1   /
  PROPS  ==================================================
  DENSITY
  45.  62.4    0.068735   /
  ROCK
  2000.      3.e-06   /
```

```
--   Rs      P       Bo   Visc
PVTO
    0.030    70.0   1.02    1.40 /
    0.0443   193.14 1.058   1.35 /
    0.119  622.48   1.088    1.164  /
    0.196   1051.8 1.121   1.011 /
    0.279   1481.17   1.159   0.881  /
    0.367    1910.5    1.202   0.768  /
    0.462    2339.9    1.249   0.671 /
    0.564    2769.35    1.302    0.587  /
    0.674    3198.7    1.36    0.515 /
    0.813   3699.5   1.434   0.446 /
    0.964   4200.5   1.516   0.391  /
   1.128    4701.5    1.605    0.348  /
   1.306   5202.3   1.702    0.317  /
   1.471    5631.6   1.791   0.300  /
   1.5     5703.0   1.806    0.298
        6000.0   1.800    0.3000 /
/
-- p     BW    CW      VW       DVW
PVTW
  14.7   1.00  0.     1.00     0.  /
-- p        Bg          vg
PVDG
    40.0    50.0     0.011
    193.14  17.8     0.0113
    622.48   3.38    0.0125
    1051.8   2.85    0.0138
    1481.17   1.959  0.0152
    1910.5   1.46    0.0166
    2339.9   1.175   0.0181
    2769.35    0.997   0.0195
    3198.7    0.873   0.021
    3699.5   0.774    0.0228
    4200.5   0.712    0.0246
    4701.5    0.659   0.0263
    5202.3    0.623   0.0281
    5631.6    0.603   0.0295
    5703.0   0.596    0.0298
    6000.0    0.590   0.0300    /
    /
```

```
SGFN
-- Sg    Krg       Pclg
 0.0000    0.000     0.0
 0.000001  0.000000000001   0.
 0.005     0.000025     0.
 0.01      0.0001    0.
 0.02      0.0004      0.
 0.04      0.0016     0.
 0.08      0.0064     0.0
 0.10      0.01       0.0
 0.12      0.0144      0.
 0.16      .0256      0.
 0.18      .0324      0.
 0.20      .04        0.
 0.22      0.0484     0.
 0.25      0.0625     0.
 0.28      0.0784     0.
 0.30      0.09       0.
 0.39      0.1521     0.
 0.40      0.16       0.
 0.8000    0.6400      0.0     /
/
--    SO       Krow          Krog
SOF3
   0.000    0.0000          0.000
   0.100    0.000           0.00
   0.2000   0.000           0.00
   0.3000   0.0900          0.09
   0.4000   0.160           0.16
   0.44     0.1936          0.1936
   0.47     0.2209          0.2209
   0.5000   0.2500          0.250
   0.525    0.2756          0.2756
   0.55     0.3025          0.3025
   0.575    0.3306          0.3306
   0.6000   0.3600          0.36
   0.63     0.3969          0.3969
   0.68     0.4624          0.4624
   0.7000   0.4900          0.49
   0.8000   0.640           0.64      /
-- SW    Krw         Pcow
SWFN
0.2      0.0       0.0
0.30      0.02      0.0
0.40      0.06      0.0
0.5       0.15      0.
0.6       0.25      0.
0.8       0.40      0. /
RPTPROPS
1  0  1   1   0   1   1    1  /
```

```
SOLUTION  ==========================================
PRESSURE
40*4502.0  /
SGAS
40*0.20   /
SWAT
40*0.30  /
RS
40*1.12 /
RPTSOL
1  1  0  1  1  0  0  1   /
SUMMARY   ==========================================
FGOR
WGOR
/
SCHEDULE  ==========================================
TUNING
0.0000001      0.0002     0.00002     /
     /
RPTSCHED
1  1  0   1    1  0    0   0   1   0   2    /
WELSPECS
                'PROD1'   'P'    1  1  0  'OIL'     /
/
COMPDAT
    'PROD1'     1  1   1  1       'OPEN'   0  0.   0.3 /
/
WCONPROD
 'PROD1'      'OPEN'       'ORAT'     500.0 /
/
TSTEP
 2*0.000029 3*0.0000579 0.000116 0.000347 0.0007
 0.00161 3*0.005 0.01 0.01 2*0.006
/
WCONPROD
 'PROD1'     'OPEN'       'ORAT'      1000.0 /
/
TSTEP
 2*0.000029 3*0.0000579 0.000116 0.000347 0.0007
 0.00161 3*0.005 0.01 0.01 2*0.006
/
WCONPROD
 'PROD1'     'OPEN'       'ORAT'     2000.0 /
/
TSTEP
2*0.000029 3*0.0000579 0.000116 0.000347 0.0007
0.00161 3*0.005 0.01 0.01 2*0.006
/
/
END
```

APPENDIX B

THE CHANGE OF $\frac{k_{ro}}{\mu_o B_o}$ WITH PRESSURE

The pressure squared solution was derived in Section 4 assuming a linear relation of $\frac{SO}{P_O B_o}$ with pressure. Throughout the derivation, this linear relation was assigned a zero intercept. It was expressed as:

$$\frac{k_{ro}}{\mu_o B_o} = a p \qquad \text{(B-1)}$$

In Eq. B-1, a is defined differently from that of Section 4, Eq. 4-21, by an absolute permeability factor. Nevertheless, the recommendations of Section 4.3 are used to evaluate the empirical slope a of Eq. B-1.

The intercept of the $k_{ro} / (\mu_o B_o)$ relation with pressure was assumed to be zero in Eq. B-1. This however is not the case for real systems (see Figs. 4-3 and 4-4). A more representative relation can be expressed as:

$$\frac{SO}{P_O B_o} = \alpha p + b \qquad \text{(B-2)}$$

here a is the actual slope and b is the intercept. Both pressure and saturation data are required to evaluate these two constants, a and b. Since saturation change during a test is normally not available, these two constants are hand to evaluate. This explains why Eq. B-1 neglected the intercept b and used an empirical slope a to replace the actual slope a.

The following sections investigate the consequences of using Eq. B-1 instead of Eq. B-2 when deriving the pressure squared approach.

B.1 Theory

In this section, Eq. B-2 is used to derive a new pressure squared solution. This solution is different from that derived in Section 4 using Eq. B-1. A comparison between both

solutions is made to show how different they are for different reservoir and testing conditions.

The logarithmic approximation of the line source solution, derived by Bøe et al. (1981) in terms of $m(p)$, is:

$$m(p_i) - m(p_{wf}) = \frac{141.2\, q_o}{k\, h} \left[0.5 \left(\ln t_D + 0.80907 + 2\, s \right) \right] \qquad \text{(B-3)}$$

where:

$$t_D = \frac{0.000264\, k\, t}{\phi\, r_w^2\, (c / \lambda)^*} \qquad \text{(B-4)}$$

and:

$$m(p) = \int_{p_{ref}}^{p} \frac{k_{ro}}{\mu_o B_o}\, dp \qquad \text{(B-5)}$$

Using Eqs. B-2 and Eq. B-5, EQ. B-3 will be:

$$\int_{p_{wf}}^{p_i} (\alpha p + b)\, dp = \frac{141.2\, q_o}{k\, h} \left[0.5 \left(\ln t_D + 0.80907 + 2\, s \right) \right] \qquad \text{(B-6)}$$

Equation B-6 may be simplified to:

$$\frac{\alpha}{2} (p_i^2 - p_{wf}^2) + b (p_i - p_{wf}) = \frac{141.2\, q_o}{k\, h} \left[0.5 \left(\ln t_D + 0.80907 + 2\, s \right) \right] \qquad \text{(B-7)}$$

Equation B-7 is the new pressure squared solution which retains the two constants, a and b. These two constants make the new solution difficult to apply in practice.

The pressure squared solution of Section 4 can be obtained by neglecting the term $[\, b\, (p_i - p_{wf})\,]$, and replacing the actual slope a by the empirical slope a, as:

$$\frac{a}{2} (p_i^2 - p_{wf}^2) = \frac{141.2\, q_o}{k\, h} \left[0.5 \left(\ln t_D + 0.80907 + 2\, s \right) \right] \qquad \text{(B-8)}$$

The simplicity of the solution given by Eq. B-8 makes it applicable to pressure transient tests.

The right hand side terms of Eqs. B-7 are different from those of Eq. B-8. To insure the accuracy of Eq. B-8 (i.e. to justify using Eq. B-1 instead of Eq. B-2), the following should

hold:

$$\alpha / 2 (p_i^2 - p_{wf}^2) + b (p_i - p_{wf}) \approx a / 2 (p_i^2 - p_{wf}^2) \quad \text{(B-9)}$$

Equation B-9 can be checked through well tests generated using a simulator. The pressure-saturation output of a simulated test can be used to plot $k_{ro} / (\mu_o B_o)$ vs. pressure. The slope of such a plot is a, and the intercept is b. On the other hand, the empirical slope, a, may be evaluated according to the recommendations discussed in Section 4.3.

B.2 Simulated Examples

Equation B-9 was checked through simulated well tests. Four drawdown tests were simulated with different magnitudes of pressure drop. Following are Examples 1 and 2 for volatile oils and Examples 3 and 4 for systems of low volatility.

Example 1

In this example, a drawdown test with a considerable pressure drop was simulated in a volatile oil system. The set of PVT data reported by Bφe et al. (1981) was used. The fluid relative permeabilities were:

$$k_{ro} = S_o^2 \quad \text{(B-10)}$$

$$k_{rg} = S_g^2 \quad \text{(B-11)}$$

Other input data is summarized in Tables B-1.

The output pressure-saturation values at the sandface were used to graph $k_{ro} / (\mu_o B_o)$ vs. pressure (Fig. B.l). Except for the starting value, most other points are on a straight line in this graph. The elapsed time from the initial value to the start of the straight line was about five seconds for this example.

Both the slope, a, and the intercept, b, of Eq. B-9 were obtained from Fig. B.l. On the other hand, the empirical slope, a, was evaluated for such volatile oils at the initial pressure, using Eq. 4-39, as:

$$a = \left(\frac{k_{ro}}{\mu_o B_o} \right)_i \frac{1}{p_i} \quad \text{(B-12)}$$

Table B.1: Reservoir properties and testing conditions for Examples 1 and 2

Parameter	Input value
h	100 ft
k	100 md
ϕ	0.15
p_i	5200 psi
S_{gi}	10 %
q_o	8000 STB/D

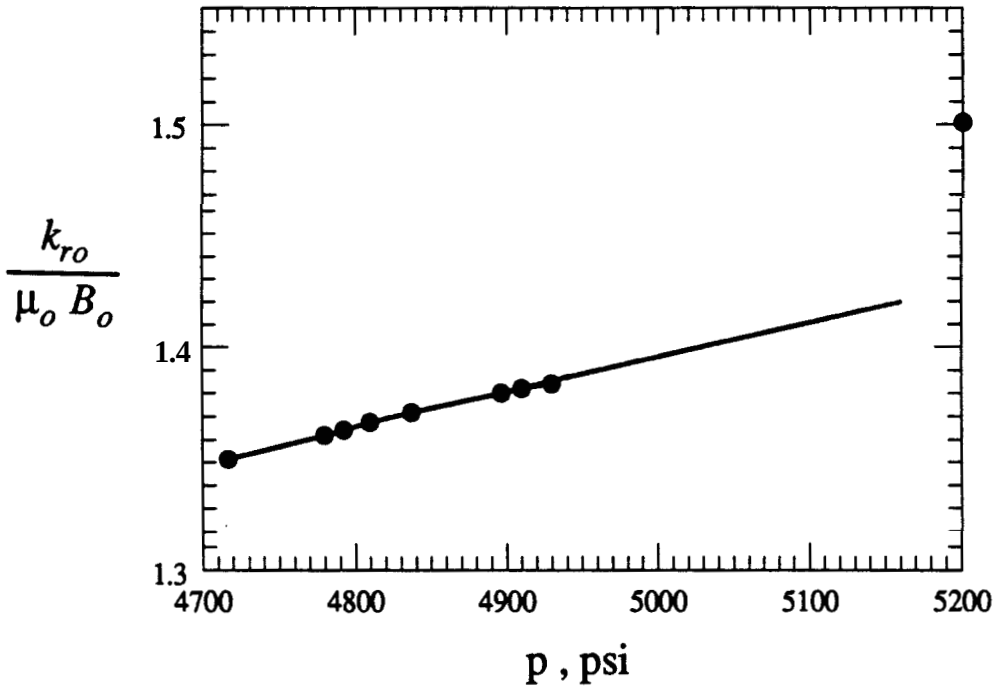

Figure B.1: k_o / ($\mu_o B_o$) vs. pressure for a simulated constant-rate drawdown test

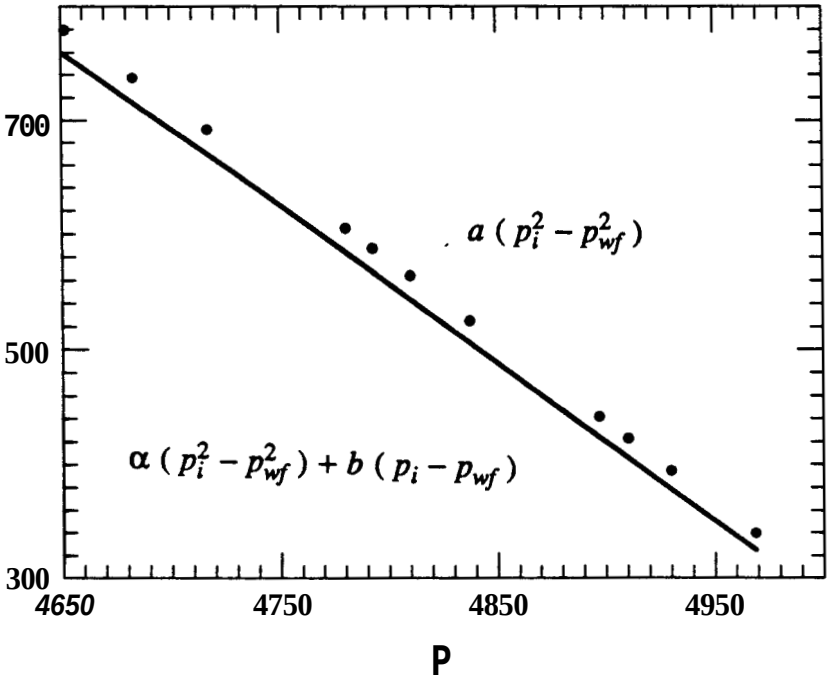

Figure B.2: The two sides of Eq. B-9 vs. pressure

$$a = 1.4629 \times 10^{-4}$$

$$b = 0.661$$

$$a = 2.88656 \times 10^{-4}$$

Using these values, the two sides of Eq. B-9 were plotted vs. pressure in Fig. B.2. The dots were for the right hand side and the solid curve was for the left hand side. The small difference between both sides, seen in Fig. B-2, verifies that Eq. B-9 holds for these conditions (large pressure drops in volatile oils). It also justifies using Eq. B-1 instead of Eq. B-2.

Example 2

In this example, a drawdown test of small pressure drop was simulated in volatile oil system. The gas saturation was 20 % and the initial pressure was 4200 psi. System properties were identical to those of Example 1.

The output pressure-saturation values at the sandface were used to graph $k_{ro} / (\mu_o B_o)$ vs. pressure, as shown in Fig. B.3. Both the slope, a, and the intercept, b, of Eq. B-9 were obtained from Fig. B.3. On the other hand, the empirical slope, a, was evaluated for such volatile oils at the initial pressure using Eq. B-12. For this simulated drawdown test, the following values were obtained:

$$a = 2.03564 \times 10^{-4}$$

$$b = 0.214522$$

$$a = 2.5705 \times 10^{-4}$$

Using these values, the two sides of Eq. B-9 were plotted vs. pressure in Fig. B.4. The dots were for the right hand side and the solid curve was for the left hand side. The difference shown in Fig. B-4 is smaller than that of Example 1. Again, such a small difference verifies that Eq. B-9 holds for these conditions (small pressure drops in volatile oils).

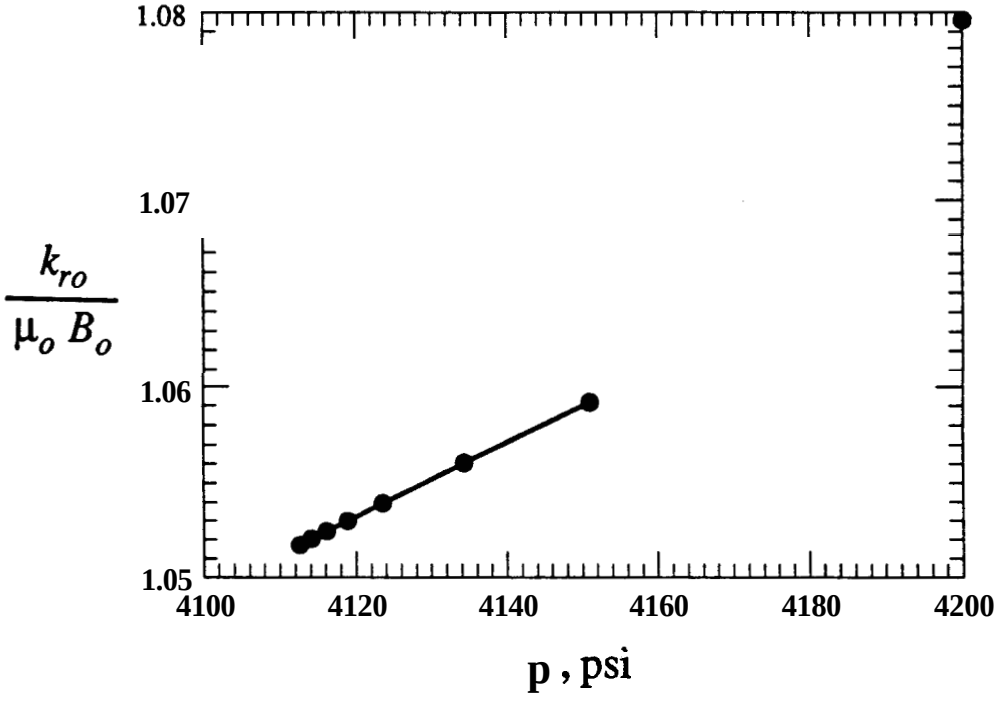

Figure B.3: $k_o / (\mu_o B_o)$ vs. pressure for a simulated constant-rate drawdown test

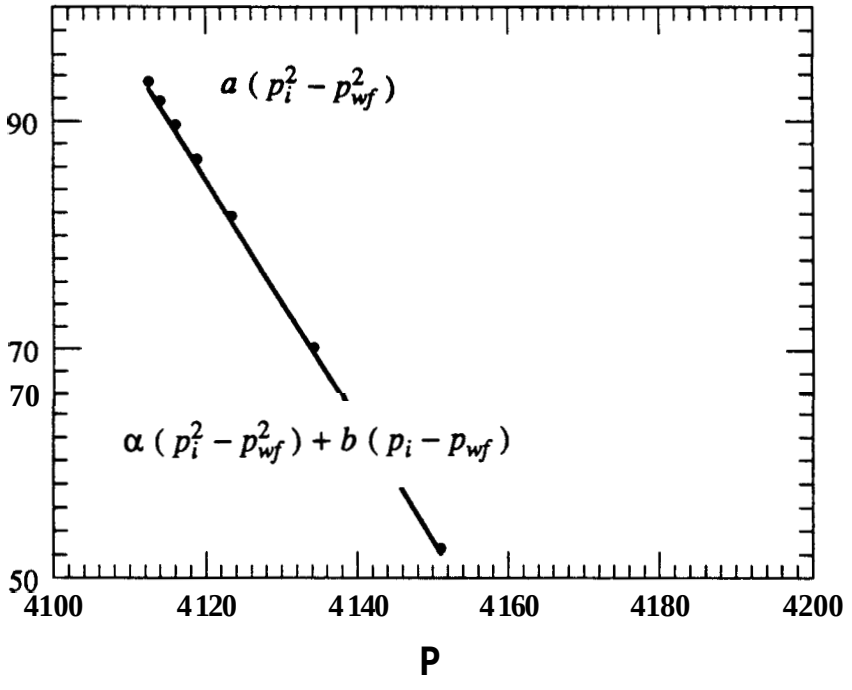

Figure B.4: The two sides of Eq. B-9 vs. pressure

Example 3

In this example, a drawdown test with a small pressure drop was simulated in oils of low volatility using the set of PVT data given in Table 4-2. The fluid relative permeabiities were given by Corey-type relation, Eqs. 5-22 and 5-23, as:

$$k_{ro} = (S_o^*)^{3.3} \qquad \text{(B-13)}$$

$$k_{rg} = 0.9\,(1 - S_o^*)^{2.0} \qquad \text{03-14)}$$

where:

$$S_o^* = \frac{S_o - S_{or}}{1 - S_{or}}$$

and

$$S_{or} = 0.20$$

Other input data are summarized in Tables B-2.

The output pressure-saturation values at the sandface were used to graph $k_{ro} / (\mu_o B_o)$ vs. pressure, as shown in Fig. B.5.

Both the slope, a, and the intercept, b, of Eq. B-9 were obtained from Fig. B.5. Because this drawdown tests was of a small pressure drop, the empirical slope, a, was evaluated at the initial pressure using Eq. B-12. For this simulated drawdown test, the following values were obtained:

$$a = 6.3646 \times 10^{-5}$$

$$b = 0.237628$$

$$a = 2.72642 \times 10^{-4}$$

Using these values, the two sides of Eq. B-9 were plotted vs. pressure in Fig. B.6. The dots are for the right hand side and the solid curve is for the left hand side. The difference between the two sides of Eq. B-9 is negligible at early times and is small for late times. Therefore, Eq. B-9 holds for these conditions (small pressure drops in oils of low volatility).

Table 8.2: Reservoir properties and testing conditions for Examples 3 and 4

Parameter	Input value
h	100 ft
k	100 md
ϕ	0.2
p_i	1137 psi
S_{gi}	9 %
q_o	300 STB/D

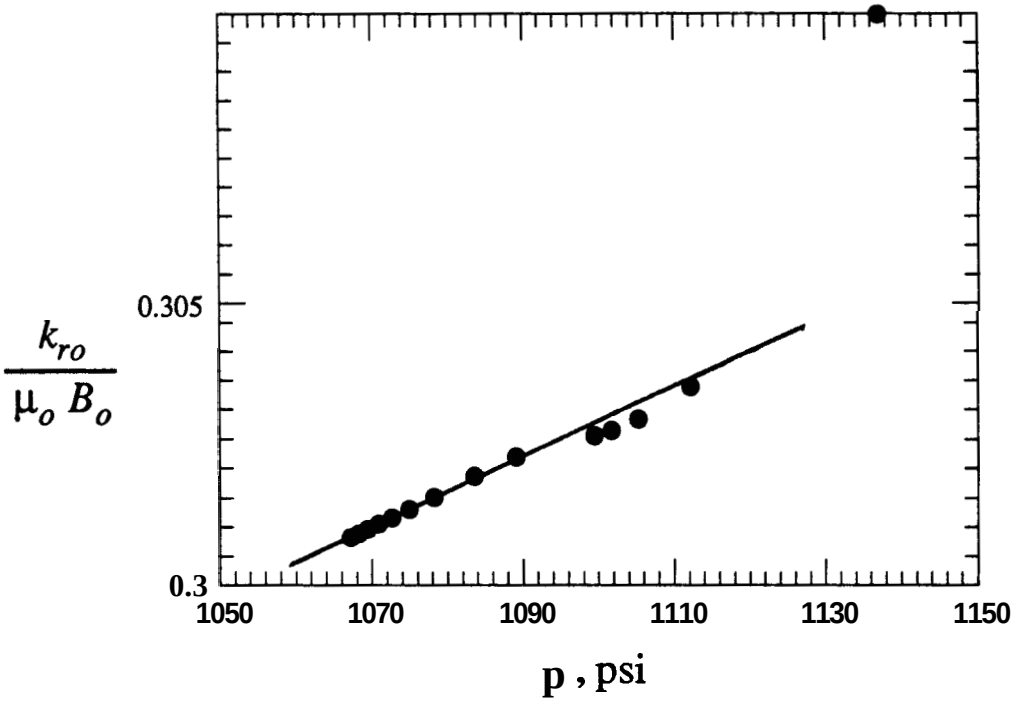

Figure B.5: $k_o / (\mu_o B_o)$ **vs. pressure for a simulated constant-rate drawdown test, Example 3**

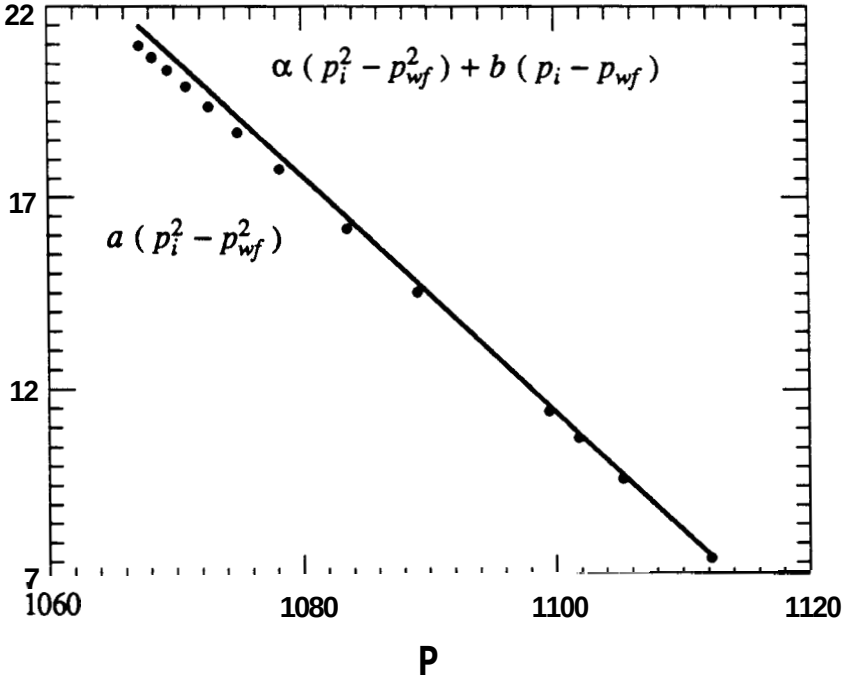

Figure B.6: The two sides of Eq. B-9 vs. pressure, Example 3

Example 4

The drawdown test of Example 3 was simulated again but with a large pressure drop. The flowing oil rate was 2000 STB/D for this run as compared to 300 STB/D for Example 3.

The output pressure-saturation values at the sandface were used to graph $k_{ro} / (\mu_o B_o)$ vs. pressure, as shown in Fig. B.7. Most of the points plotted on a straight line in such a graph.

Both the slope, α, and the intercept, b, of Eq. B-9 were obtained from Fig. B.7. For such drawdown tests with a large pressure drop in oils of low volatility, the empirical slope, a, was evaluated at $p_{0.1\,hr}$ using Eq. 4-41, as:

$$a = \left(\frac{k_{ro}}{\mu_o B_o} \right)_{p_{0.1\,hr}} \frac{1}{p_{0.1\,hr}} \qquad \text{(B-15)}$$

For this simulated drawdown test, the following values were obtained:

$$a = 7.61818 \times 10^{-5}$$

$$b = 0.223375$$

$$\alpha = 3.5064 \times 10^{-4}$$

Using these values, the two sides of Eq. B-9 were plotted vs. pressure in Fig. B.8. The dots are for the right hand side and the solid curve is for the left hand side. As can be seen in Fig. B.8, the difference is significant at early times, but tends to decrease with time. The considerable difference between the two sides of Eq. B-9, and most importantly the curved-shape of the dots, indicate that Eq. B-9 does not hold for these conditions (drawdown tests with large pressure drops in oils of low volatility). This, in essence, explains the rate sensitivity of the pressure squared approach in oils of low volatility seen in Figs. 4.16 and 4.17 and discussed in Appendix C.

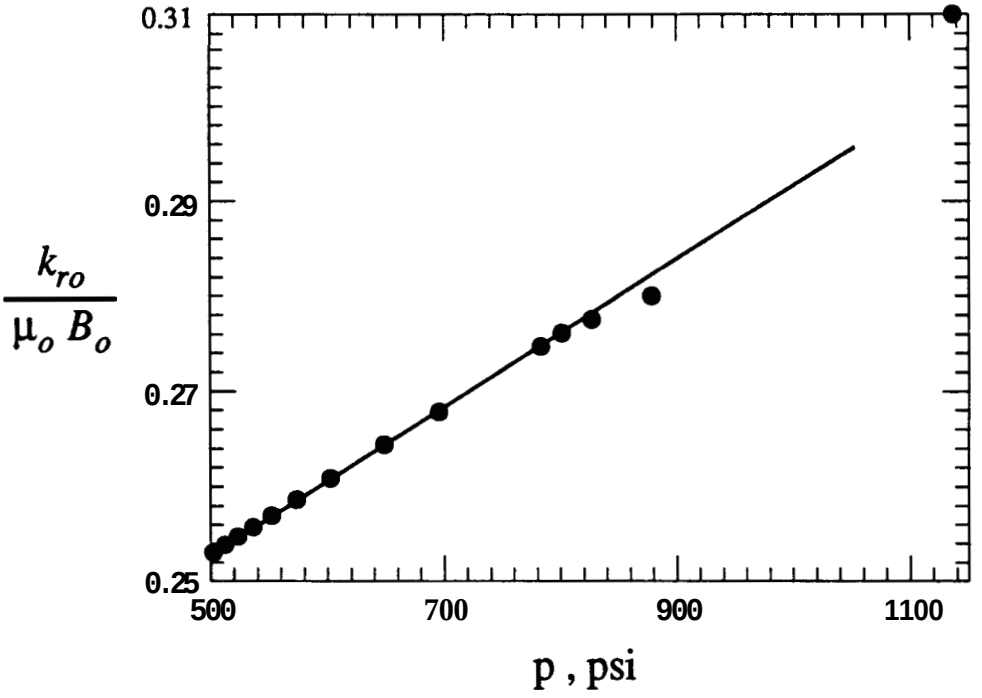

Figure B.7: k_o / ($\mu_o B$,) **vs. pressure for a simulated** constant-rate **drawdown test, Example 4**

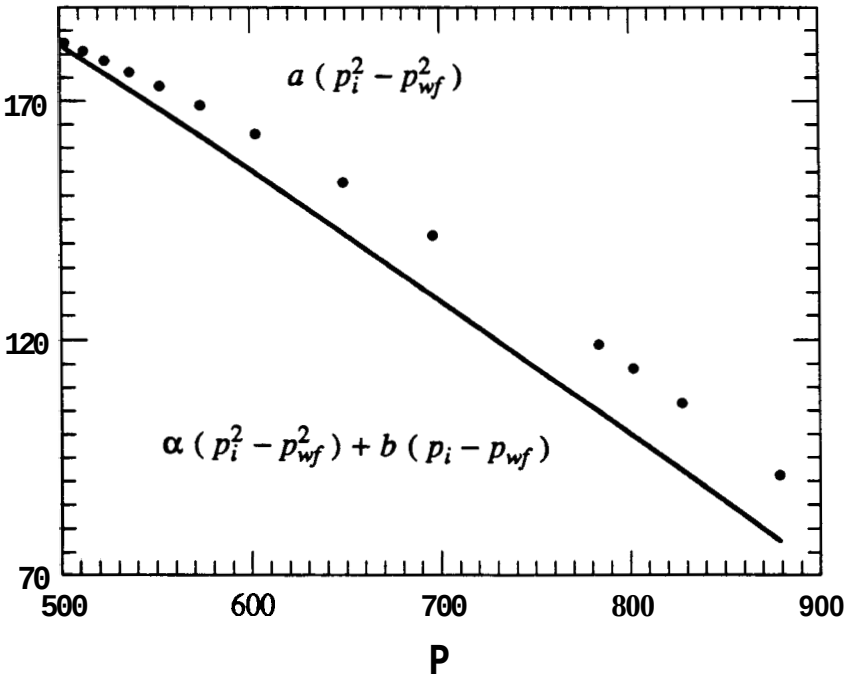

Figure B.8: **The two sides of Eq. B-9 vs. pressure, Example 4**

B.3 Summary

The rate sensitivity of the pressure squad approach was not seen for drawdown tests with either large or small pressure drop in volatile oils (Examples 1 and 2), nor was it seen for drawdown tests of small pressure drop in oils of low volatility (Example 3). Such a rate sensitivity developed only for the case of drawdown tests with a large pressure drop in systems of low volatility (Example 4). This rate sensitivity was pointed out in Section 4.4, where it developed for drawdown tests run under similar conditions (see Figs. 4.16 and 4.17) but it did not develop for subsequent buildups (see Figs. 4.18 and 4.19).

The pressure squared solution, given by Eq. B-8, holds to a good engineering accuracy for volatile oils. For oils of low volatility, the pressure squared approach applies better for drawdown tests with small pressure drops. For drawdown tests of large pressure drops in such systems, assumptions implicit in Eq. B-1 are not justified, resulting in a loss of accuracy.

Appendix C

Rate Normalization of Multiphase Well Tests

Solutions of well test equations are derived based on the assumption of constant rate or constant wellbore pressure. In practice, neither of these parameters can be held constant during a pressure transient test. The variation of rate may be attributed to afterflow effects in a buildup test or wellbore unloading effects in a drawdown test, which for some tests dominate most of the transient response. This distorted transient response can only be analyzed when it is properly normalized to obtain the pressure response of a fictitious constant rate test. Such normalization has become possible with the development of bottomhole rate and pressure measurement devices (Meunier et al. ,1983).

There are several ways to normalize the pressure-rate data of a single phase test. The first and most straightforward is that proposed by Gladfelter et al. (1955). They suggested that the pressure rise after shut-in divided by the instantaneous change in rate caused by afterflow should be plotted versus the logarithm of shut-in time to obtain a modified Miller-Dyes-Hutchinson buildup plot. Ramey (1965) confirmed such normalization which he then extended to wellbore unloading effects during drawdown tests. Winestock and Colpitts (1965) proposed a similar rate normalization of pressure for drawdown tests in gas wells with monotically declining rate. Using numerical simulation, Lee et al. (1975) confirmed Winestock-Colpitts approach for gas wells. Ramey (1976) provided further discussion of Gladfelter et al. and Winestock-Colpitts normalization procedure. Kucuk (1986) stated that Gladfelter normalization works for any change in rate that is linear with time.

Rate normalization of multiphase tests has not been studied in much detail. Fetkovich and Vienot (1984) followed a normalization procedure based on Penine's (1956) pressure solution. Applying Gladfelter normalization, they utilized the change in total afterflow rates to normalize the pressure rise after shutin. As a result, they obtained the total system mobility but not individual phase mobilities. Along the same lines, Raghavan (1986) normalized the

drawdown response using the instantaneous total rate and the buildup response using the total rate at shut-in, $q_t\ (\Delta t = 0.0)$, (Uraiet and Raghavan, 1980). Raghavan also indicated that such normalization yields only the total system mobility as:

$$\lambda_t = (k/\mu)_t = \frac{162.6}{m^* h} \tag{C-1}$$

where:

$$(k/\mu)_t = (k/\mu)_o + (k/\mu)_g + (k/\mu)_w \tag{C-2}$$

and m^* is the semilog slope of a $(p_i - p_{wf}) / q_t$ versus time plot for a drawdown test and of a $(p_{ws} - p_{wf,s}) / q_t\ (\Delta t = 0.0)$ versus time plot for a buildup test. The total rate, q_t in RB/D is defined as:

$$q_t = q_o B_o + [\, q_g - q_o R_s + q_w R_{sw} \,] B_g + q_w B_w \tag{C-3}$$

The normalization applied by Fetkovich-Vienot and Raghavan was based on Penine's pressure solution, Eq. C-1. With the new approach derived in Section 4, a better normalization scheme is possible for systems in which gas phase is present. This scheme applies at all rates and results in individual phase mobilities as well as in total system mobility. The following is a presentation of the theory as well as demonstrations of the scheme using several example well tests simulated under varying rate profiles.

C.I Theory

Multiphase flow was modeled in Section 4 by the diffusivity equation with p^2 as the dependent variable, Eq. 4-25. Line source solution of this equation was also derived. When this solution was used to analyze drawdown and buildup tests (Section 4.4), they yielded reasonable estimates of individual phase mobilities. Unliie Pemne's (1956) approach, the proposed solution was insensitive to oil rates in volatile oils. For oils of low volatility, both approaches were sensitive to rates. This has already been discussed in Sections 4.6, 4.7 and Appendix B, and will be investigated in more detail here.

Penine's solution to obtain oil permeability, Eq. 2-8, is :

$$k_o = \frac{162.6\, q_o\, B_o\, \mu_o}{m^*\, h} \qquad \text{(C-4)}$$

Equation C-4 is based on the solution of Martin's diffusivity equation, Eq. 2-12, using the linearized inner boundary condition, Eq. 447. This solution can be written as:

$$p_i - p_{wf} = \frac{q_o\, B_o\, \mu_o}{4\,\pi\, k_o\, h}\ \left[-E_i\left(-\frac{\phi\, r_w^2\, c_t}{4\, t\, \lambda_t} \right) \right] \qquad \text{(C-5)}$$

Assuming that Eqs. C-4 and C-5 hold, the unit response can be computed through dividing the pressure change by the oil rate, $\Delta p / q_o$. In essence, this is the basis of Gladfelter et al. normalization applicable to single phase oil flow. When several drawdown tests are run in the same system but at different rates, their responses can be collapsed to that of a unit rate when normalized using their different rates. If the responses do not collapse to that of a unit rate, then the underlying assumption, that Eqs. C-4 and C-5 hold, is not valid.

Perrine's approach was tested through three drawdown tests simulated at 1000, 3000 and 5000 STB/D oil rates in volatile oil system (every other parameter was held the same for all tests). The PVT set of data reported by Bφe et al. (1981) was used. Test responses were then normalized as $(p_i - p_{wf}) / (q_o)_j$, where j refers to a specific test, and plotted in Fig. C.1. Only the normalized response for the 1000 STB/D oil rate test resulted in the correct unit response. The higher the oil rate the more the normalized response shifts from the correct one and the more oil permeability is underestimated. Penine's approach was also tested in oils of low volatility using the PVT set given in Table 4-2. Two tests were simulated at 300 and 2000 STB/D , see Examples 3 and 4 in Appendix B. Test responses were then normalized as $(p_i - p_{wf})_j / (q_o)_j$, where j refers to a specific test, and plotted in Fig. C.2. This diversion of the correct slope indicates the importance of the neglected terms in deriving Penine's solution. It also magnifies the consequences of the improper linearization of the inner boundary condition applied to obtain Eq. 4-47.

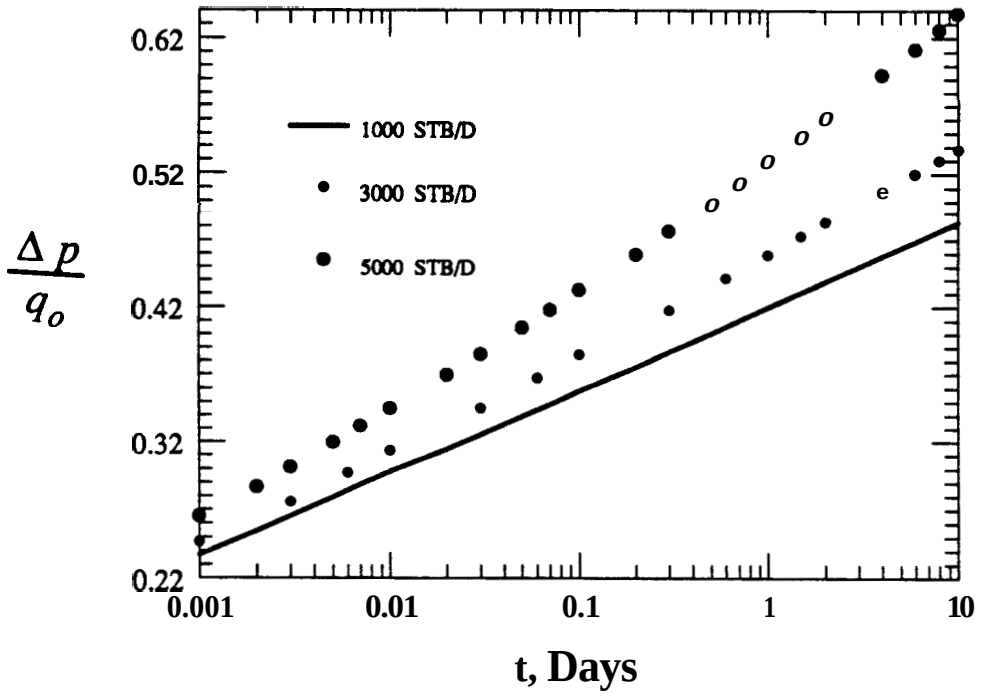

Figure C.1: $\Delta p / q_o$ for three drawdown tests simulated at different rates in volatile oil systems.

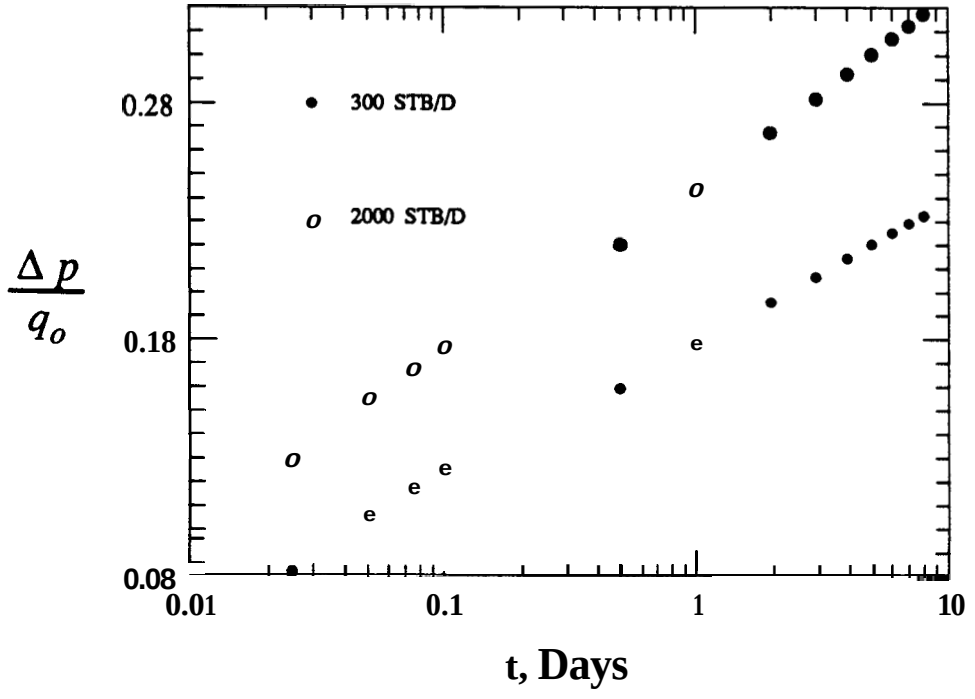

Figure C.2: $\Delta p / q_o$ for two drawdown tests simulated at different rates in oils of low volatility.

The line source solution of the multiphase difisivity equation, Eq. 4-25, in terms of p^2, was given by Eq. 4-30 and written as:

$$p_i^2 - p_{wf}^2 = \frac{q_o}{2\pi a h} \left[-E_i \left(-\frac{\phi r_w^2 c_t}{4 t \lambda_t} \right) \right] \qquad \text{(C-6)}$$

where a is the empirical slope whose definition (which is different for oils of different volatilities, Section 4.3) is combined with Eq. C-6 to estimate effective oil permeability. For example, the following relation can be derived for volatile oils:

$$k_o = \frac{325.2 B_o \mu_o p_i}{m h} \qquad \text{(C-7)}$$

where m is the semilog slope of a $(p_i^2 - p_{wf}^2)/q_o$ versus time for a drawdown test, and of a $(p_{ws}^2 - p_{wf,s}^2)/q_o$ $(\Delta t = 0.0)$ versus time for a buildup test. The oil rates are in STB/D.

The unit response can be computed through dividing the change in p^2 by the surface oil rate, $\Delta p^2 / q_o$. This solution was also tested with the same three drawdown tests run in volatile oil system. These tests were simulated at 1000, 3000 and 5000 STBD oil rates. Test responses were then normalized as $(p_i^2 - p_{wf}^2)_j / (q_o)_j$, where j refers to a specific test, and plotted in Fig. C.3. The responses of the three drawdown tests collapsed to a single straight line of the correct slope. For very high rates, there is a tendency towards lower slope at late times which results in a small overestimation of oil phase permeability. Therefore for volatile oil systems, surface oil rate can be used to normalize the multiphase response in terms of p^2. This normalization allows the determination of estimates for individual phase permeabilities to good accuracy. The pressure squared solution was also tested with the same two drawdown tests run in the system of low oil volatility. These tests were simulated at 300 and 2000 STBD oil rates. Test responses were then normalized as $(p_i^2 - p_{wf}^2)_j / (q_o)_j$, where j refers to a specific test, and plotted in Fig. C.4. This deviation from the correct slope indicates the importance of the intercept neglected in deriving the pressure squared solution, see Appendix B. This behavior was also seen in Section 4.4 (see Figs. 4.16 and 4.17).

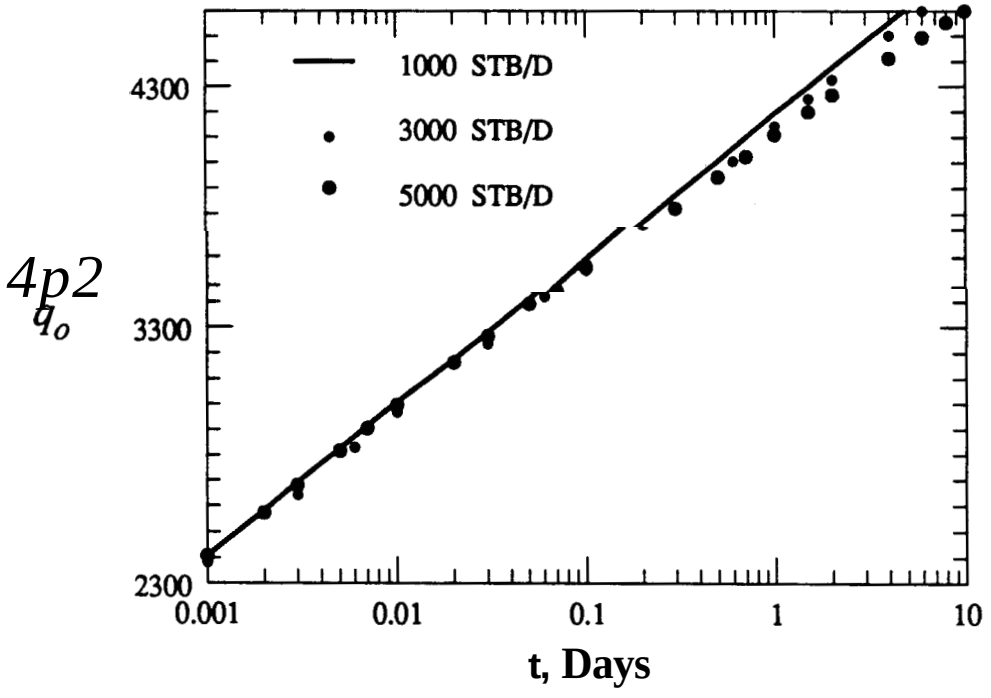

Figure C.3: A p^2 / q_o for three drawdown tests simulated at different rates in volatile oil systems.

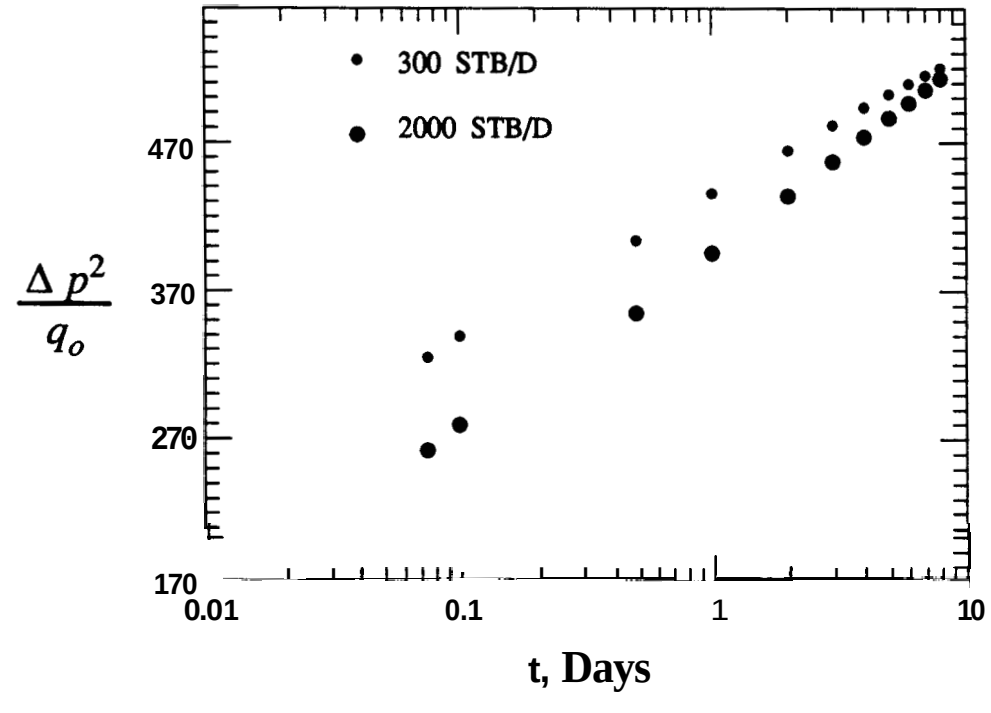

Figure C.4: A p^2 / q_o for two drawdown tests simulated at different rates in oils of low volatility.

The rate normalization applied by Fetkovich-Vienot (1984) and Raghavan (1986) utilizes the total and not the oil rate. This normalization is based on Penine's pressure solution for Martin's diffusivity equation, Eq. 2-12, but with an inner boundary condition that is different from Eq. 447. This inner boundary condition is written as:

$$\lim_{r \to r_w} \left(r \frac{\partial p}{\partial t} \right) = \frac{q_t}{2 \pi \lambda_t h} \qquad \text{(C-8)}$$

where q_t is delined by Eq. C-3 and λ_t is delined by Eq. C-2.

The solution obtained is formulated in Eq. C-1 which yields total system mobility using the total voidage rate, Eq. C-3. This normalization is also tested with four drawdown tests simulated at 2000, 6000, 13000 and 18000 RB/D total rates (The corresponding surface oil rates were 990, 2750,5300 and 6700 STB/D). These four tests were run with the volatile oil system (all other parameter were held the same for all tests). Test responses were then normalized as $(p_i - p_{wf})_j / (q_t)_j$, where j refers to a specific test, and plotted in Fig. C.5. Only the normalized response for the 2000 RB/D total rate test resulted in the correct unit response through the whole test. The normalized response for the 6000 RB/D total rate test asymptotically matches the correct slope after a long time. Higher rates shifted from the correct unit response and had no definite semilog slope. In general, their slopes were higher than the correct slope which resulted in underestimates of total system mobility. In general, the deviation from the correct slope, pronounced at high rates, indicates that total rate *can* not be used to normalize pressure response under such conditions.

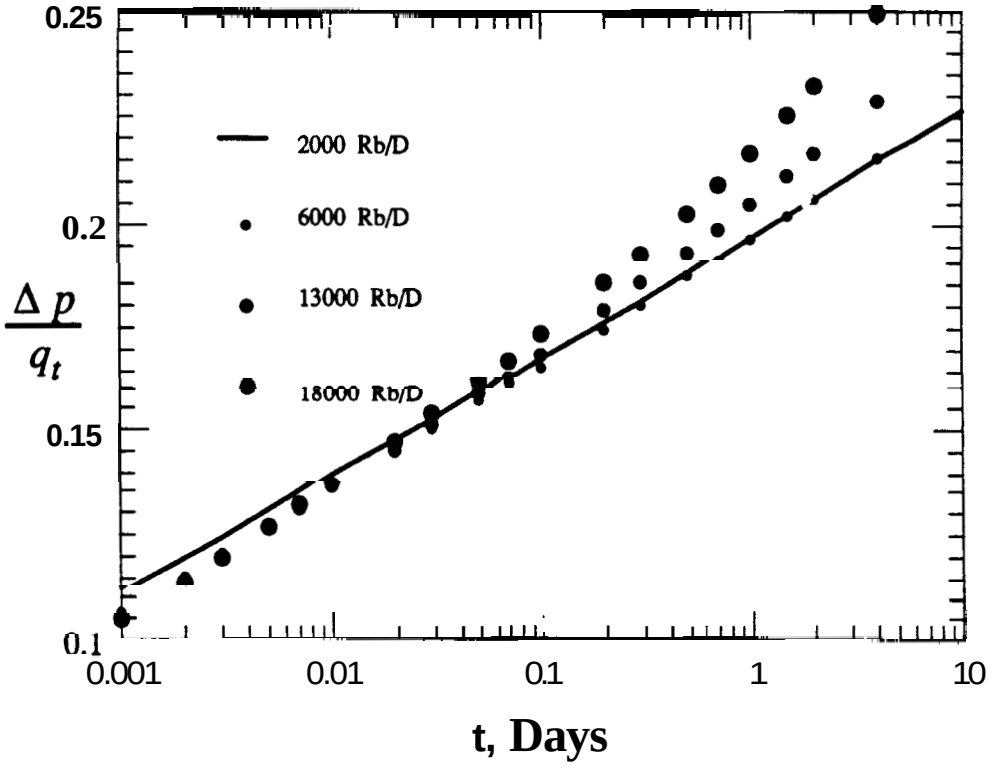

Figure C.5 : **The normalized response of four drawdown tests run at different voidage rates in the same system, Pemne's approach.**

C.2 Example Applications

Example well tests were generated using the ECLIPSE simulator, where rate! is made to vary with time to resemble that of an afterflow following a buildup or wellbore unloading during a drawdown. The currently used normalization (Fetkovich-Vienot, 1984, and Raghavan, 1986). is applied using total voidage rates to normalize the change in pressure. Also, the normalization scheme, proposed in this work, is demonstrated using surface oil rates to normalize the change in p^2.

Gladfelter et al. (1955) normalization is applied here to simplify the demonstration. Such normalization is applicable when the rate changes are linear with time (Kucuk, 1986). Results can be generalized for applications in more robust deconvolution techniques.

Example 1

A drawdown test with the rate profile shown in Fig. C.6 was simulated utilizing the set of PVT properties provided by Bçe et al. (1981). The relative permeability relations were given by Eqs. 5-22 and 5-23, Corey-type relations with a 3.3 exponent for oil and a 2.0 exponent for gas. The reservoir had a thickness of 100 ft, a porosity of 0.15 and a permeability of 20 md. The test started at an initial pressure of 5202 psi and 10 96 gas saturation.

The pressure response is plotted in Fig. C.7. It does not exhibit a single semilog slope in the transient period. When the total voidage rate was used to normalize the pressure change, the response exhibited a single slope, Fig. C.8. This slope was used in Eq. C-1 and resulted in a total mobility of 22.18 md/cp compared to the input value of 56.85 md/cp. This underestimation of total system mobility is significant. In order to resolve this problem, the proposed normalization is applied. The change in p^2 is normalized using surface oil rates. Figure C.9 shows the normalized response which exhibited a single slope. This slope was used in Eq. C-7 and yielded an oil permeability of 11 md which compared reasonably to the input value of 13.1 md.

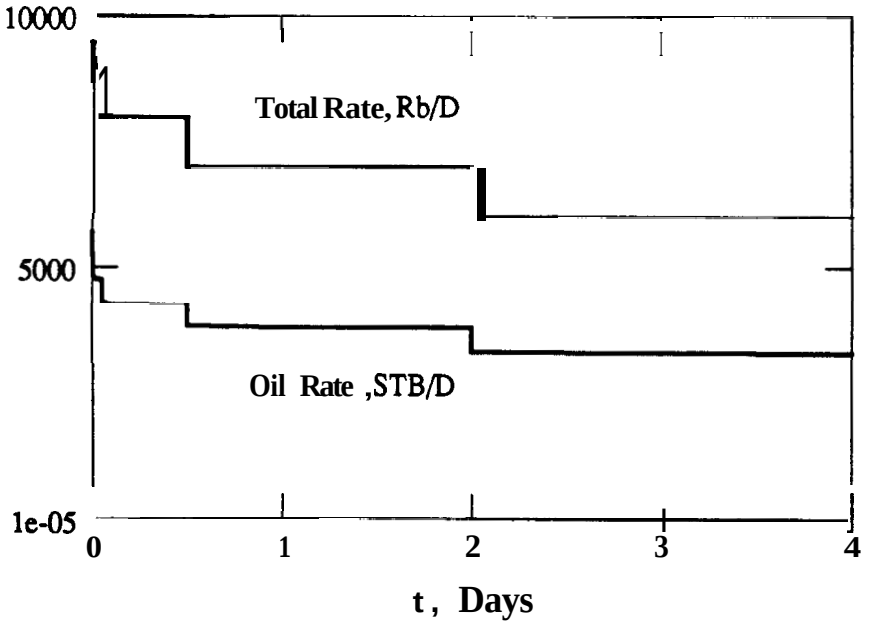

Figure C.6 : The rate profile for Example 1.

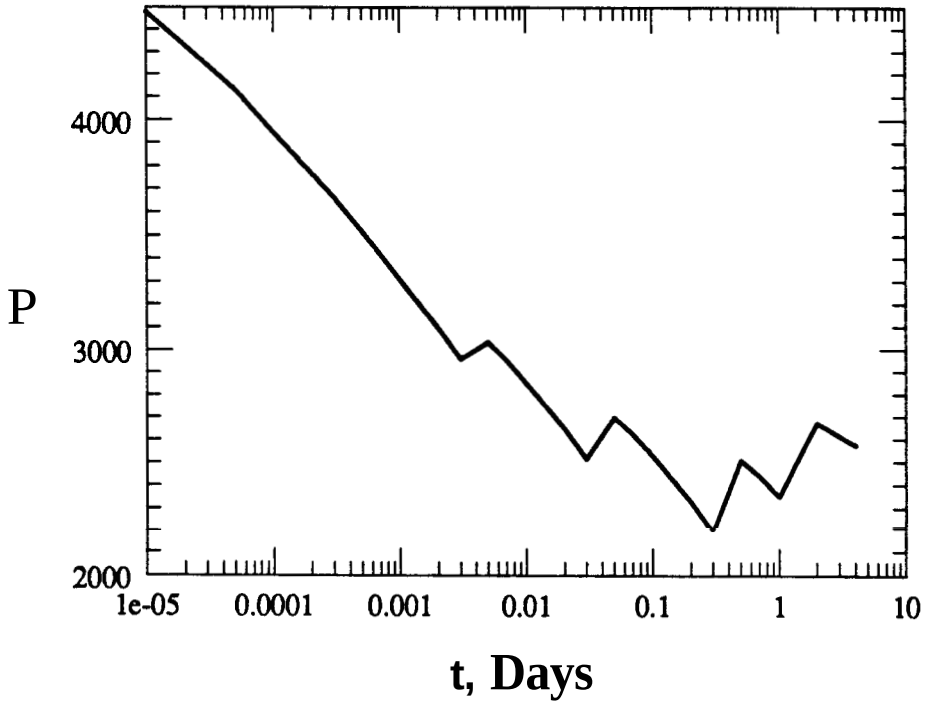

Figure C.7 : The pressure response of Example 1.

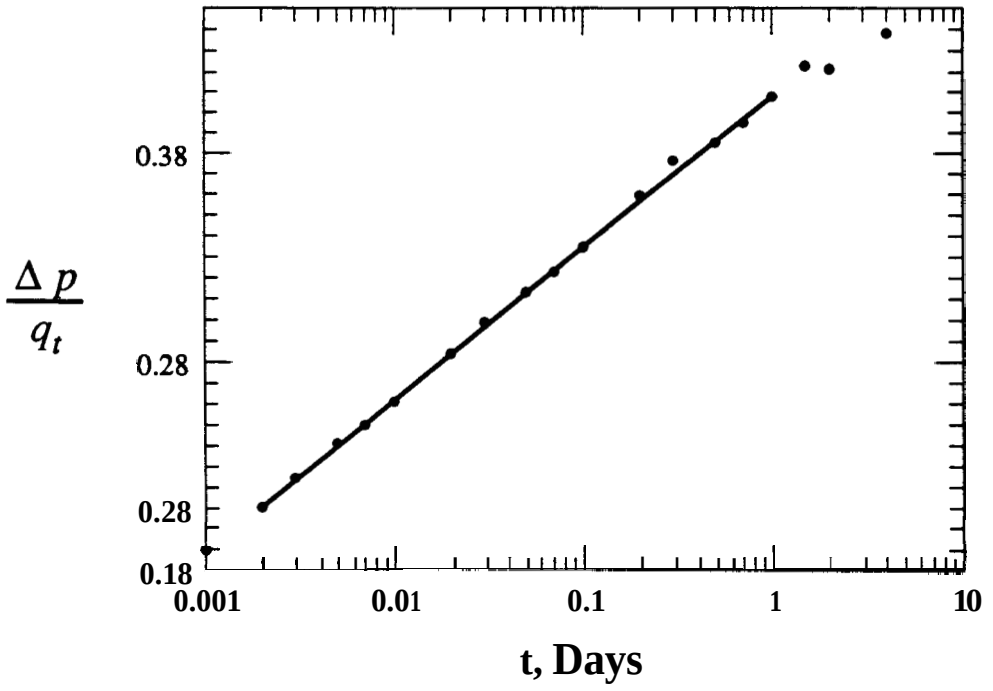

Figure C.8 : The normalized response of Example 1, Perrine's approach.

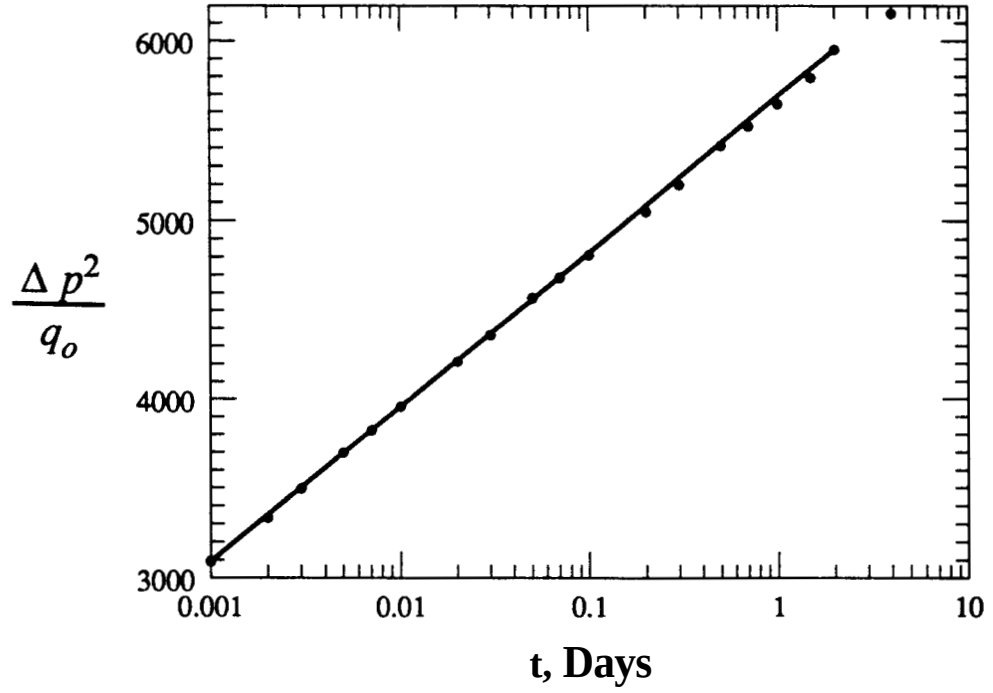

Figure C.9 : The normalized response of Example 1, the new approach.

Example 2

This drawdown test was simulated with the rate profile shown in Fig. C.10. The reservoir thickness was 40 ft and the absolute permeability was 10 md. All other parameters were similar to those used in Example 1.

Neither the pressure response plotted in Fig. C.11 or the pressure square response plotted in Fig. C.12 exhibited a single semilog slope in the transient period. When total rates were used to normalize pressure changes, the response exhibited two semilog slopes, Fig. C.13. Such a response may be misinterpreted as an indication of a composite system. In order to resolve this problem, the proposed normalization is applied. Changes in p^2 were normalized using changes in surface oil rate. Figure C.14 showed the normalized response which exhibited a single slope. This slope was used in Eq. C-7 and yielded an oil permeabiity of 5.3 md which compared reasonably to the 6.5 md input value.

Example 3

This drawdown test was simulated with the rate profile shown in Fig. C.15. This rate profile was simulated to reflect wellbore unloading effects that result in a linear change of rate with time. The resewoir thickness was 100 ft and the absolute permeability was 50 md. All other parameters were similar to those used in Example 1.

The pressure response plotted in Fig. C.16 and the pressure squared response plotted in Fig. C.17 were dominated by the unloading effects of wellbore fluids. When total voidage rates were used to normalize pressure changes, the response exhibited a late semilog slope in addition to an early asymptotic semilog slope, Fig. C.18. This shape of the semilog plot was expected for a linear change of rate with time (Kucuk, 1986). The second semilog slope was used in Eq. C.1 and resulted in 78.44 md/cp.

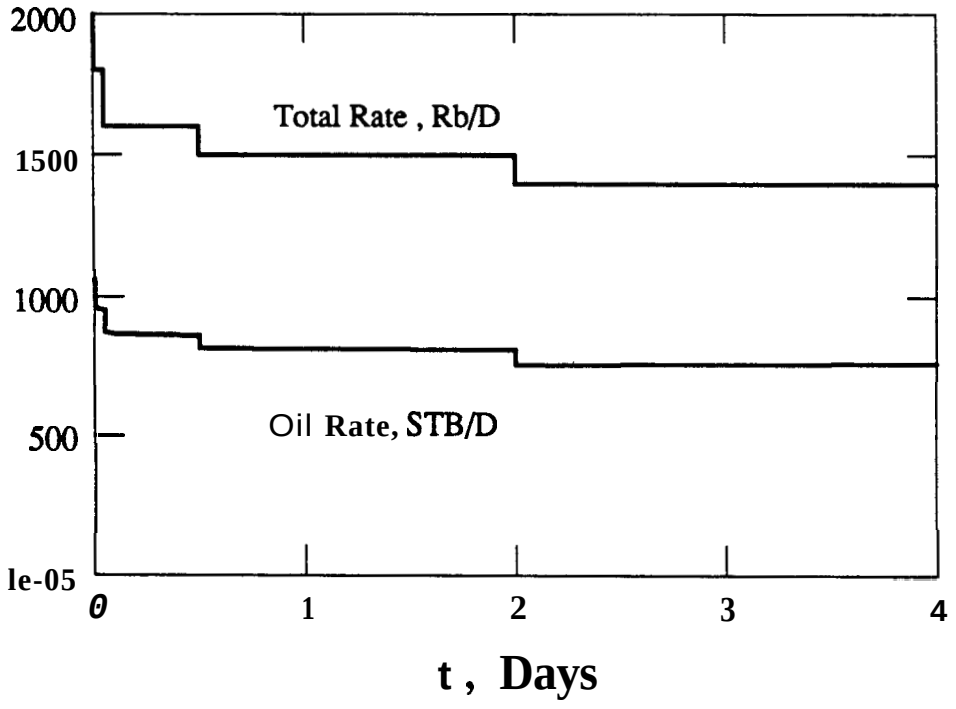

Figure C.10: **The** rate **profile for Example 2.**

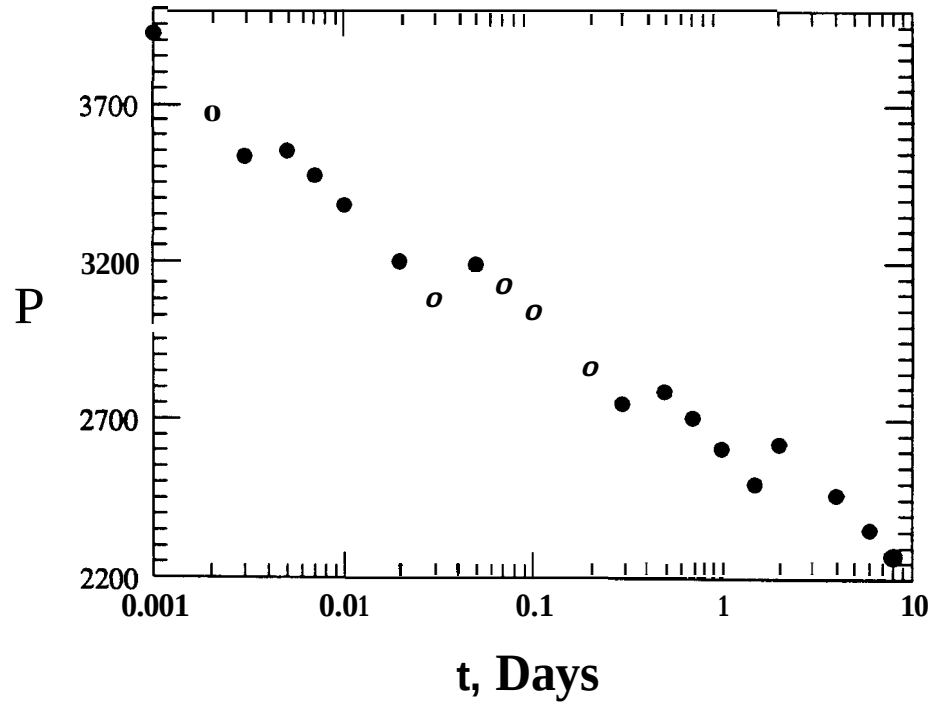

Figure C.11: **The response of Example 2, in terms of p.**

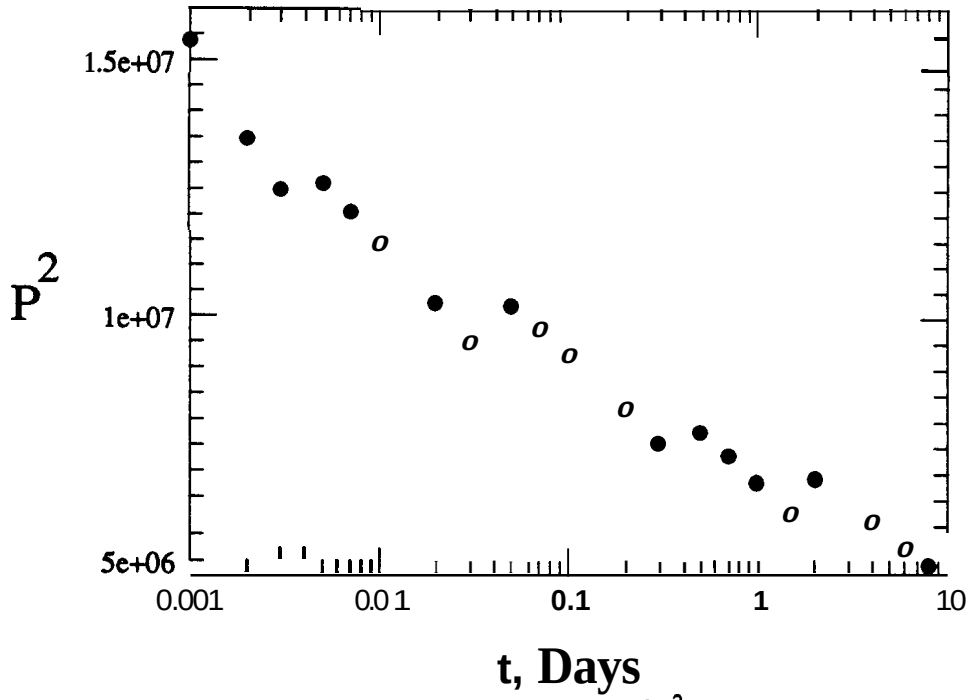

Figure C.12: **The response of Example 2, in terms of p^2.**

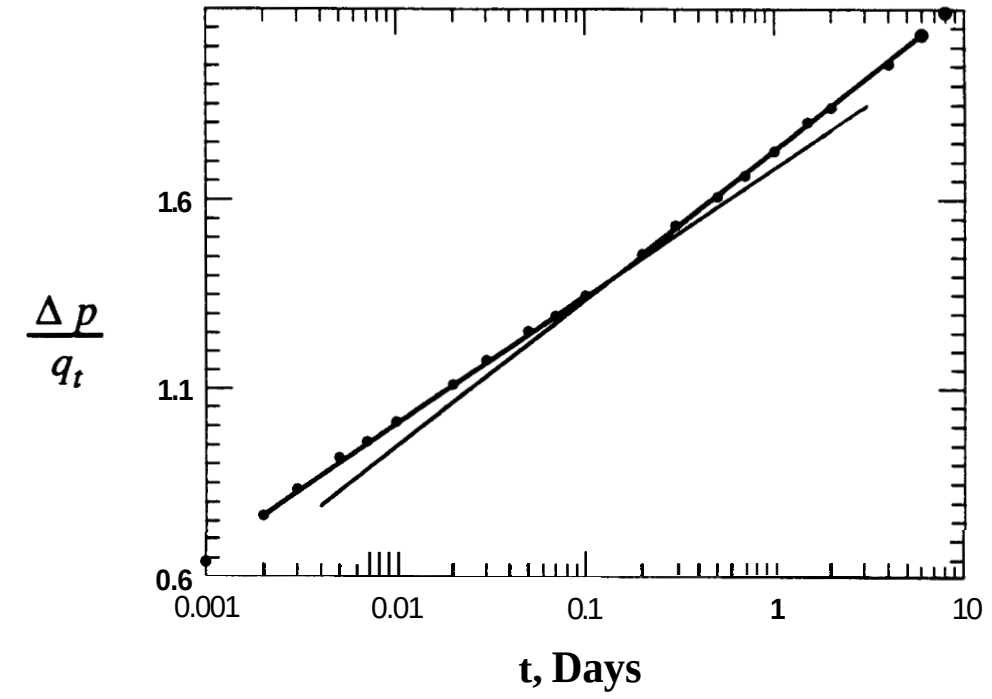

Figure C.13: The normalized response of Example 2, Perrine's approach.

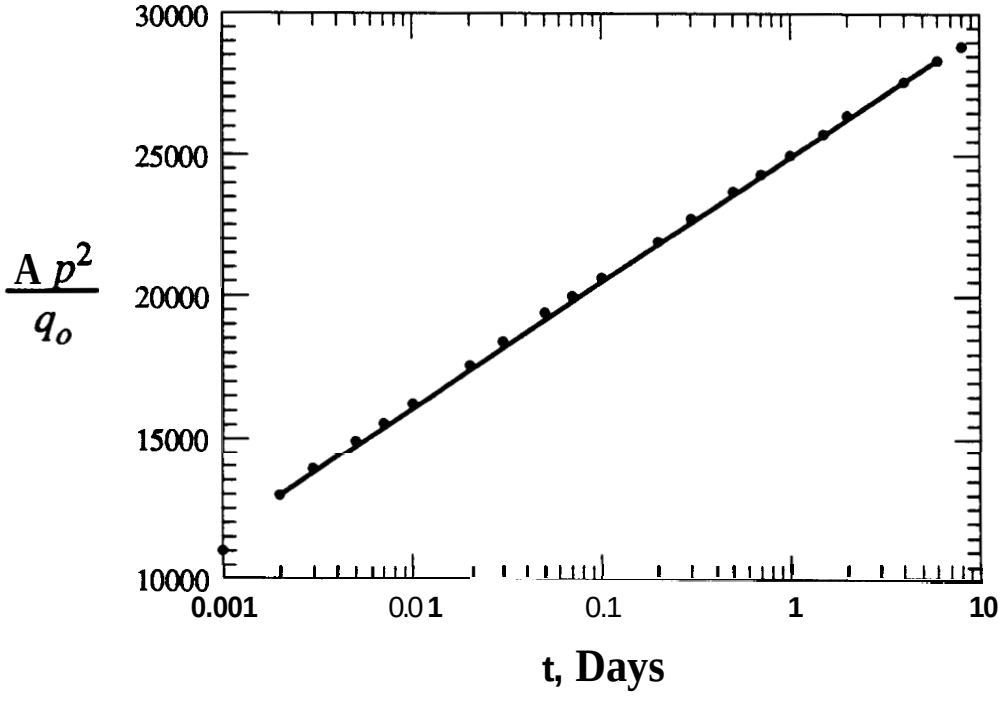

Figure C.14: The normalized response of Example 2, the new approach.

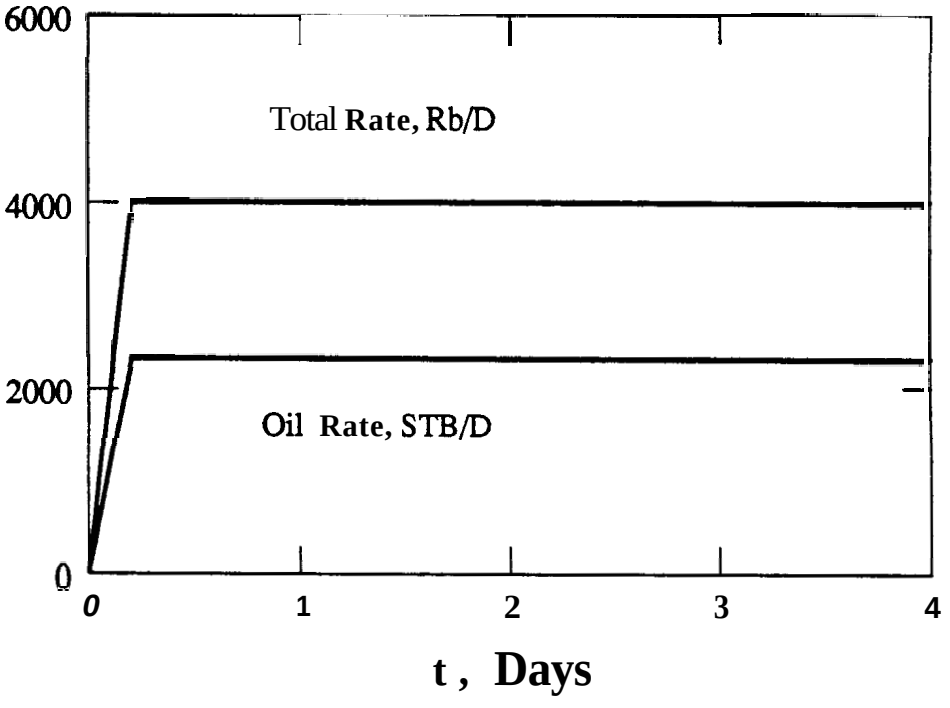

Figure C.15: The rate profile for Example 3.

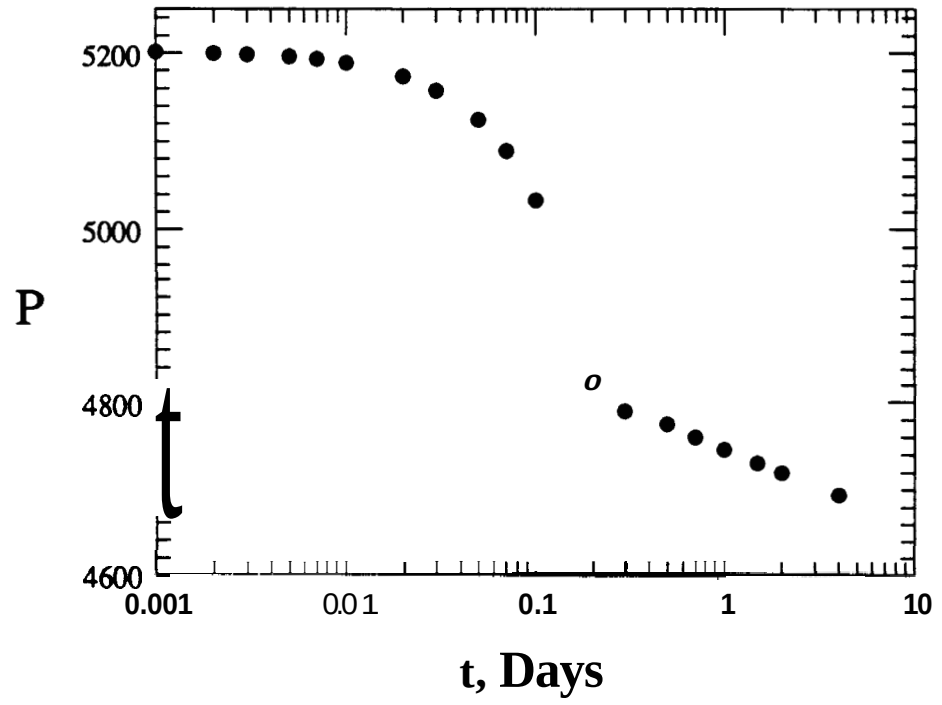

Figure **C.16:** **The response of Example 3,** in **terms of** p.

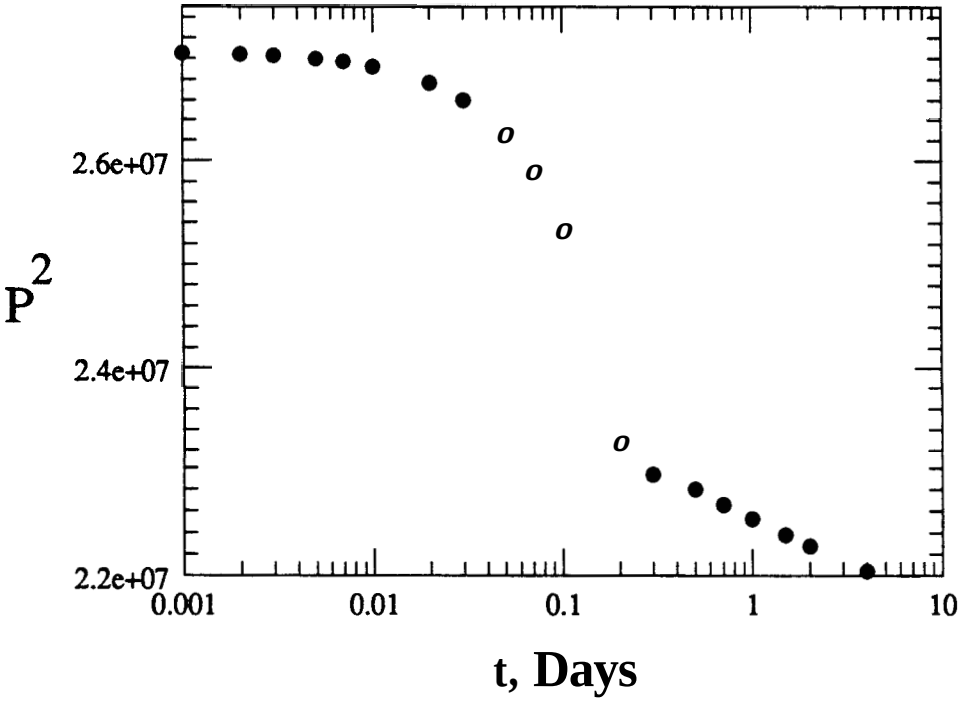

Figure **C.17:** **The response of Example 3,** in **terms of** p^2.

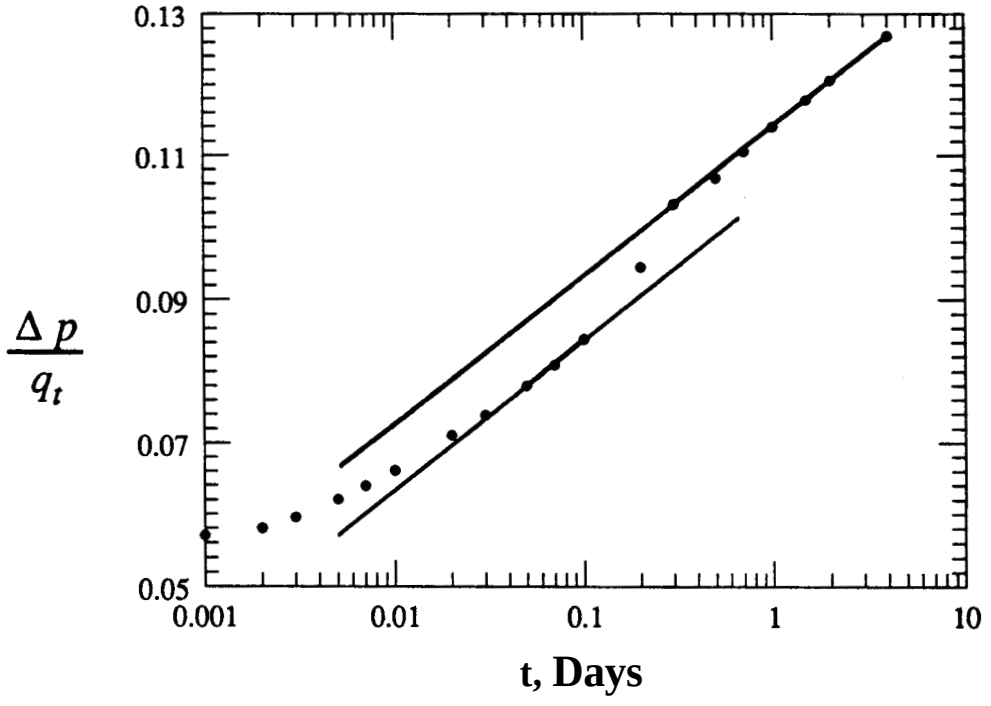

Figure C.18: The normalized response of Example 3, Penine's approach

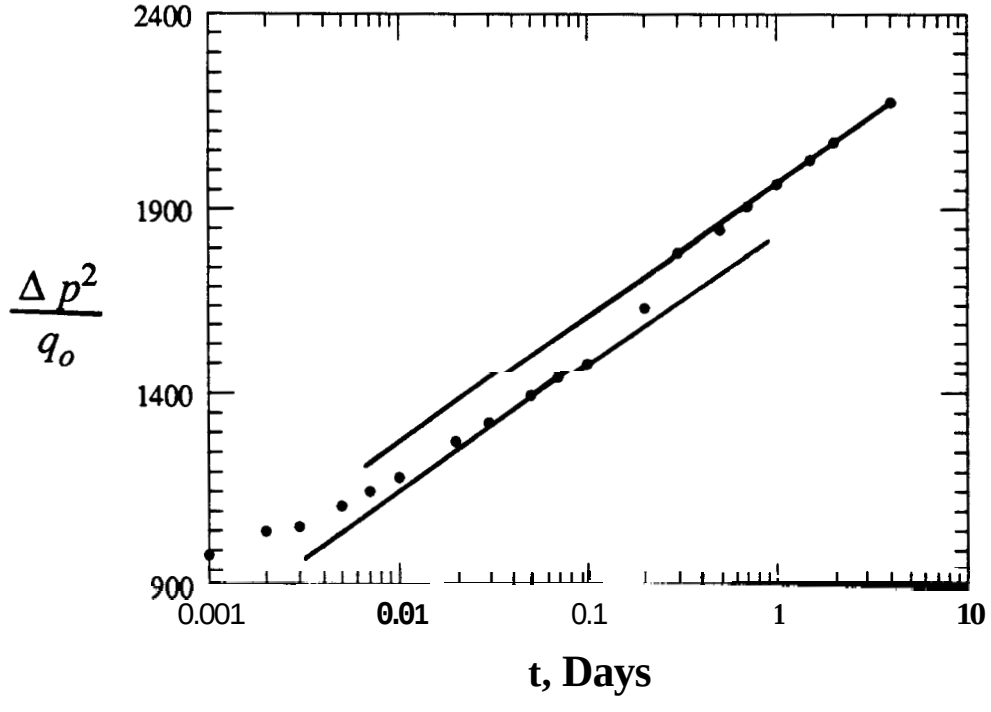

Figure C.19: The normalized response of Example 3, the new approach.

Another approach (Kucuk, 1986) to analyze such response is to utilize the difference in $\Delta p / q_t$ at any given time between the late slope and the extension of the early slope in the following relation:

$$\lambda_t = (k / \mu)_t = \frac{70.6}{[(\Delta p / q_t)_2 - (\Delta p / q_t)_1] \; h} \qquad \text{(C-9)}$$

where the index 2 refers to the value on the late slope and the index 1 refers to the value on the early slope. When Eq. C-9 was used, the estimate obtained for the total system mobility was 81.3 md/cp which is close to 78.44 md/cp obtained using the late slope in Eq. C-1. Both values were underestimates of the input total mobility of 128.4 md/cp. In order to resolve this problem of underestimation, the proposed normalization is applied where the change in p^2 is normalized using the change in surface oil rate. Fig. C.19 showed the normalized response which exhibited a late slope, and an early slope similar to that seen in Fig. C.18. The late slope was used in Eq. C-7 and yielded an oil permeability of 28.08 md compared to the 32.8 md input value. A relation similar to Eq. C-9 can be derived in terms of p^2 as:

$$a = \frac{141.2}{[(\Delta p^2 / q_o)_2 - (\Delta p^2 / q_o)_1] \; h} \qquad \text{(C-10)}$$

where a is the empirical slope defined in Section 4.3. When this definition for volatile oil is applied to Eq. C-10, the following relation results:

$$k_o = \frac{141.2 \; p_i \; B_{o,i} \; \mu_{o,i}}{[(\Delta p^2 / q_o)_2 - (\Delta p^2 / q_o)_1] \; h} \qquad \text{(C-11)}$$

The use of Eq. C.1 resulted in a 31.7 md oil permeability which is close to the input value of 32.8 md. This shows the improvement in accuracy obtained using the proposed approach

Example 4

This is a buildup test simulated with an afterflow profile shown in Fig. C.20. The rate profile was made to reflect afterflow effects. The reservoir thickness was 100 ft and the absolute permeability was 30 md. The well was shut-in after 100 days of production time at an average pressure of 5125 psia and at an average gas saturation of 12 %. All other parameters were similar to those used in Example 1.

The pressure response plotted in Fig. C.21 and the pressure squared response plotted in Fig. C.22 were dominated by the afterflow effects. When the total voidage rate was used to normalize pressure change, the response exhibited a single slope, Fig. C.23. This slope was used in Eq. C-1 and resulted in a 49.5 md/cp total mobility. compared to the input value of 78.9 md/cp. In order to resolve this problem, the proposed normalization was applied where the change in p^2 was normalized using the change in surface oil rate in STB/D. Figure C.24 showed the normalized response which exhibits a single slope. This slope was used in Eq. C-7 and yielded an oil permeability of 16 md compared to the input value of 18 md. Again, this example shows the reasonable accuracy obtained using the proposed normalization compared to the underestimation of that currently used in the oil industry.

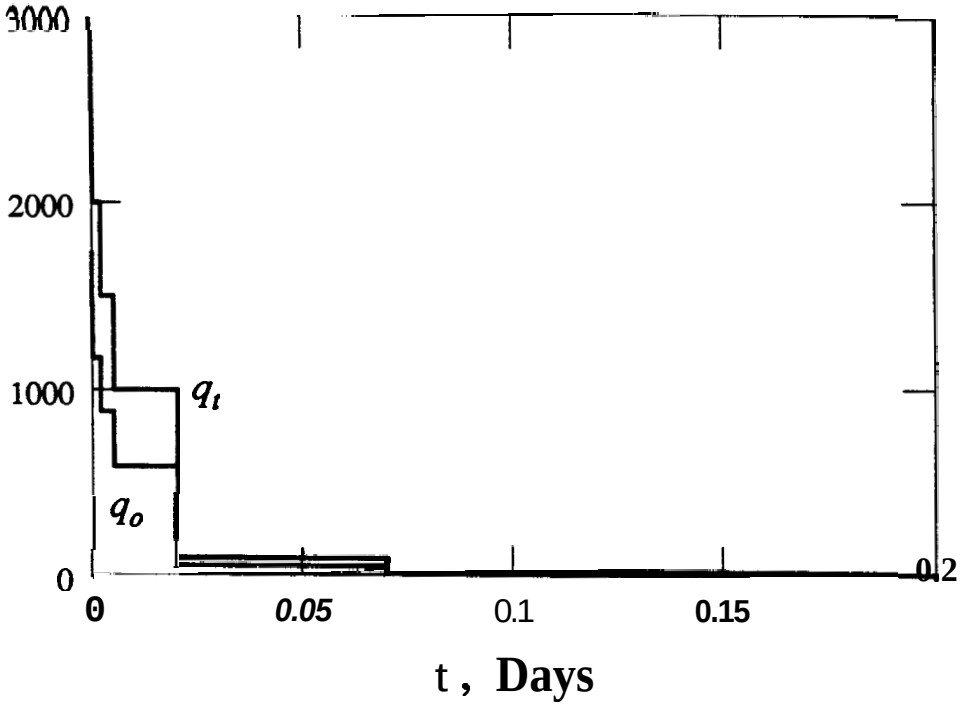

Figure C.20: The afterflow profile, oil rate in STBD and total rate in Rb/D, for Example 4.

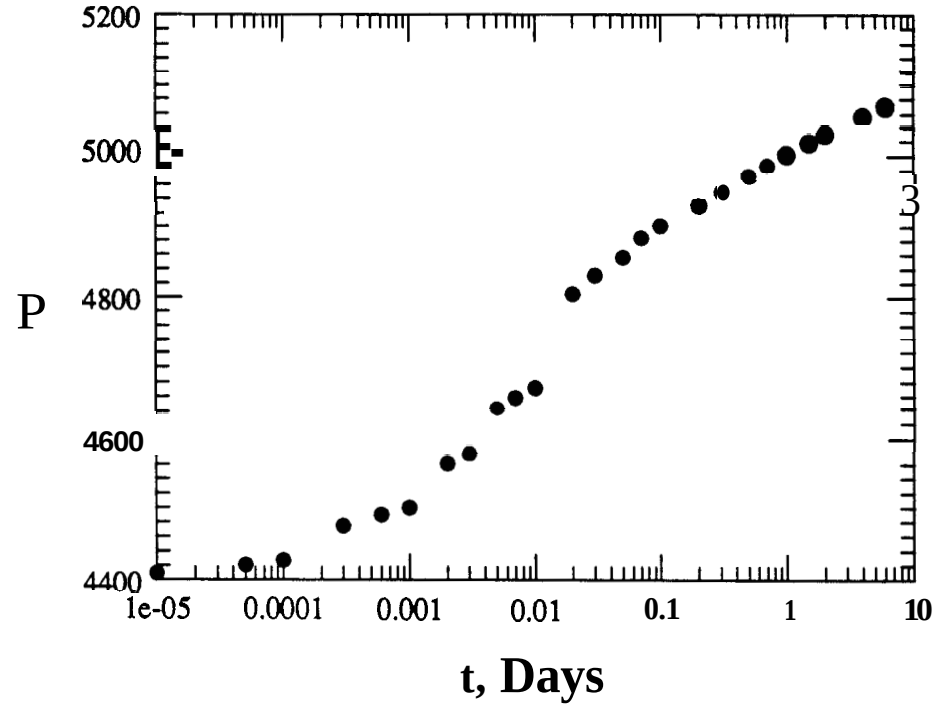

Figure C.21: The response of Example 4, in terms of p.

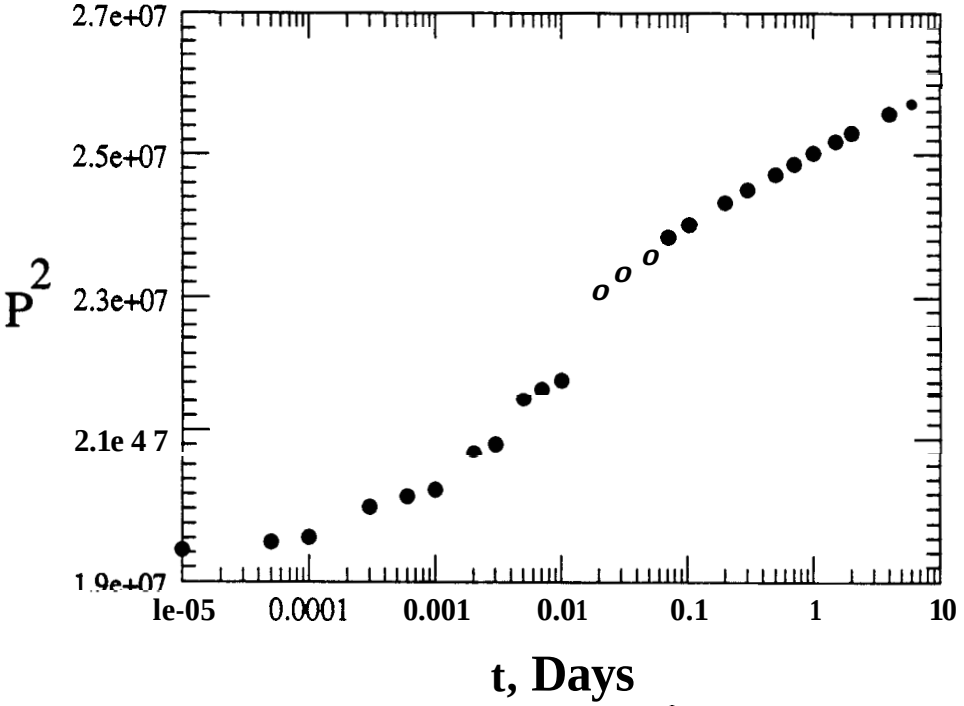

Figure C.22: The response of Example 4, in terms of p^2.

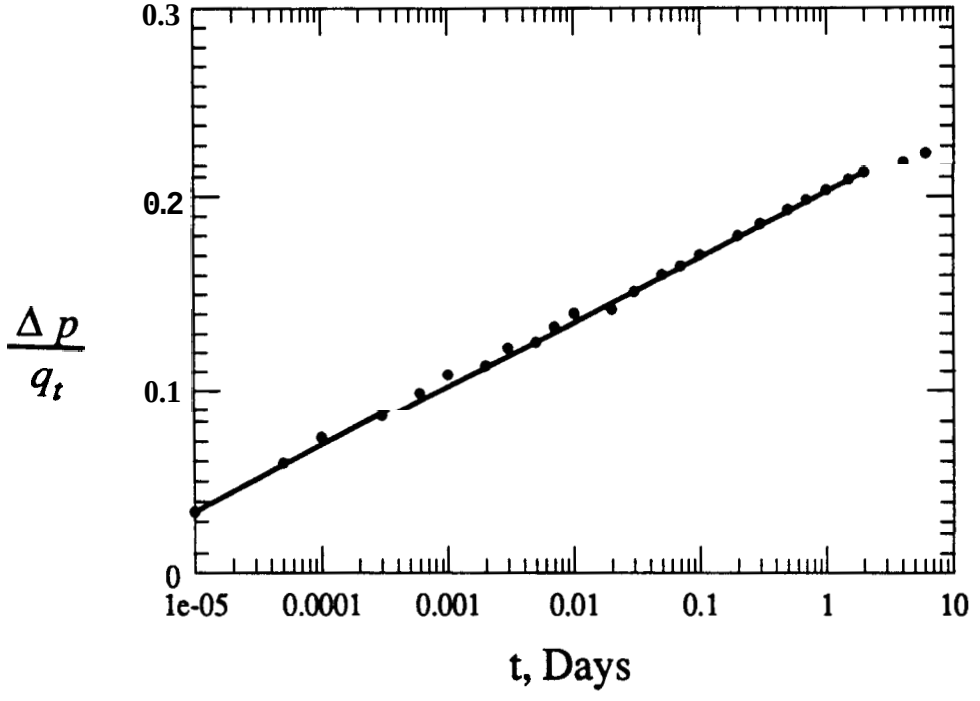

Figure C.23: **The normalized** response **of Example 4. Penine's approach**

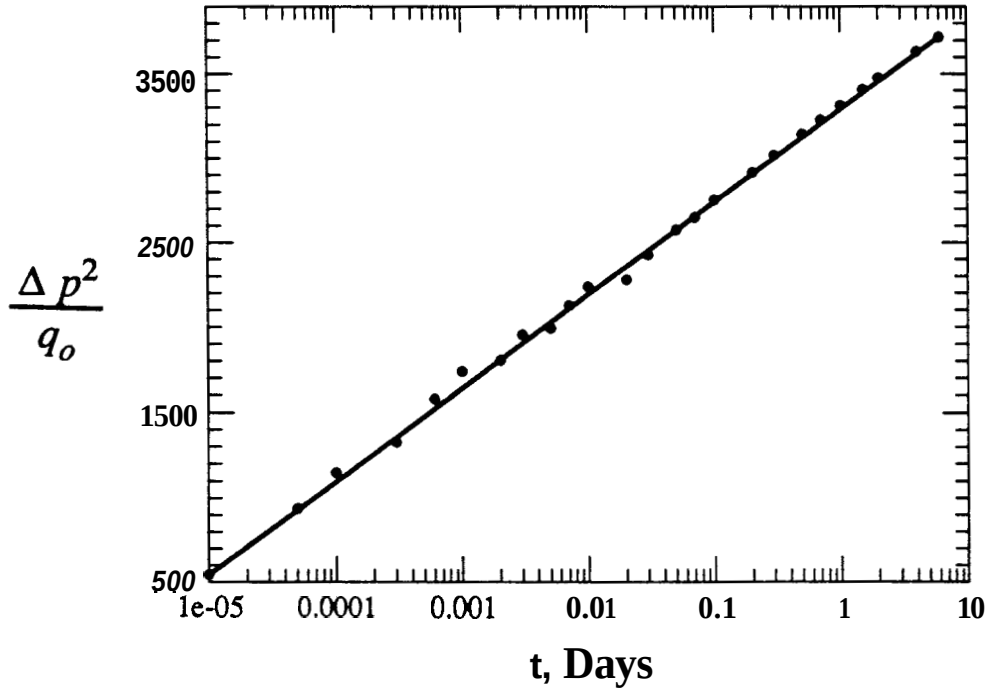

Figure C.24: **The normalized response of Example 4, the new approach.**

C.3 Discussion

The Gladfelter et al. (1955) normalization was applied to simply demonstrate certain points of interest to multiphase flow. These observations are discussed here, and considered to apply to other robust deconvolution schemes.

The rate normalization, based on Penine's approach and currently used in the industry for multiphase flow, was shown to apply only at low rates. Its sensitivity to rate for oils of both high and low volatility is due to the terms neglected in deriving Penine's approach and the improper linearization of the inner boundary condition in terms of pressure. This normalization requires that the total rate in RB/D be monitored throughout the test. This is not easily satisfied in practice due to the difficulties encountered in measuring gas rates. Furthermore, this normalization results in underestimated values for total system mobility and yields no individual phase mobility.

The rate normalization proposed in this work was shown to be insensitive to rates for volatile oils, due to the proper linearization of the inner boundary condition and improved treatment of the nonlinear terms when deriving the diffusivity equation in terms of p^2, Eq. 4-25. This normalization requires only surface oil rates. Moreover, it results in reasonable estimates of individual phase permeabilities and thereby accurate values of total system mobility. On the other hand, the proposed rate normalization was also seen to be sensitive to rate for oils of low volatility.

This section also investigated the limits of Perrine's approach and the rate normalization currently applied in the industry. The Perrine (1956) approach was seen to be sensitive to flow rates in oils of both high and low volatility. Perrin's solution was also seen to underestimate the total system mobility for high rate tests. On the other hand, the pressure squared solution applies for all rates in volatile oils, and yields reasonable estimates of individual phase as well as total system mobilities. For oils of low volatility, the pressure squared approach applies at low rates, but may develop several semilog slopes at high rates.